

**Thèse de doctorat de l'Université de Bourgogne Franche-Comté**

**Préparée à L'UFR Sciences Vie Terre Environnement**

**Laboratoire Biogéosciences – UMR 6282**

Ecole doctorale n°554

Environnement - Santé

Doctorat de Paléontologie - Evolution

Par

DUBIED Morgane

Développement postnatal et évolution du complexe craniofacial chez les rongeurs

Postnatal development and evolution of the rodents' craniofacial complex

Thèse présentée et soutenue à Dijon, le 9 Novembre 2022

Composition du Jury :

M, FARA, Emmanuel  
Mme, RUF, Irina  
M, SANCHEZ-VILLAGRA, Marcelo  
Mme, EVIN, Allowen  
M, DEBAT, Vincent  
Mme, MONTUIRE, Sophie  
M, NAVARRO, Nicolas

Professeur, Université de Bourgogne Franche-Comté Président du jury  
Professeure, Senckenberg Museum (Allemagne) Rapporteure  
Professeur, Université de Zurich (Suisse) Rapporteur  
Directrice de recherche, Université de Montpellier Examinatrice  
Maître de conférences, MNHN Examineur  
Directrice d'études, EPHE Directrice de thèse  
Maître de conférences, EPHE Codirecteur de thèse

## Abstract

Understanding developmental mechanisms in evolution is crucial to apprehend the diversification of organismal forms. In mammals, changes occur during all development phases (prenatal and postnatal). Postnatal growth plays an essential role in the acquisition of the adult shape. During this period, the craniofacial complex undergoes many changes in functional constraint forcing the different tissue to accommodate while adjusting, along the growth and at the adult stage, to a certain level of functional performance. These different developmental interactions respond to several influencing factors such as molecular, genetic and cellular processes but also the environment. The latter will play on these interactions, but in different ways between the prenatal and postnatal phases, as gestational environment and environment at birth are different. For testing the interactions between the developing organism and its environment and the potential evolutionary consequences, Rodentia is a good example of broad diversity in all aspects (wide variety of forms, in diets, behavior and ecology) and thus a study group of choice. It is a very diverse and disparate mammal order, in which changes can be observed on a large scale. In addition, it includes model organisms that can be easily reared in laboratory following a precise experimental configuration to test the effects of diverse sources of variation. The craniofacial complex is a highly integrated structure, architecturally complex, as it is composed of many skeletal elements, and functionally, as it is involved in various tasks essential to the organism. At the same time, and somewhat paradoxically, this unit is highly scalable and presents a great diversity of forms. The basis of craniofacial shape variation and its control are as much, related to the additive effects of genes as to their epigenetic and context-specific interactions during development. These epigenetic interactions during growth will respond to mechanical and other stimuli between the ossification centers, the tissues and organs making up the head. In particular, these interactions control the spatialization and intensity of bone remodeling in response to other tissue strain. They will thus compensate and coordinate the growth of the different tissues and organs in order to acquire and/or maintain certain functions, such as the occlusion between the upper and lower jaws. These epigenetic interactions are thus essential to the normal development of the skeleton in general and the skull in particular. By responding to changes in forces and movements, they will be a potential driver of microevolutionary changes (and thus macroevolutionary changes) at the morphological level favoring adaptive directions of variation and generating new functional covariations between traits. Despite this central role, the importance of these interactions in the expression of inter-specific differences and in the longer term in the dynamics of clades remains poorly understood. Analysis of the tempo of adult disparity acquisition during ontogeny is a key element in understanding the differential filling of the shape space by clades. This project aimed I) at studying the establishment of craniofacial disparity in rodents during development on a macroevolutionary scale and then on a finer taxonomic scale; and II) at estimating the importance of the epigenetic processes during this postnatal growth.

## Résumé

La compréhension des mécanismes de développement dans l'évolution est cruciale pour appréhender la diversification des organismes. Chez les mammifères, des changements se produisent tout au long du développement (prénatal et postnatal). La croissance postnatale joue un rôle essentiel dans l'acquisition de la forme adulte. Durant cette période, le complexe craniofacial subit de nombreux changements de contraintes fonctionnelles obligeant les différents tissus à s'adapter tout en s'ajustant, tout au long de la croissance et au stade adulte, à un certain niveau de performance fonctionnelle. Ces différentes interactions développementales répondent à plusieurs facteurs forçants tels que les processus moléculaires, génétiques et cellulaires mais aussi l'environnement. Ce dernier va jouer sur ces interactions, mais de manière différente entre les phases prénatale et postnatale, car l'environnement gestationnel et l'environnement à la naissance sont différents. Pour tester les interactions entre l'organisme en développement et son environnement et les conséquences potentielles sur l'évolution, les Rodentia constituent un bon exemple de grande diversité à tous égards (grande variété de formes, de régimes alimentaires, de comportements et d'écologie) et donc un groupe d'étude de choix. Il s'agit d'un ordre de mammifères très diversifié et disparate, dans lequel des changements peuvent être observés à grande échelle. En outre, ce groupe comprend plusieurs organismes modèles qui peuvent être facilement élevés en laboratoire, afin de tester les effets de diverses sources de variation grâce à des protocoles expérimentaux précis. Le complexe craniofacial est une structure hautement intégrée, complexe sur le plan architectural, car il est composé de nombreux éléments squelettiques, et sur le plan fonctionnel, car il participe à diverses tâches essentielles pour l'organisme. En même temps, et de façon quelque peu paradoxale, cet ensemble est très évolvable et présente une grande diversité de formes. La base de la variation de la forme craniofaciale et son contrôle sont autant liés aux effets additifs des gènes qu'à leurs interactions épigénétiques et contextuelles au cours du développement. Ces interactions épigénétiques pendant la croissance vont répondre aux stimuli mécaniques et autres, entre les centres d'ossification, les tissus et les organes qui composent la tête. En particulier, ces interactions contrôlent la spatialisation et l'intensité du remodelage osseux en réponse aux contraintes subies par les autres tissus. Elles vont ainsi compenser et coordonner la croissance des différents tissus et organes afin d'acquérir et/ou de maintenir certaines fonctions, comme l'occlusion entre les mâchoires supérieure et inférieure. Ces interactions épigénétiques sont donc essentielles au développement normal du squelette en général et du crâne en particulier. En répondant aux changements de forces et de mouvements, elles seront un moteur potentiel de changements microévolutifs (et donc macroévolutifs) au niveau morphologique favorisant des directions adaptatives de variation et générant de nouvelles covariations fonctionnelles entre les traits. Malgré ce rôle central, l'importance de ces interactions dans l'expression des différences interspécifiques et à plus long terme dans la dynamique des clades reste mal comprise. L'analyse du rythme d'acquisition de la disparité chez l'adulte au cours de l'ontogenèse est un élément clé pour comprendre le remplissage différentiel de l'espace des formes par les clades. Ce projet a visé à étudier I) la mise en place de la disparité craniofaciale chez les rongeurs au cours du développement à échelle macroévolutive, puis à une échelle taxonomique plus fine ; et II) d'évaluer l'importance des processus épigénétiques lors de cette croissance postnatale.





## Remerciements

Après quatre années de thèse, plusieurs centaines d'heures de segmentation, plus de vingt mille landmarks posés, deux changements de bureau, trois luxation de l'épaule, une vis flambant neuve dans cette dernière et deux passages par la case Covid, il est enfin temps pour moi, avant toute chose, de remercier ceux sans qui cette grande aventure aurait été impossible.

Je voudrais ensuite remercier l'Ecole Doctorale Environnement-Santé ainsi que son conseil de m'avoir permis d'obtenir cette bourse de thèse, puis de m'avoir accueilli en tant que membre. Merci à Thierry, Christelle et Virginie pour leur soutien et leur confiance indéfectible durant tout ce temps. Je souhaite aussi remercier le laboratoire Biogéosciences pour son accueil, notamment Emmanuel et Pascal, pour leur écoute de la première heure, tant au sein du labo lui-même, qu'au sein des différents conseils auxquels j'ai pu participer à leurs côtés. Je remercie aussi les membres de l'équipe BioME.

Je tiens également à adresser mes remerciements aux membres de mon comité de suivi, Dr. Yann Heuzé et Dr. Vincent Debat, pour leur regard critique et bienveillant tout au long de ces années de thèse, avec un merci de plus pour Vincent qui a très agréablement accepté d'examiner ce manuscrit. J'adresse également mes remerciements aux autres membres de mon jury, Pr. Irina Ruf et Pr. Marcelo Sanchéz-Villagra me faisant l'honneur d'accepter de rapporter ce travail de thèse ; Dr. Allowen Evin et Pr. Emmanuel Fara, qui ont accepté, à mon plus grand plaisir, d'examiner mon travail.

De tout mon cœur, un immense merci à mes directeurs. Sophie, tout d'abord merci de m'avoir proposé ce sujet. Merci pour ton soutien et ton enthousiasme de tous les jours, dans les bons comme les mauvais moments ; merci pour ces grandes expéditions en collection ; merci pour toutes nos discussions, professionnelles ou non, jamais sans nos cafés ; merci pour ce gardiennage de chat de qualité ; je garderai toute ma vie dans coin de ma tête tes histoires de campagnols.

Nicolas, merci de m'avoir toi aussi accepté en thèse, malgré mon handicap R-èsque évident, promis un jour j'y arriverai, toutes ces journées à fixer R avec toi n'auront pas été veines ; merci pour ton enthousiasme ; merci pour ton temps, malgré ton calendrier multicolore. Merci à vous deux pour votre soutien tout au long des élevages et des confinements, qui n'ont clairement été un bon moment pour personne. Ce fut un immense plaisir et un honneur de vivre ce voyage avec vous.

Je remercie également Dr. Catherine Paul et Dr. Nesrine Mabrouk du LIIC pour leur aide durant les essais de quantification de myosine ; ainsi que Dr. Marielle Guéguen Minerbe et Issam Nour de l'IFSTTAR de m'avoir donné accès à leur microscope à fluorescence.

Un grand merci aux membres du laboratoire sans qui rien de tout cela n'aurait été possible. Merci Emilie de m'avoir formé sur la plateforme Morphoptics, tu as été (et restera) un soutien sans faille, prenant toujours de ton temps pour chaque crise de rire ou de larmes. Merci Lauriane pour ton sourire toujours présent, aux animaleries (sans toi j'aurai jeté l'éponge sur la fin) comme en morpho ou au pied d'un arbre pendant les confinements à attendre désespérément qu'un piou-piou pointe le bout de son bec, merci pour tes tests ainsi que tes images et montage de haute qualité. Merci Rémi de ne jamais avoir mis à exécution ta menace d'effacer « sans faire exprès » toutes mes données du serveur. Merci à vous trois pour les crises de déconcentration en morpho, ça a sauvé

quelques-uns de mes neurones (ou ça les as achevé, au choix) et merci d'avoir sauvé mes bébés scripts ainsi que quelques parties de Civ'. Merci Claire pour ces vraies pauses café sur le toit et merci Ludo pour les pause-café/bière (PS : mon genou n'est toujours pas un levier de vitesse). Une petite pensée pour Edwige, qui n'a jamais hésité à rentrer dans ce bureau de l'apocalypse, toujours avec un sourire et un petit mot doux. Merci Seb pour ton soutien, ton réconfort, et la petite virée à Bâle, toujours à pic. Merci Carmela pour tes corrections et nos discussions de couloir ou de bar. Merci Morphoptics et surtout merci petit micro-CT d'avoir bien voulu fonctionner jusqu'au bout, sans m'irradier, cher surfacique d'avoir tenu juste le temps de mes échantillons, Cintia la fidèle tablette d'avoir tenu plus longtemps que ses stylets.

Merci aux masters, doctorants et post-doctorants du 3ème et 4ème étage, Petite Morgane mon petit homonyme, « Raspoutitine » alias Justine, Adeline, Cédric, Margot, Paulo, Louis, Pierre, Gaëtan, Alice, Chris, Alexandrine, Agathe, Justine B., Robin, Maiwenn, Mégane, Giovanni, Mathilde, Thomas et tous ceux que j'oublie en écrivant ces lignes...

Mention spéciale à celles qui sont là depuis mon arrivée à Dijon et avec qui nous nous sommes relayés dans les bobos, Ophélie et Pauline ; ainsi qu'à celui qui prend soin de mon cher binôme et qui amène toujours de l'amour, Nicolas. Ma paulette, moi aussi je pourrais t'écrire des pages de remerciements. Toujours là depuis ce premier jour à Dijon, binôme un jour, binôme toujours. Avec notre karma nous allons bien finir dans un vieux bureau poussiéreux comme deux mames à nous plaindre des étudiants. Merci d'avoir toujours été là même si plusieurs larges kilomètres nous séparaient momentanément, pour ces soirées koh-lanta/riz au thon/bières. Tu vois moi aussi j'ai fini par finir !

Clémence et Thierry, comment vous oublier, on s'est suivi dans les conseils, asso et commissions en tout genre, nous avons même affronté le Forum des Jeunes Chercheurs ensemble, de tout coeur merci. Et biensûr Charles, nous nous sommes jetés dans la fosse de la Commission recherche ensemble et je n'aurais pu rêver meilleur binôme.

Je souhaite aussi remercier Aurélien, tu m'as accueilli dans ton bureau pour cette fin de thèse et pour encore quelques temps et a toujours été la voix de la sagesse. Promis j'essaye de faire survivre les plantes.

Merci aux étudiants, du meilleur au plus mauvais, de la L1 au master, j'espère vous en avoir autant enseigné que ce que vous m'avez appris.

Je ne peux écrire ces lignes sans avoir une pensée pour les petites bêtes sans lesquels j'aurais moins perdu le sommeil mais aussi sans lesquels les deux tiers de cette thèse seraient tombés à l'eau, aux soixante hamsters, quarante-deux gerbilles et quarante souris ; vous n'avez pas eu le choix de votre sacrifice mais vous m'avez tant apporté, tous mes remerciements et tout mon respect.

Merci aux amis proches, Méli et Clem, mes femmes, mes pétoncles, mes furieux, mon coeur. Sans vous j'aurais très sûrement craqué. On en aura fait des trajets Dijon-Paris-Fribourg-Lyon dans des ordres pas du tout optimaux pour voir nos frimousses mais aussi gérer nos joies et nos peines à coup de petits pots en poteries et de prouts sur les joues. Léo, mon grand frère dino, tu m'as toujours soutenu, tu es maintenant loin mais tu es toujours là, tu restes un pilier de ma vie et je ne remercierai jamais assez pour ça. Maxou, merci pour ces années de sacrifice, de distance, mais aussi

de rire, de soutien, de jeu avec des plateformes (malgré ton coaching j'y arrive vraiment pas mais je ne désespère pas), tu restes un ami cher et sans toi cette thèse n'aurait pas été possible, en aucun cas. Kevin et Oli, cœur sur vous, tant de soirées, de weekends, de péripéties de congrès, d'aventures en tout genre, merci à vous pour votre soutien et votre love.

Les papas paleux, je ne vous avais pas oublié ! Bastien merci pour ta confiance de la première heure, ça n'a pas toujours été facile mais tu as toujours cru en moi et je n'en serai pas là sans toi. Floréal, Choupinou, merci d'être toujours là même si je suis méchante mais qu'après tout je dessine pas trop les endocrânes chewing-gum et je ne sers pas trop mal les pintes. Je vous tire tous les deux mon chapeau messieurs, promis un jour on arrive à publier Barbie.

J'ai encore tant de monde à remercier, je vais donc passer aux copains ! Les parisiens : Paul(o), Lionel, Matthieu, Jeremy, Romain (Rominou), Justine. Les toulousains : Maxime (Kuku) et Alexis. Les dijonnais en général mais surtout : Renan, Manu, Johanna, Hugo, Romain (Mouillon), Laurent, Léopoldine (Léo), Nicolas (Dudu), Alicio, Julien, Emeric (Marty) et tous les autres.

Au meilleur des dijonnais, Ivan, tu as vu la fin et m'as soutenu sans faillir, j'espère te rendre la pareille bientôt. Nous avons encore tant d'aventures à vivre ensemble, le plus longtemps possible, avec tout mon amour et la boule de poil/saucisse roulante/écureuil volant Jack.

Ma famille, maman Sylvine, papa Max et papa François, G-P Philippe, Colette, on ne s'est pas beaucoup vu, vous m'avez inondé d'amour mais aussi laissé de l'air. Vous faites partie de mes premiers supporters et je ne vous remercierai jamais assez pour tout, puisque vous avez tout fait pour moi. Le chemin n'a largement pas été facile mais vous m'avez toujours porté et soulevé plus haut que je n'aurai jamais pu le faire moi-même. Vous m'avez donné le goût de la nature, de la science et de la curiosité, tout comme ceux qui sont partis avant cette thèse. Grand-père Raymond, Grands-mères Jeannine, Colette et Sylviane, Alice, sans vous je ne serai pas là non plus aujourd'hui. On dit « jamais deux sans trois », je serais donc la troisième en titre.

Cher lecteur, je sèche donc mes petits yeux et mon petit nez, dans lesquels il a plu comme il pleut sur la ville pendant la rédaction de ces ultimes lignes, te laisse à mon manuscrit et te remercie d'avance de ta lecture.



# Table of contents

Chapter 1 - Introduction.....	1
1.1 Generalities on the group.....	3
1.2 Craniofacial anatomy.....	4
1.2.1 Cranial anatomy.....	4
1.2.2 Mandibular anatomy.....	8
1.2.3 Tooth anatomy.....	9
1.2.4 Masticatory muscle anatomy.....	10
1.3 Tissue growth.....	11
1.3.1 Bone modeling and remodeling.....	11
1.3.2 Masseter muscle growth.....	12
1.3.3 Tooth growth.....	12
1.4 Objectives.....	13
Chapter 2 - Development and divergence of the mandible shape at a macroevolutionary scale.....	21
Chapter 3 - Ontogenetic changes and plasticity across Myomorpha: experimental design.....	43
3.1 Experimental design.....	44
3.2 Fluorochromes study.....	45
3.2.1 Material and methods.....	45
3.2.2 Why it probably did not work.....	48
3.2.3 If it had worked.....	49
3.3 Bone microstructure.....	49
3.4 Myosin study.....	50
3.4.1 Material and methods.....	50
3.4.2 Why it probably did not work.....	52
3.4.3 If it had worked.....	52
3.5 Acquisition of 3D models and landmarks.....	53

Chapter 4 - Postnatal development of the craniofacial complex.....	61
4.1 Functional constraints channel mandible shape ontogenies.....	62
4.2 Skull postnatal development.....	80
4.2.1 Material and methods.....	80
4.2.2 Results.....	80
4.2.3 Discussion.....	82
4.3 Covariation between the skull and the mandible.....	83
4.3.1 Material and methods.....	83
4.3.2 Results.....	83
4.3.3 Discussion.....	85
4.4 Conclusions.....	86
 Chapter 5 - Plasticity in postnatal development.....	 83
5.1 Material and methods.....	85
5.2 Results.....	86
5.3 Discussion.....	88
5.4 Conclusion.....	89
 Conclusions & Perspectives.....	 93
Conclusions.....	94
Perspectives.....	97
 Annexes.....	 103







## Chapter 1 - Introduction



Understanding developmental mechanisms in evolution is crucial to apprehend the diversification of organismal forms (Alberch 1980, Darwin 1859, Smith *et al.* 1985). In mammals, changes occur during all development phases (prenatal and postnatal). Postnatal growth plays an essential role in the acquisition of the adult shape. During this period, the craniofacial complex undergoes many changes in functional constraint forcing the different tissue to accommodate while adjusting, along the growth and at the adult stage, to a certain level of functional performance. These different developmental interactions respond to several influencing factors such as molecular, genetic and cellular processes but also the environment. The latter will play on these interactions, but in different ways between the prenatal and postnatal phases, as gestational environment and environment at birth are different.

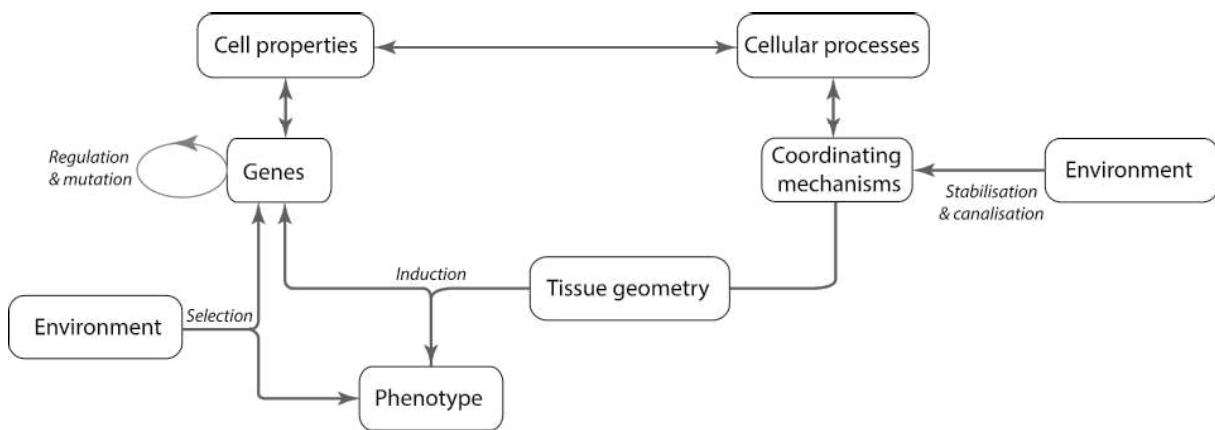


**Figure 1.1.** Schematic diagram of the feedback loop between genetic and epigenetic levels which characterize developmental processes (After Alberch 1991, Oster & Alberch 1982).

In this context, taking into account the existing diversity in mammals, variation in time and space of developmental processes within an anatomical context will influence the mapping from genotypes to phenotypes (Debat *et al.* 2001, Alberch, 1982, Salazar-Ciudad *et al.* 2003, Milocco *et al.* 2020, Hallgrímsson *et al.* 2014). Physical constraints undergone by organisms in development could be similar in a certain range of anatomical contexts, and would structure in a comparable way the phenotypic variation by influencing the spatialization of underlying developmental processes. These processes lead to discontinuities and directionalities in the space of shape (Alberch 1980, Gerber 2014, Salazar-Ciudad 2021). They induce biases in the phenotypic outcomes of random mutations (Alberch 1982, Halgrímsson *et al.* 2006, Uller *et al.* 2020) and therefore in the evolutionary trajectories (Kavanagh *et al.* 2013, Uller *et al.* 2018). During mammalian postnatal growth, major biomechanical changes, in response to change in diet (i.e. weaning) and behavior influence the spatialization of tissue modeling and remodeling (Zelditch *et al.* 2008, Zelditch & Swiderski 2011). Changes in muscle strain, tooth growth, development of sensory organs etc. led to convergences in the developmental processes imposing some directionality in the ontogenetic trajectories despite a diversified anatomical context. Consequently, these changes constrained the evolution of ontog-

enies and adult shape variation (Hallgrímsson & Hall 2011). These developmental biases result in some parallelism between developmental and evolutionary trajectories (Alberch *et al.* 1979, Gould 1977, Webster & Zelditch 2005). Still, early shape differentiation has a profound effect on the directionality and intensity of shape changes during ontogeny (Goswami *et al.* 2016, Conith *et al.* 2022). Developmental processes and their degree of freedom influence the phenotypic production, questioning the importance of evolution of the ontogenetic trajectories in shaping the diversity of organismal shapes.

For testing the interactions between the developing organism and its environment and their potential evolutionary consequences, Rodentia is a good example of broad diversity in all aspects and thus a study group of choice. It is a very diverse and disparate mammal order, in which changes can be observed on a large scale. The mandible and cranium present a wide variety of forms across this order. Rodents present also wide diversity in diets, behavior and ecology. In addition, it includes model organisms that can be easily reared in laboratory following a precise experimental configuration to test the effects of diverse sources of variation.

### 1.1 Generalities on the group

The order Rodentia is taxonomically very diverse, with over 2500 living species among 34 families (Fig. 1.2). All along this manuscript, the classification followed is that proposed by Wilson *et al.* 2016. Rodents form the richest order of mammals in terms of taxa. Indeed, 40% of known mammal species belong to the Rodentia (Lacher *et al.*, 2016). They occur in all continents and most oceanic islands, the most noticeable exception being Antarctica. Their size range is very wide, from 3g for the African pigmy mouse (*Nannomys*) to 60kg for the capybara (*Hydrochoerus hydrochaeris*). However, most species are small to medium in size (15g to 15 kg). The majority of rodents have a hairy body, some are fully or partially covered with spines. They have a wide range of ecologies, from arboreal to burrowing, from aquatic to desert, and are found in most environments throughout the world. This multitude of sizes and habitats implies the existence of very diverse diets (frugivorous, herbivorous, insectivorous, omnivorous, granivorous, etc., Nowak & Walker, 1999). This diversity is closely linked to the morphology of the masticatory apparatus (skull, mandible, muscles).

The first occurrence in the fossil record is described during the Paleocene (-60 to -55 Ma, Hartenberger 1998, Van Itterbeeck *et al.* 2007). Principal adaptive radiation of most of the modern families took place in the Paleocene/Eocene, these families were then well established in the Early Oligocene (Vianey-Liaud 1985).

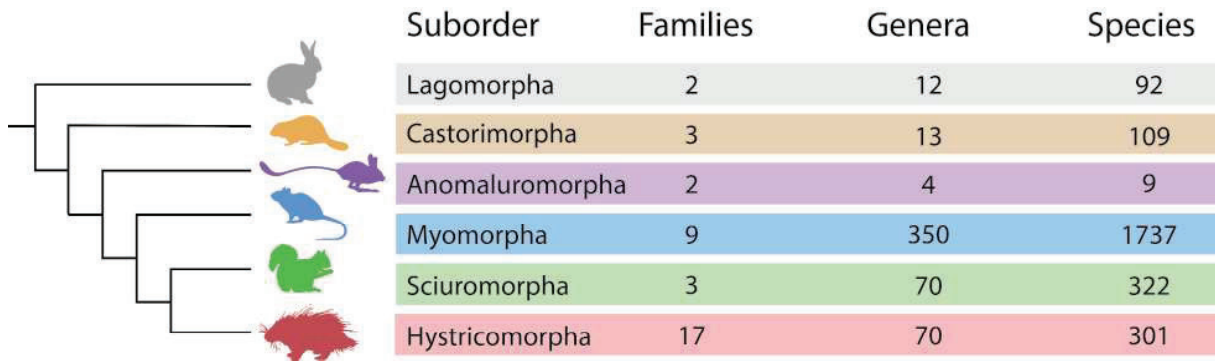


**Figure 1.2.** Number of families, genera and species per suborder in Rodentia. Lagomorpha are present as an outgroup.

## 1.2 Craniofacial anatomy

### 1.2.1 Cranial anatomy

**Lower view** (Fig. 1.3) - The skull of rodents is generally elongated and broad, with a laterally compressed anterior part. The nasals extend to the anterior part of the snout, spilling outwards through the nasal openings. The premaxillae extend across the median part of the rostrum. They inhabit the incisor alveolus, which extends a little further posteriorly in adult specimens, sometimes to the squamosal (*Hydrochaeris*). In inferior view, the palatine foramina are located at the contact of the premaxillae and maxillae, and form two large elongated slits. The maxillae extend posteriorly to the contact with the squamosal (*Hydrochaeris* and *Cavia*), but in most species end at the pterygoid. The palatine is most often with parallel lateral margins, but in some cases may be reduced anteriorly, with the rows of teeth converging forward (*Spalax* and *Myocastor*). The pterygoids are placed behind the palatine, and bear posteriorly projecting apophyses. They are fused early to the basisphenoid. The tympanic bulla is formed by a bony bulla pierced by the auditory meatus, exiting to the outside of the ear canal. The basioccipital, placed on the posterior part of the skull in inferior view, bears at each of its lateral ends the paraoccipital processes. The supraoccipital has occipital condyles on its lower part.

**Superior view** (Fig. 1.4) - The frontals are large, with a length of one quarter to one third of the total length of the skull. The parietals are positioned behind the frontals. The interparietal joins the parietals and supraoccipital and is sometimes absent in some burrowing rodents.

**Lateral view** (Fig. 1.5) - The zygomatic arch includes the maxilla, jugal and squamosal. In addition to containing the inner tips of the incisors, the maxilla supports the jugal teeth (molars and premolars). Its height therefore varies according to the structure of the roots. The maxilla has a strong zygomatic apophysis perforated by the infra-orbital foramen, which varies greatly in size depending on the species but can reach dimensions as large as the orbit. The jugal is positioned

laterally to the orbit but can also sometimes extend to its anterior part. The posterior end of the jugal is placed under the zygomatic process of the squamosal. The posterior part of the zygomatic arch consists of the squamosal.

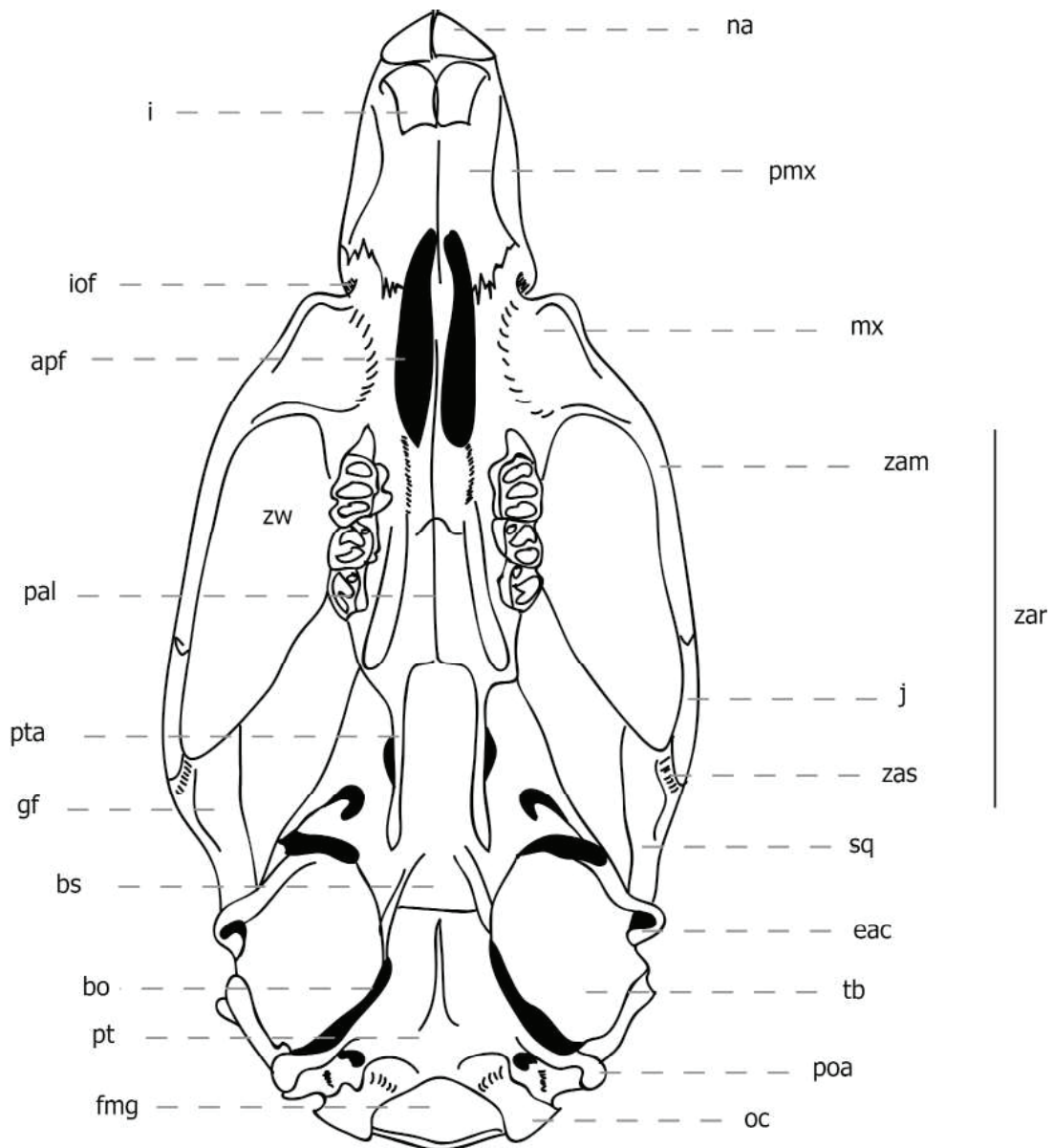


**Figure 1.3.** Cranial anatomy of rodents in inferior view (*Rattus rattus*). apf: anterior palatine foramen, bo: basioccipital, bs: basisphenoid, eac: external auditory canal, fmg: foramen magnum, gf: glenoid fossa, i: incisor, iof: infraorbital foramen, j: jugal, mx: maxilla, na: nasal, oc: occipital condyle, pal: palatine, pmx: premaxilla, poa: paraoccipital apophysis, pt: pterygoid, pta: pterygoid apophysis, sq: squamosal, tb: tympanic bulla, zam: zygomatic apophysis of the maxilla, zar: zygomatic arch, zas: zygomatic apophysis of the squamosal, zw: zygomatic window.

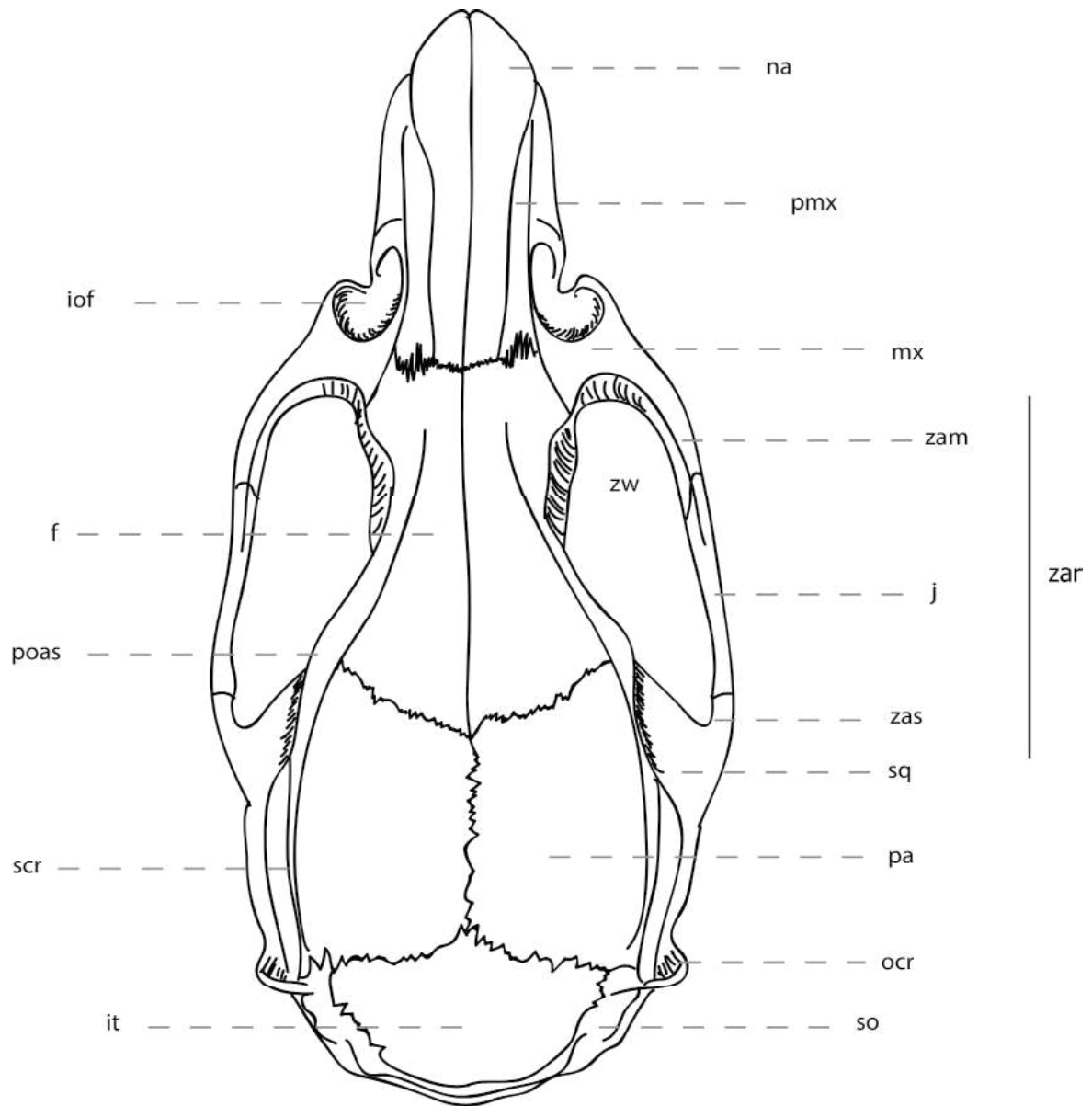


**Figure 1.4.** Cranial anatomy of rodents in superior view (*Rattus rattus*). f: frontal, iof: infra-orbital formaen, it: interparietal, j: jugal, mx: maxilla, na: nasal, ocr: occipital crest, pa: parietal, pmx: pre-maxilla, poas: post-orbital apophysis of the squamosal, scr: squamosal crest, so: supraoccipotal, sq: squamosal, zam: zygomatic apophysis of the maxilla, zar: zygomatic arch, zas: zygomatic apophysis of the squamosal, zw: zygomatic window.

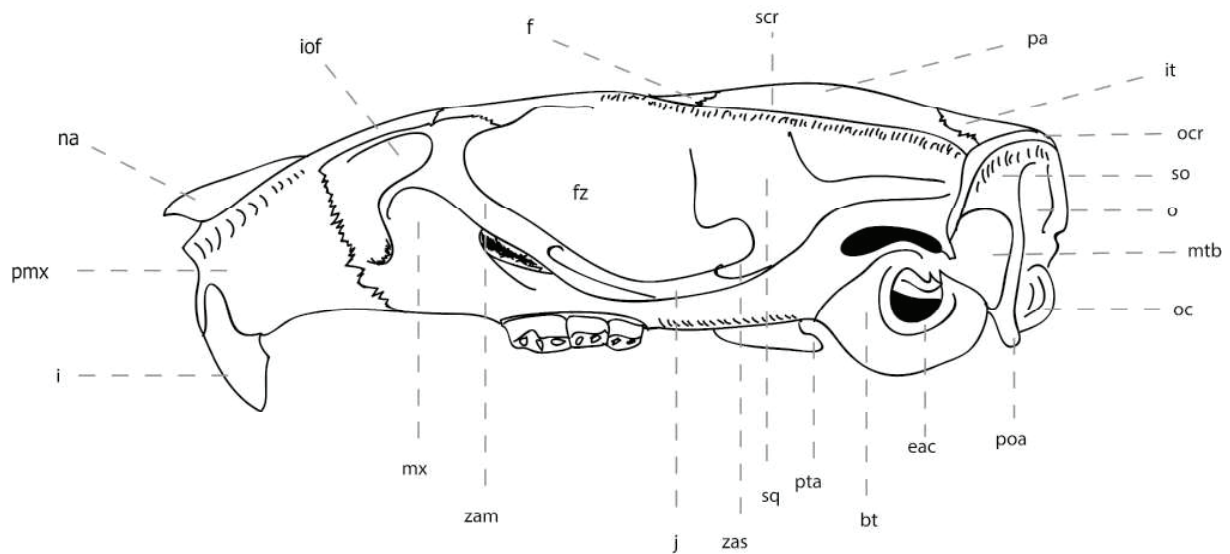


**Figure 1.5.** Cranial anatomy of rodents in lateral view (*Rattus rattus*). eac: external auditory canal, f: frontal, i: incisor, iof: infra-orbital foramen, it: interparietal, j: jugal, mtb: mastoid part of the tympanic bulla, mx: maxilla, na: nasal, o: occipital, oc: occipital condyle, ocr: occipital crest, pa: parietal, pmx: premaxilla, poa: paraoccipital apophysis, pta: pterygoid apophysis, zam: zygomatic apophysis of the maxilla, scr: squamosal crest, so: supraoccipital, sq: squamosal, tb: tympanic bulla, zam: zygomatic apophysis of the maxilla, zas: zygomatic apophysis of the squamosal, zw: zygomatic window.

1.2.2 Mandibular anatomy

The mandible is the bone under the skull with which it is articulated. It is composed of two hemimandibles, which are therefore two bones connected by their anterior part (Fig. 1.6). The size and shape of the various mandibular processes vary according to the size and placement of the muscles attached to them. The coronoid process can be very high for example in the genus *Ondatra* to completely absent in *Ctenodactylus* (Potapova 2020). Consequently the curvilinear length of the lunate notch will vary accordingly. The condylar process allows the mandibular articulation in the squamosal and is most often of large size. The angular process, placed posteroinferiorly on the mandible, is very variable in shape and length. The lower incisor and its alveolus extend over a large part of the mandible and may extend to the condylar process.

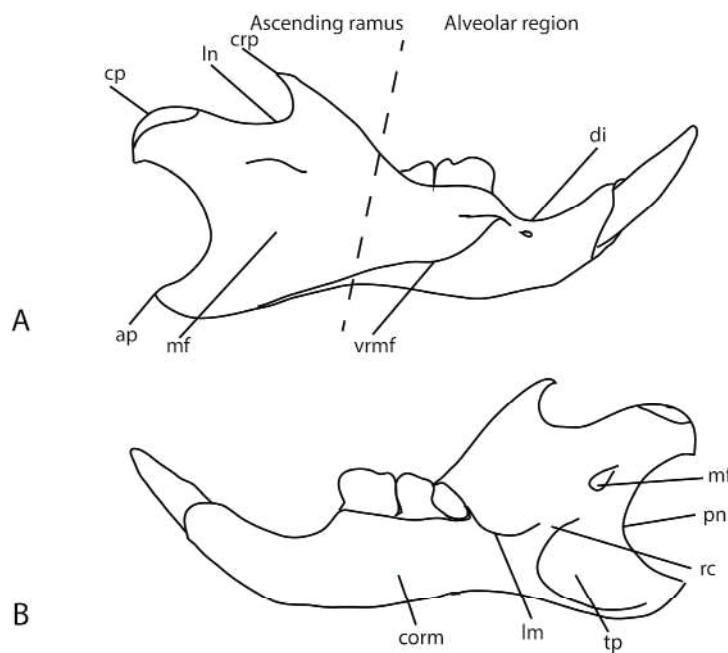


**Figure 1.6.** Mandibular anatomy in rodents in labial (A) and lingual view (B). ap: angular process, corm: mandibular corpus, cp: condylar process, crp: coronoid process, di: diastema, lm: line of the mylohyoid, ln: lunar notch, mf: masseter fossa, pn: posterior notch, rc: ramus crest, rf: ramus fossa, tp: tuberosity of the pterygoid, vrmf: ventral ridge of masseter fossa.

Tullberg used the structure of the mandible (Fig. 1.7) and the position of the masseters (infra-orbital structure, Fig. 1.8) to establish the systematics of rodents as early as 1899. Two main mandibular forms were then distinguished:

- **Hystricognaths**, which have a strong angular apophysis that is inwardly projecting, while their condyloid apophysis is outwardly directed.
- **Sciurognaths**, which, unlike hystricognaths, have an angular process directed outwards and a condyloid process directed inwards.

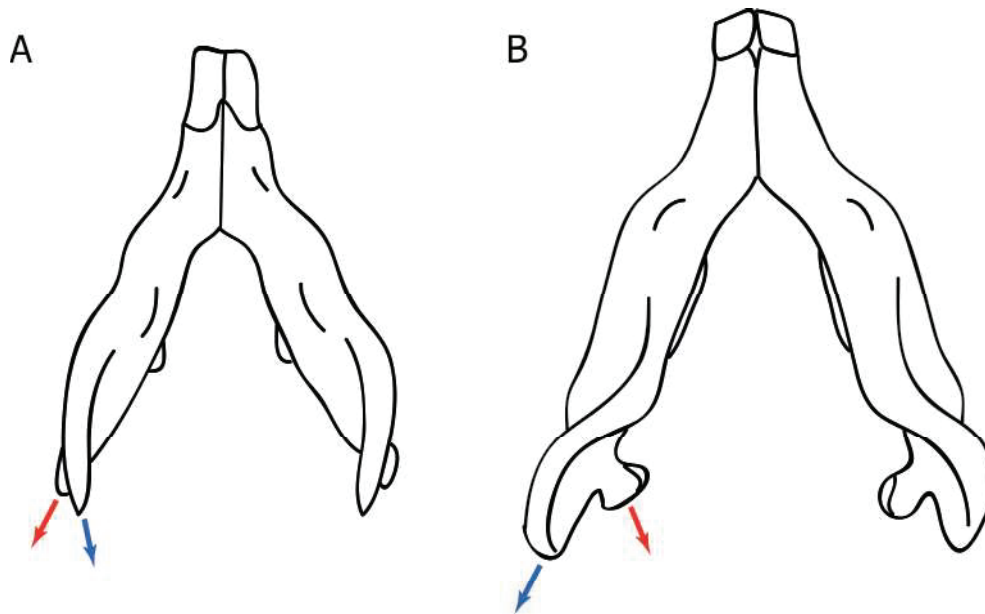


**Figure 1.7.** Mandibular structures in rodents (After Courant, 2000). A) Hystricognath. B) Sciurognath. Red arrow: orientation of the condylar process, blue arrow: orientation of the angular process.

### 1.2.3 Tooth anatomy

Rodents have continuously growing incisors with a reinforced enamel band on the anterior surface. The canines are absent, leaving large diastemas separating the incisors from the jugal teeth. This anatomy is directly related to the gnawing function of the incisors.

Rodents exhibit a high degree of dental diversity, based on tooth pattern and growth habit associated with crown height. There are two main dental formulae:  $I^1/1, C^0/0, P^0/0, M^3/3$  and  $I^1/1, C^0/0, P^2/2, M^3/3$  (Wilson *et al.*, 2016), in some species, only a fourth premolar persists in the dental row. The pattern on the occlusal surface varies, as does the number of cusps (Fig. 1.8). The four main types of tooth pattern for molars are: bunodont (*Mus*), lophodont (*Chinchilla*), lopho-bunodont (*Nectomys*), prismatic (*Lemmus*) and loxodont (*Hydrochoerus*).

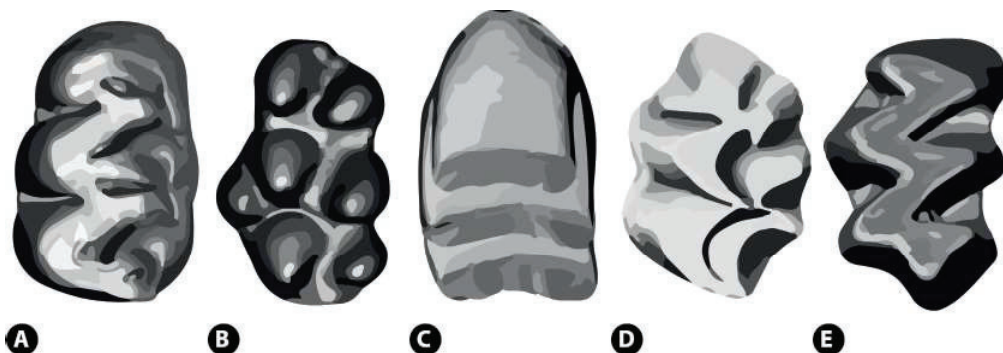


**Figure 1.8.** Patterns of tooth occlusal surface. A) lopho-bunodont. B) bunodont. C) lophodont D) lopho-bunodont. E) prismatic. (Modified from Lazzari *et al.* 2015).

### 1.2.4 *Masticatory muscle anatomy*

The morphology of the craniofacial complex varies according to the arrangement of the masticatory muscles of rodents. Three skeletal parts are closely related to the arrangement of this muscle complex (zygomasseteric complex): the infraorbital foramen, the zygomatic arch and the mandible.

The zygomasseteric complex is a complex of four muscles: the masseter, the temporalis, the pterygoid and the digastricus.

The masseter has two distinct parts: the lateral masseter and the medial masseter. The lateral masseter extends from the lower border of the zygomatic arch to the anterior part of the angular process. It is itself divided into two parts, one anterior and superficial, one posterior and deep. The medial masseter attaches to the medial side of the zygomatic arch or to the inner wall of the orbit. It also attaches to the mandibular bone above the insertion of the lateral masseter. It is divided into two parts, one anterior and one posterior.

The temporalis is smaller than the masseter. It inserts at the level of the squamosal on the occipital crest and in the interorbital region. Its main function is to ensure the closure of the jaw.

The pterygoid separates into an internal and an external branch. The medial branch is short and thick, it attaches to the pterygoid fossa (and sometimes to the orbit) and is inserted behind the medial side of the angular process of the mandible. The lateral is a small muscle extending from the pterygoid area to the medial side of the condylar process.

The digastricus extends from the paraoccipital process to the lower edge of the mandible. It allows the retraction and lowering of the mandible.

The infraorbital foramen allows the passage of the medial masseter muscle. The shape and size of this foramen is very variable. Depending on the different insertions of the muscles, four infraorbital structures can be found (Brandt 1855, Wood 1965, Fig. 1.9):

- **Protogomorph**, with a small to medium infraorbital foramen, a reduced masseter and a predominant temporalis.
- **Sciurormorph**, with a very small infraorbital foramen and a lateral masseter inserted in the anterior part of the orbital arch
- **Myomorph**, which is intermediate between the two previous types. The infra-orbital foramen is narrow at the base and widened in its upper part.
- **Hystricomorph**, with a highly developed, almost circular infraorbital foramen.

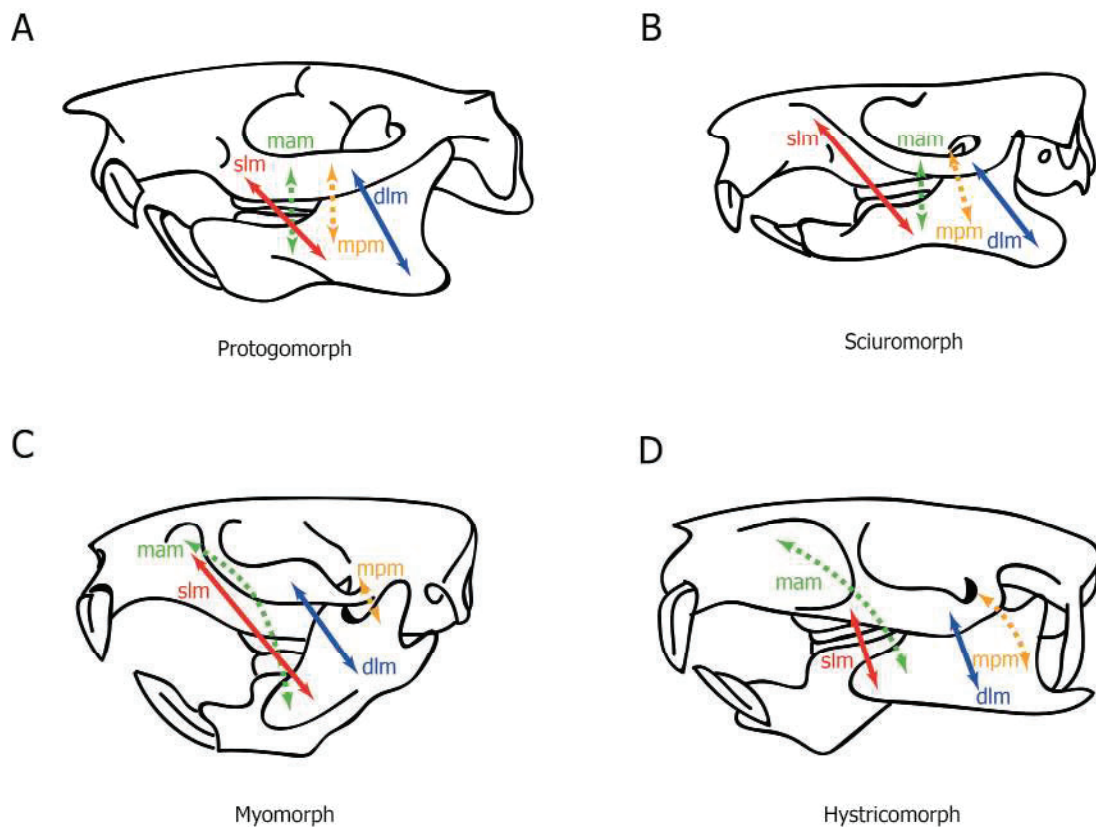


**Figure 1.9.** Infra-orbital structures in rodents (After Courant, 2000). A) protogomorph. B) sciurormorph. C) myomorph. D) hystricomorph. slm: superficial lateral masseter (red arrow); dlm: deep lateral masseter (blue arrow); mam: medial anterior masseter (green dotted arrow); mpm: medial posterior masseter (yellow dotted arrow).

### 1.3 Tissue growth

#### 1.3.1 Bone modeling and remodeling

During life and thus during growth, bone undergoes modeling and remodeling. Bone modeling is defined as the formation of bone by osteoblasts on a given surface (Allen & Burr 2014), while bone remodeling is the result of resorption of the bone synchronized with formation (by osteoblasts, Table 1.1). In this manuscript, I will talk about bone remodeling, as it treats of post-natal development and the majority of the primary bone is already present in the organism (Lee *et al.* 2017). Bone is a dynamic tissue (Zaidi 2007) that must maintain the stability and integrity of the organ (Proff & Römer 2008). Bone remodeling is an active process by which the bone can change in shape, size and microstructure in response to physiologic influences and mechanical strains maintaining strength and mineral homeostasis (Katsimbri 2017). This process relies on the balance between bone resorption and deposition. These two functions must be coupled in time and space to ensure the stability of bone mass (Rucci 2008). Bone resorption is performed by osteoclasts, some large multicellular cells (Teitelbaum & Ross 2003). Bone deposition is made by osteoblasts,

which are specialized bone-forming cells. They produce bone by synthesis and secretion of type I collagen (Katsimbri 2017). Bone strength, size and shape depends on various factors as bone mass, geometry and microstructure that varies during life. During this thesis, the molecular aspects of this process will not be discussed. However, it is an important factor to keep in mind as these mechanisms are directly involved in shape changes during growth.

	<b>Modeling</b>	<b>Remodeling</b>
<b>Goal</b>	Shape bone, increase bone mass	Renew bone
<b>Cells</b>	Osteoclasts or osteoblasts and precursors	Osteoclasts, osteoblasts and precursors
<b>Bone envelope</b>	Periosteal, endocortical, trabecular	Periosteal, endocortical, trabecular, intracortical
<b>Mechanism</b>	Activation-formation or activation-resorption	Activation – resorption – formation
<b>Timing</b>	Primarily childhood but continues throughout life	Throughout life
<b>Net effect on bone Mass</b>	Increase	Maintain and slight decrease

**Table 1.1.** Characteristics of modeling and remodeling in bone (After Allen & Burr 2014).

### 1.3.2 *Masseter muscle growth*

The muscle fiber is produced from myoblasts, which are stem cells that differentiate into myotubes and then into muscle fibers, made of myosin and actin. During the development of the masseter muscle, the differentiation of myoblasts occurs the most actively between the 13<sup>th</sup> embryonic day and birth for mice. The activation of muscles fibers in mouse, begins at the 15<sup>th</sup> embryonic day and continue after weaning (Yamane *et al.* 2000, Yamane 2005, Saito *et al.* 2004). Around weaning, the membrane proteins responsible of muscle fibers synthesis are progressively eliminated (Saito *et al.* 2002, Yamane *et al.* 2004, Yamane 2005).

### 1.3.3 *Tooth growth*

Growth can be continuous or finite, so molars can be brachydont, mesodont, hypsodont to hypselodont (Lazzari *et al.* 2015, Fig. 1.10). The growth of these teeth mechanically constrains the growth of other tissues as it implies a different volume occupied by the teeth in the mandible and skull. This is why this factor is important to consider during growth and certainly plays a role in bone remodeling. It is therefore integrated into this work, particularly in Chapter 2.

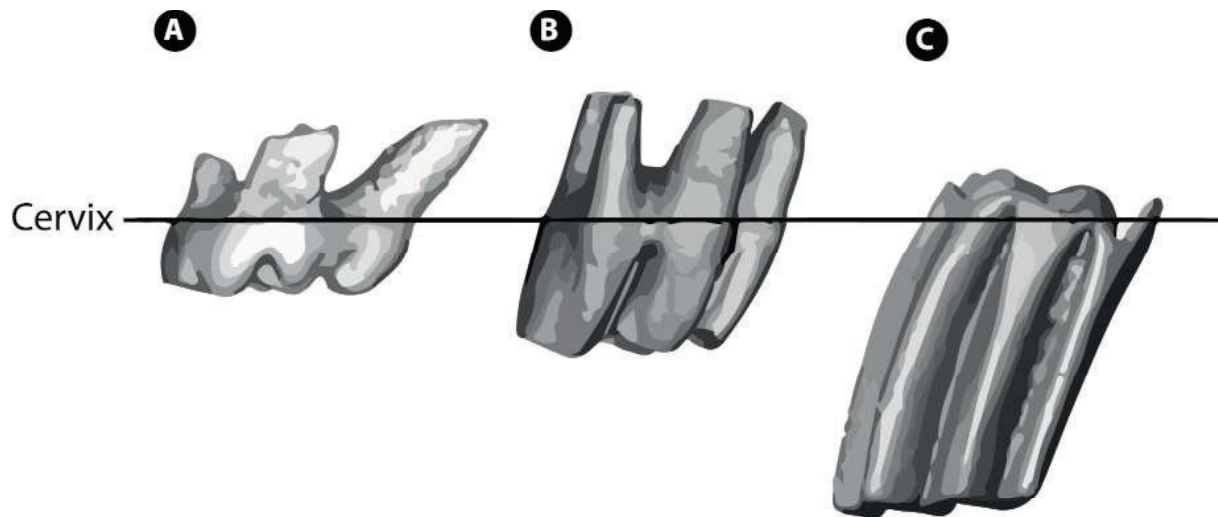


**Figure 1.10.** Hypsodonty index. A) brachyodont. B) mesodont. C) hypsodont. (Modified from Lazzari *et al.* 2015).

#### 1.4 Objectives

The skull is a highly integrated structure, architecturally complex, as it is composed of many skeletal elements, and functionally, as it is involved in various tasks essential to the organism. At the same time, and somewhat paradoxically, this unit is highly evolvable and presents a great diversity of forms. The basis of craniofacial shape variation and its control are as much, related to the additive effects of genes as to their epigenetic and context-specific interactions during development. In this manuscript, epigenetics is defined by the “Sum of the genetic and nongenetic factors acting upon cells to control selectively the gene expression that produces development and evolution” (Hallgrimson & Hall 2011). These epigenetic interactions during growth will respond to mechanical and other stimuli between the ossification centers, the tissues and organs making up the head. In particular, these interactions control the spatialization and intensity of bone remodeling in response to other tissues strain. They will thus compensate and coordinate the growth of the different tissues and organs in order to acquire and/or maintain certain functions, such as the occlusion between the upper and lower jaws. These epigenetic interactions are thus essential to the normal development of the skeleton in general and the skull in particular. By responding to changes in forces and movements, they will be a potential driver of microevolutionary changes (and thus macroevolutionary changes) at the morphological level favoring adaptive directions of variation and generating new functional covariations between traits. Despite this central role, the importance of these interactions in the expression of inter-specific differences and in the longer term in the dynamics of clades remains poorly understood. Analysis of the tempo of adult disparity acquisition during ontogeny is a key element in understanding the differential filling of the shape space by clades. The level of disparity within a clade generally appears to be already present in the young and the evolution of ontogenetic trajectories would little affect this level of disparity. The early

postnatal stages would therefore appear to be more flexible than the late stages, which are subject to greater functional constraints. Thus, in sciuridae, a relatively conservative clade, the disparity in mandibular shape seems to be generated prenatally and maintained by compensation for ontogenetic variation (Zelditch *et al.* 2016). On the other hand, rodents as a very diversified group in term of species, dental types, muscles architectures, diet, ecologies etc... is likely to present an increase in mandibular and cranial disparity between juvenile and adult changes, it is therefore crucial to pay attention to ontogenetic changes. These changes appear to be concomitant with tooth eruption and the acquisition of mastication; radically different between clades. A disparity established prenatally would suggest a secondary, compensatory role for epigenetic processes during growth. On the contrary, the post-weaning establishment of inter-specific differences would imply a central role for epigenetic processes in the expression of specific and potentially the integration within the variation of the craniofacial complex of ecological and behavioral differences between taxa.

To begin this manuscript (Fig 1.11), I will take a broad view to obtain a macroevolutionary picture of postnatal mandibular development in rodents, in order to map general growth patterns between and within clades (Chapter 2). Subsequently, I will focus on the different developmental processes undergone by the craniofacial complex, this time on a finer taxonomic and temporal scale. For this purpose, I will describe the different experimental techniques envisaged and implemented (Chapter 3). Postnatal development will then be described in three model species (Chapter 4). Finally, in these three species, the role of mechanical constraints during growth will be questioned using variations in diet (Chapter 5).

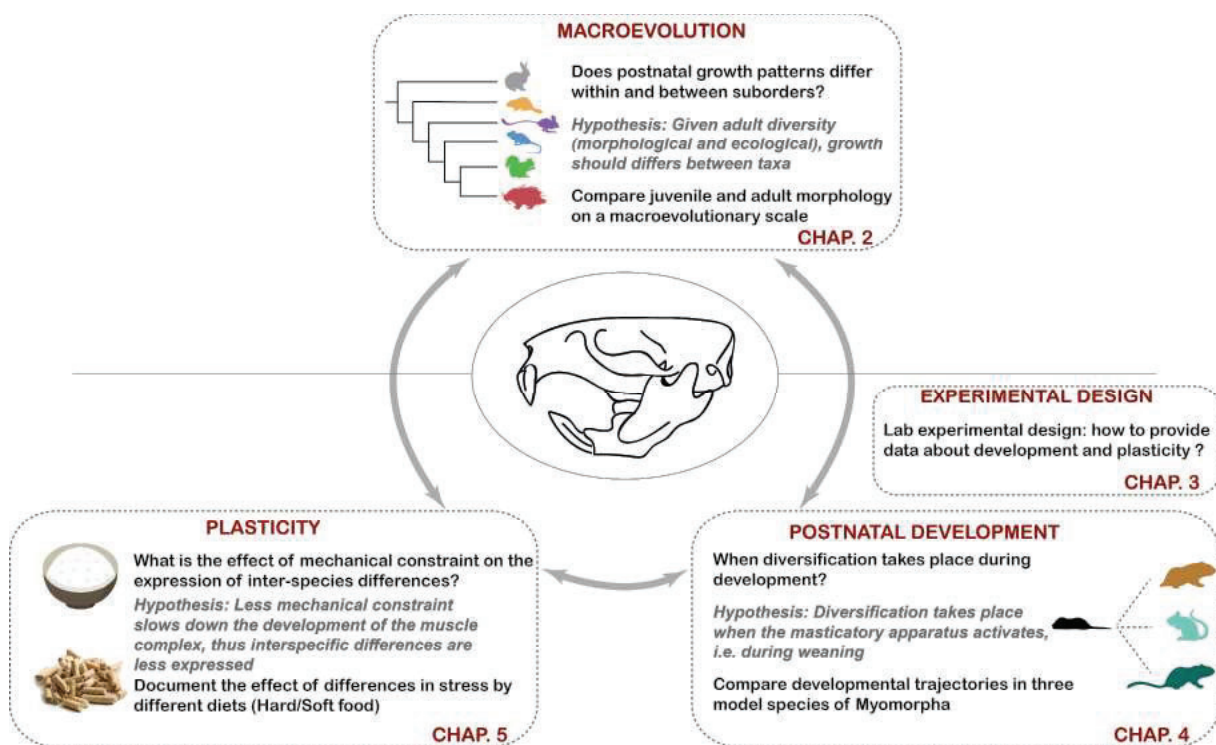


Figure 1.11. Diagram representing the plan followed throughout this manuscript.

References

- ALBERCH, P. Ontogenesis and morphological diversification. *American zoologist*, 1980, vol. 20, no 4, p. 653-667.
- ALBERCH, P. Developmental constraints in evolutionary processes. In : *Evolution and development*. Springer, Berlin, Heidelberg, 1982. p. 313-332.
- ALBERCH, P. From genes to phenotype: dynamical systems and evolvability. *Genetica*, 1991, vol. 84, no 1, p. 5-11.
- ALBERCH, P., GOULD, S. J., OSTER, G. F., and WAKE, D. B. Size and shape in ontogeny and phylogeny. *Paleobiology*, 1979, vol. 5, no 3, p. 296-317.
- ALLEN, M. R., and BURR, D. B. Bone modeling and remodeling. In : *Basic and applied bone biology*. Academic Press, 2014. p. 75-90.
- BRANDT, J. F. *Beiträge zur nähern Kenntniss der Säugethiere Russland's*. Kaiserl. Academ. d. Wiss., 1855.
- CONITH, A. J., MEAGHER, M. A., and DUMONT, E. R. The influence of divergent reproductive strategies in shaping modularity and morphological evolution in mammalian jaws. *Journal of Evolutionary Biology*, 2022, vol. 35, no 1, p. 164-179.
- COURANT, F. *Approches morphométrique et cladistique de la diversité et de la disparité dans l'ordre des rongeurs*. 2000. PhD thesis. Dijon.
- DARWIN, C. *The origin of species by means of natural selection*. EA Weeks, 1859.
- DEBAT, V., and DAVID, P. Mapping phenotypes: canalization, plasticity and developmental stability. *Trends in ecology & evolution*, 2001, vol. 16, no 10, p. 555-561.
- GERBER, S. Not all roads can be taken: development induces anisotropic accessibility in morphospace. *Evolution & Development*, 2014, vol. 16, no 6, p. 373-381.
- GOSWAMI, A., RANDAU, M., POLLY, P. D., WEISBECKER, V., BENNET, C. V., HAUTIER, L., SANCHEZ-VILLAGRA, M. R. Do developmental constraints and high integration limit the evolution of the marsupial oral apparatus?. *Integrative and comparative biology*, 2016, vol. 56, no 3, p. 404-415.
- GOULD, S. J. *Ontogeny and Phylogeny*. Harvard University Press, 1977.
- HALLGRÍMSSON, B., and HALL, B. K. (ed.). *Epigenetics: linking genotype and phenotype in development and evolution*. University of California Press, 2011.

- HALLGRÍMSSON, B., BROWN, J. JY., FORD-HUTCHINSON, A. F., SHEETS, D. H., ZELDTCH, L. M., and JIRIK, F. R. The brachymorph mouse and the developmental-genetic basis for canalization and morphological integration. *Evolution & development*, 2006, vol. 8, no 1, p. 61-73.
- HALLGRIMSSON, B., MIO, W., MARCUCIO, R. S., and SPRITZ, R. Let's face it—complex traits are just not that simple. *PLoS genetics*, 2014, vol. 10, no 11, p. e1004724.
- HARTENBERGER, J.-L. Description de la radiation des Rodentia (Mammalia) du Paléocène supérieur au Miocène; incidences phylogénétiques. *Comptes Rendus de l'Académie des Sciences-Series IIA-Earth and Planetary Science*, 1998, vol. 326, no 6, p. 439-444.
- KATSIMBRI, P. The biology of normal bone remodelling. *European journal of cancer care*, 2017, vol. 26, no 6, p. e12740.
- KAVANAGH, K. D., SHOVAL, O., WINSLOW, B. B., ALON, U., LEARY, B. P., KAN, A., and TABIN, C. J. Developmental bias in the evolution of phalanges. *Proceedings of the National Academy of Sciences*, 2013, vol. 110, no 45, p. 18190-18195.
- LACHER, T. E., MITTERMEIER, R. A., and WILSON, E (ed.). *Handbook of the mammals of the world: vol. 6: lagomorphs and rodents I*. Lynx editons, 2016.
- LAZZARI, V., GUY, F., SALAIS, P.-E., EURIAT, A., CHARLES, C., VIRIOT, L., TAFFOREAU, P, and MICHAUX, J. Convergent evolution of molar topography in Muroidea (Rodentia, Mammalia): connections between chewing movements and crown morphology. *Evolution of the rodents: advances in phylogeny, functional morphology and development*, 2015, p. 448-477.
- LEE, C., RICHTSMEIER, J. T., and KRAFT, R. H. A computational analysis of bone formation in the cranial vault using a coupled reaction–diffusion-strain model. *Journal of mechanics in medicine and biology*, 2017, vol. 17, no 04, p. 1750073.
- MILOCCO, L., and SALAZAR-CIUDAD, I. Is evolution predictable? Quantitative genetics under complex genotype-phenotype maps. *Evolution*, 2020, vol. 74, no 2, p. 230-244.
- NOWAK, R. M. et WALKER, E. P. *Walker's Mammals of the World*. JHU press, 1999.
- OSTER, G., and ALBERCH, P. Evolution and bifurcation of developmental programs. *Evolution*, 1982, p. 444-459.
- POTAPOVA, E. G. Morphofunctional transformations of the jaw muscles in rodent evolution. *Biology Bulletin Reviews*, 2020, vol. 10, no 5, p. 394-406.
- PROFF, P., and RÖMER, P. The molecular mechanism behind bone remodelling: a review. *Clinical oral investigations*, 2009, vol. 13, no 4, p. 355-362.

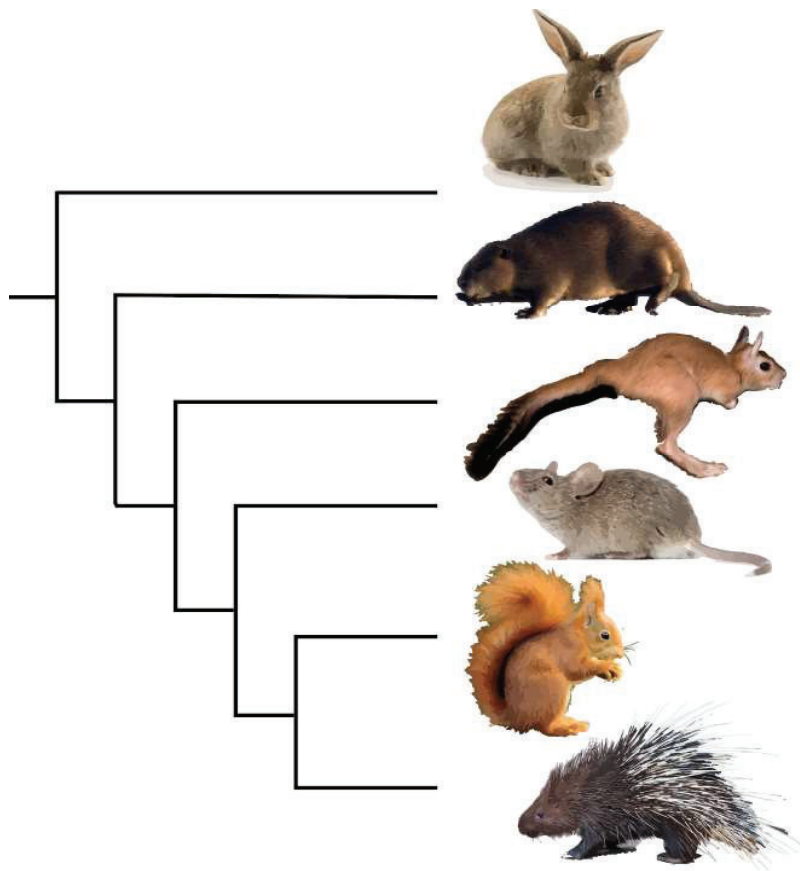
- RUCCI, N. Molecular biology of bone remodelling. *Clinical cases in mineral and bone metabolism*, 2008, vol. 5, no 1, p. 49.
- SAITO, T., FUKUI, K., AKUTSU, S., NAKAGAWA, Y., ISHIBASHI, K., NAGAT, J., Shuler, C. F., and Yamane, A. Effects of diet consistency on the expression of insulin-like growth factors (IGFs), IGF receptors and IGF binding proteins during the development of rat masseter muscle soon after weaning. *Archives of Oral Biology*, 2004, vol. 49, no 10, p. 777-782.
- SAITO, T., OHNUKI, Y., YAMANE, A., and SAEKI, Y. Effects of diet consistency on the myosin heavy chain mRNAs of rat masseter muscle during postnatal development. *Archives of Oral Biology*, 2002, vol. 47, no 2, p. 109-115.
- SALAZAR-CIUDAD, I. Why call it developmental bias when it is just development?. *Biology Direct*, 2021, vol. 16, p. 1-13.
- SALAZAR-CIUDAD, I., JERNVALL, J., and NEWMAN, S. A. Mechanisms of pattern formation in development and evolution. 2003.
- SMITH, J. M., BURIAN, R., KAUFFMAN, S., ALBERCH, P., CAMPBELL, J., GOODWIN, B., LANDE, R., RAUPE, D., and WOLPERT, L. Developmental constraints and evolution: a perspective from the Mountain Lake conference on development and evolution. *The Quarterly Review of Biology*, 1985, vol. 60, no 3, p. 265-287.
- TEITELBAUM, S. L. and ROSS, F. P. Genetic regulation of osteoclast development and function. *Nature Reviews Genetics*, 2003, vol. 4, no 8, p. 638-649.
- TULLBERG, T. *Ueber das System der Nagethiere: eine phylogenetische Studie*. Akademische Buchdruckerei, 1899.
- ULLER, T., FEINER, N., RADERSMA, R., JACKSON, I. S. C., and RAGO, A. Developmental plasticity and evolutionary explanations. *Evolution & Development*, 2020, vol. 22, no 1-2, p. 47-55.
- ULLER, T., MOCZEK, A. P., WATSON, R. A., BRAKEFIELD, P. M., and LALAND, K. N. Developmental bias and evolution: A regulatory network perspective. *Genetics*, 2018, vol. 209, no 4, p. 949-966.
- VAN ITTERBEECK, J., MISSIAEN, P., FOLIE, A., MARKEVICH, V. S., VAN DAMME, D., GUO, D.-Y., and SMITH, T. Woodland in a fluvio-lacustrine environment on the dry Mongolian Plateau during the late Paleocene: Evidence from the mammal bearing Subeng section (Inner Mongolia, PR China). *Palaeogeography, Palaeoclimatology, Palaeoecology*, 2007, vol. 243, no 1-2, p. 55-78.

- VIANEY-LIAUD, Monique. Possible evolutionary relationships among Eocene and lower Oligocene rodents of Asia, Europe and North America. In : *Evolutionary relationships among rodents*. Springer, Boston, MA, 1985. p. 277-309.
- WEBSTER, M., and ZELDITCH, M. L. Evolutionary modifications of ontogeny: heterochrony and beyond. *Paleobiology*, 2005, vol. 31, no 3, p. 354-372.
- WOOD, A. E. Grades and clades among rodents. *Evolution*, 1965, p. 115-130.
- YAMANE, A. Embryonic and postnatal development of masticatory and tongue muscles. *Cell and tissue research*, 2005, vol. 322, no 2, p. 183-189.
- YAMANE, A., MAYO, M., SHULER, C., CROWE, D., OHNUKI, Y., DALRYMPLE, K., and SAEKI, K. Expression of myogenic regulatory factors during the development of mouse tongue striated muscle. *Archives of oral biology*, 2000, vol. 45, no 1, p. 71-78.
- YAMANE, A, URUSHIYAMA, T., and DIEKWISCH, T. G. H. Roles of insulin-like growth factors and their binding proteins in the differentiation of mouse tongue myoblasts. *International Journal of Developmental Biology*, 2004, vol. 46, no 6, p. 807-816.
- ZAIDI, M. Skeletal remodeling in health and disease. *Nature medicine*, 2007, vol. 13, no 7, p. 791-801.
- ZELDITCH, M. L., CALAMARI, Z. T., and SWIDERSKI, D. L. Disparate postnatal ontogenies do not add to the shape disparity of infants. *Evolutionary Biology*, 2016, vol. 43, no 2, p. 188-207.
- ZELDITCH, M. L. and SWIDERSKI, D. L. Epigenetic interactions: the developmental route to functional integration. *Epigenetics: linking genotype and phenotype in development and evolution*, 2011, p. 290-316.
- ZELDITCH, M. L., WOOD, A. R., BONETT, R. M., and SWIDERSKI, D. L. Modularity of the rodent mandible: integrating bones, muscles, and teeth. *Evolution & development*, 2008, vol. 10, no 6, p. 756-768.





## Chapter 2 - Development and divergence of the mandible shape at a macroevolutionary scale



Rodents represent a very diverse order and therefore harbour a multitude of different morphologies and life history traits. This mammalian order is therefore a very good playground for studying macroevolutionary divergence. Many studies deal with morphological diversity by taking into account only adult specimens (Hautier *et al.* 2012, Wilson, 2013, Zelditch *et al.* 2015). The starting point of this axis is to compare postnatal developmental trajectories in a larger number of taxa, in order to reveal patterns of growth at a macroevolutionary scale. I therefore sought to collect both adult and juvenile (pre-weaning) specimens in order to compare the disparity at these two stages to observe developmental dynamics on a large scale.

Two strategies were available to me. The first would have been to restrict the sampling to a suborder and sample a large number of individuals per species. This strategy implies sampling more stages per species, in terms of age (adding subadults, adults, ageing adults), allometry, and more individuals per stage in order to establish more accurate trajectories. It could have been applied to the Myomorpha, as the individuals are numerous in collections because they come from trapping and breeding. The other strategy is the one I have chosen, i.e. to try to cover as much of the rodent phylogenetic tree as possible by sampling more species but fewer individuals per taxon. By taking this approach, it is possible to cover a greater diversity of life history traits. To provide information on morphological changes occurring between birth and adulthood, juvenile stage was taken as youngest as possible to make sure to be before weaning. In the same time, it ensures the covering of an important portion of postnatal development. As weaning is both dietary and behavioral, it is spread out in different ways in different species, so it is important to cover as much of the development as possible. The main difficulty of this approach is to find juvenile specimens in good condition. Indeed, many collection specimens are either already sub-adult, too fragile or deteriorated (due to incomplete ossification at a young age). Due to the difficulty of obtaining juvenile specimens in good condition, it was not possible to include Castorimorpha and Anomalomorpha in this study. The same applies to Sciuromorpha, for which only two species could be sampled, but these allow us to compare our results with those of Zelditch *et al.* (2016), whose study focused on Sciuridae. A lagomorph, *Oryctolagus cuniculus*, was used to root the phylogenetic tree of the sampled species (Fig. 2.1).

Classically, life history traits taken into account in morphological studies are locomotion (Hautier *et al.* 2012, Munoz 2021, Samuels & Van Valkenburgh 2008), habitat (Camargo *et al.* 2019, Duraõ *et al.* 2019) and more specifically for studies concerning the craniofacial complex, diet (Hautier *et al.* 2012, Samuels 2009). This seems logical given the importance of the diet, since the cranium and mandible must allow the animal to eat. However, it seemed appropriate to me, when dealing with the development of the adult form of these bones, to take into account factors inherent to growth itself. In other words, I wished to assess the traits surrounding the first stages of life, and more specifically to test the impact of gestation duration, weaning age and number of litters per year for each species. Indeed, these factors are usually considered in single species studies (behavioral and immunity studies, Wolff & Sherman 2008) but rarely in broad taxonomic studies.

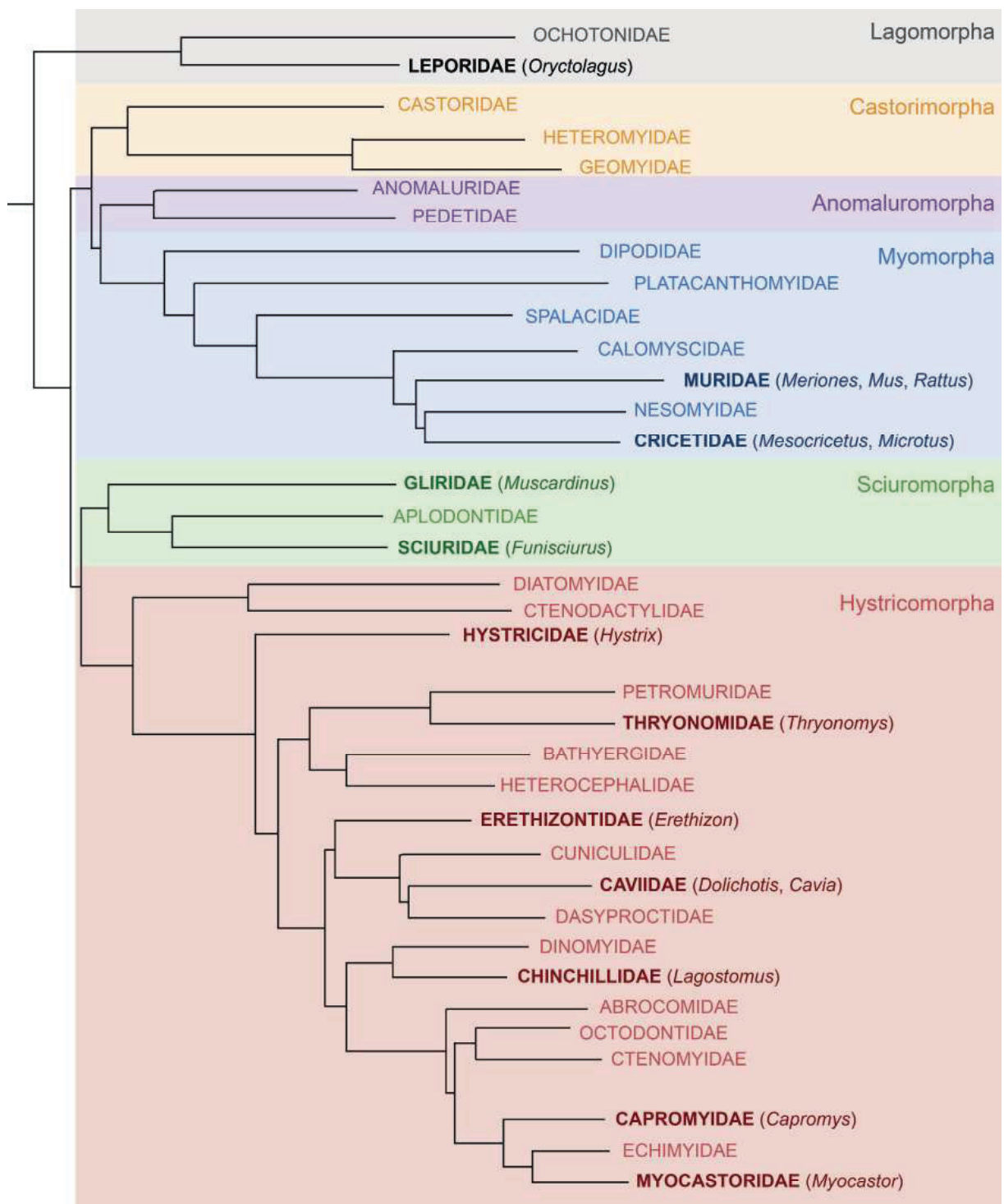


**Figure 2.1.** Phylogeny of rodents (After Lacher *et al.* 2016). Sampled families are shown in dark, corresponding genera are added in brackets.

References

- CAMARGO, N. F., MACHADO, L. F., MENDONÇA, A. F., and VIEIRA, A. M. Cranial shape predicts arboreal activity of Sigmodontinae rodents. *Journal of Zoology*, 2019, vol. 308, no 2, p. 128-138.
- DURÃO, A. F., VENTURA, J., and MUÑOZ-MUÑOZ, F. Comparative post-weaning ontogeny of the mandible in fossorial and semi-aquatic water voles. *Mammalian Biology*, 2019, vol. 97, no 1, p. 95-103.
- HAUTIER, L., LEBRUN, R., and COX, P. G. Patterns of covariation in the masticatory apparatus of hystricognathous rodents: implications for evolution and diversification. *Journal of Morphology*, 2012, vol. 273, no 12, p. 1319-1337.
- LACHER, T. E., MITTERMEIER, R. A., and WILSON, D. E. Handbook of the mammals of the world: vol. 6: lagomorphs and rodents I. 2016.
- MUÑOZ, N. A. Locomotion in rodents and small carnivorans: Are they so different?. *Journal of Mammalian Evolution*, 2021, vol. 28, no 1, p. 87-98.
- SAMUELS, J. X. Cranial morphology and dietary habits of rodents. *Zoological Journal of the Linnean Society*, 2009, vol. 156, no 4, p. 864-888.
- SAMUELS, J. X. and VAN VALKENBURGH, B. Skeletal indicators of locomotor adaptations in living and extinct rodents. *Journal of morphology*, 2008, vol. 269, no 11, p. 1387-1411
- WILSON, L. AB. Allometric disparity in rodent evolution. *Ecology and Evolution*, 2013, vol. 3, no 4, p. 971-984.
- WOLFF, J. O. and SHERMAN, P. W. (Ed.). *Rodent societies: an ecological and evolutionary perspective*. University of Chicago Press, 2008.
- ZELDITCH, M. L., CALAMARI, Z. T., and SWIDERSKI, D. L. Disparate postnatal ontogenies do not add to the shape disparity of infants. *Evolutionary Biology*, 2016, vol. 43, no 2, p. 188-207.
- ZELDITCH, M. L., LI, J., TRAN, L. AP, and SWIDERSKI, D. L.. Relationships of diversity, disparity, and their evolutionary rates in squirrels (Sciuridae). *Evolution*, 2015, vol. 69, no 5, p. 1284-1300.

Received: 8 January 2021 | Revised: 17 August 2021 | Accepted: 19 August 2021

DOI: 10.1111/jeb.13920

RESEARCH PAPER

JOURNAL OF Evolutionary Biology  WILEY

# Commonalities and evolutionary divergences of mandible shape ontogenies in rodents

Morgane Dubied<sup>1</sup>  | Sophie Montuire<sup>1,2</sup>  | Nicolas Navarro<sup>1,2</sup> <sup>1</sup>Biogeosciences, UMR 6282 CNRS, EPHE, Université Bourgogne Franche-Comté, Dijon, France<sup>2</sup>EPHE, PSL University, Paris, France**Correspondence**Nicolas Navarro, Biogeosciences, UMR 6282 CNRS, EPHE, Université Bourgogne Franche-Comté, Gabriel, Dijon.  
Email: nicolas.navarro@u-bourgogne.fr**Funding information**

EPHE, Grant/Award Number: AP EPHE 2019

**Abstract**

In mammals, significant changes take place during postnatal growth, linked to changes in diet (from sucking to gnawing). During this period, mandible development is highly interconnected with muscle growth and the epigenetic interactions between muscle and bone control the spatialization of bone formation and remodelling in response to biomechanical strain. This mechanism contributes to postnatal developmental plasticity and may have influenced the course of evolutionary divergences between species and clades. We sought to model postnatal changes at a macroevolutionary scale by analysing ontogenetic trajectories of mandible shape across 16 species belonging mainly to two suborders of Rodents, Myomorpha and Hystricomorpha, which differ in muscle attachments, tooth growth and life-history traits. Myomorpha species present a much stronger magnitude of changes over a shorter growth period. Among Hystricomorpha, part of the observed adult shape is set up prenatally, and most postnatal trajectories are genus-specific, which agrees with nonlinear developmental trajectories over longer gestational periods. Beside divergence at large scale, we find some collinearities between evolutionary and developmental trajectories. A common developmental trend was also observed, leading to enlargement of the masseter fossa during postnatal growth. The tooth growth, especially hypselodonty, seems to be a major driver of divergences of postnatal trajectories. These muscle- and tooth-related effects on postnatal trajectories suggest opportunities for developmental plasticity in the evolution of the mandible shape, opportunities that may have differed across Rodent clades.

**KEYWORDS**

geometric morphometrics, macroevolution, mandible shape, postnatal growth, rodents

## 1 | INTRODUCTION

Understanding developmental mechanisms in evolution is crucial to apprehend the diversification of organismal forms (Alberch, 1980; Darwin, 1859; Smith et al., 1985). It is well recognized nowadays that these mechanisms lead to discontinuities and directionalities in the space of shapes (Alberch, 1980; Gerber, 2014; Salazar-Ciudad,

2021). Indeed, they induce biases in the phenotypic outcomes of random mutations (Alberch, 1982; Hallgrímsson et al., 2006; Uller et al., 2020) and therefore in the evolutionary trajectories (Kavanagh et al., 2013; Uller et al., 2018). The existence of such developmental bias results in some parallelism between developmental and evolutionary trajectories (Alberch et al., 1979; Gould, 1977; Webster & Zelditch, 2005). Despite the abundant theoretical literature about

Data deposited at Dryad: <https://doi.org/10.5061/dryad.70rxwdbz4>.

the role of development in evolution (Arthur, 2001; Uller et al., 2020), there are practical problems to gather ontogenetic data at a large scale. Empirical works are still needed to assess whether directions in the morphospace supported by developmental variation are also the most evolvable. Developmental processes influence thus the phenotypic production and the availability of variation to selection, questioning the importance of evolution of the ontogenetic trajectories themselves in shaping the diversity of organismal shapes.

The evolution of ontogenetic trajectories involves a complex interplay of the rate and timing of development of the various parts constituting an organism as well as with the internal and/or external environment. During pre- and postnatal development, organismal growth responds to many genetic, biomechanical and environmental factors. As organs grow, they compete for space and resources, while maintaining a functional phenotype under a variety of selection regimes (Dibner et al., 2007; Nijhout & Emlen, 1998; Olsen et al., 2000). In vertebrates, for example, epigenetic interactions will compensate for, and coordinate, the growth of the organs that form the head, to acquire and/or maintain functions such as occlusion between the lower and upper jaws (Hallgrímsson & Hall, 2011; Lieberman, 2011). Similarly, changes in muscle forces during development regulate the spatialization and intensity of bone remodelling (Herring, 2011; Zelditch & Swiderski, 2011; Zelditch et al., 2008), which may change not only the structure but also the shape of the bone (Martinez-Maza et al., 2016). Organ interactions may drive the occurrence and intensity of developmental plasticity and the indirect response to selection (Fusco, 2008). By responding to developmental changes in forces and movements, epigenetic interactions between bones and other tissues could drive morphological variation (Hallgrímsson & Hall, 2011). Epigenetics could therefore structure evolutionary trajectories, potentially biasing diversification among taxa (Renvoisé et al., 2017; Young & Badyaev, 2007) and thus becoming a major determinant of plasticity-led evolution (Uller et al., 2020; West-Eberhard, 2003).

Postnatal growth is a key period in mammals, during which skull variation is strongly modified (Mitteroecker & Bookstein, 2009) and then stabilized (Zelditch et al., 2003). During this transition from the juvenile to the adult head, major biomechanical changes occur in response to changes in the use of the masticatory apparatus related to weaning, from sucking to gnawing and chewing movements (Curley et al., 2009). An important component of adult anatomy is the eruption and growth of teeth, in relation to the acquisition of mastication. Tooth development partly determines the complexity of the ontogenetic trajectory of the mouse mandible (Swiderski & Zelditch, 2013). The ever-growing incisor leads to bone remodelling during mandible growth (Renvoisé & Montuire, 2015). This simple, highly integrated, skeleton element strongly responds to changes in mechanical constraints related to food hardness (Anderson et al., 2014; Menegaz & Ravosa, 2017), or to muscle dystrophy (Renaud et al., 2010). The mandible is an ideal model system to observe organ interactions and thus to test their evolutionary consequences, as its development is tightly integrated with that of teeth and muscles (Atchley, 1993; Klingenberg & Navarro, 2012).

Rodentia is a very diverse and disparate mammal order, in which postnatal changes can be observed on a large scale. The muscle

attachment to the cranium is used to classify rodents into three main suborders: Myomorpha, Sciuromorpha and Hystricomorpha (Hautier, 2010; Hautier et al., 2008; Simpson, 1945; Wood, 1965). The mandible presents a wide variety of forms across these suborders (Hautier, 2010), which group into two mandibular structures (Tullberg, 1899): hystricognaths (with a strong inwardly projecting angular process and an outwardly projecting condyloid process) or sciurognaths (with an outwardly projecting angular process and an inwardly projecting condyloid process). The insertions of the masseter muscles to the mandible and the cranium were used by early authors (Brandt, 1855; Wood, 1965) to describe four different morphologies across rodents: protrogomorphy (small-to-medium infraorbital foramen, a reduced masseter and a predominant temporalis), sciuroomorphy (very small infraorbital foramen and a lateral masseter inserted in the anterior part of the orbital arch), hystricomorphy (infraorbital foramen is very developed and almost circular) and myomorphy (infraorbital foramen is narrow at the base and widened in its upper part). Rodents present also three main types of molar growth (Renvoisé & Montuire, 2015): root apex closed after tooth maturation (brachyodonty), ever-growing with open root (hypselodonty) or with no root (hypselodonty); and molars take up a great deal of space in the mandible as they develop, particularly in hypselodont species.

Beyond intricate interconnections with postnatal developing structures (muscles and tooth), shape disparity of the mandible seems to be generated prenatally, at least in Sciuridae, with compensated postnatal ontogenetic variations (Zelditch et al., 2016), suggesting a relatively reduced role for biomechanical plasticity in the establishment of species differences. Data supporting this result include most species belonging to the Sciuridae, which is relatively conservative in terms of skull shape (Cardini & Thorington, 2006). Myomorpha and Hystricomorpha are diversified in shape, probably because of their high diversification rate and high diversity (Alhajeri & Stepan, 2018; Wilson, 2013). Therefore, studying the evolution of their ontogenies will likely provide additional contrasts to better understand the importance of postnatal growth in the set-up of species divergences.

These two suborders and the evolution of their ontogenies will be the focus of this study, mainly because they exhibit diverse life-history traits among species (Wilson et al., 2016; Wolff & Sherman, 2008). Gestation and weaning are shorter in Myomorpha, which generally give birth to large litters many times a year. This behaviour involves a short *in utero* development and a rapid and therefore mechanically brutal weaning (Curley et al., 2009). Hystricomorpha give birth to small litters a few times a year. Parental care is therefore different, with longer behavioural weaning and less brutal dietary weaning, over a much longer period (Wolff & Sherman, 2008). The potential for postnatal plasticity could likely be different between the two suborders. A wide variety of diets is also found within these two groups (Nowak & Walker, 1999). Changes in diet might correlate with evolutionary changes in muscle attachment, direction of mastication and mandible shape (Álvarez & Pérez, 2019).

Geometric morphometrics is used to describe postnatal trajectories of the mandible shape on specifically collected species with

identified juveniles (before weaning), instead of using static allometry from a series of specimens varying in size. Comparing these post-natal growths within and between Myomorpha and Hystricomorpha suborders—together with two Sciuromorpha species for comparison—will provide valuable data about the influences of development in evolution, for instance if evolutionary and developmental directions in the morphospace coincide (Erwin, 2007; Gerber, 2014; Wilson, 2013; Zelditch et al., 2016). It will also provide data about the evolution of ontogenesis in rodents, if these evolutionary changes sustain species divergences, and if postnatal growth is a key period for the establishment of adult disparity. Contrasting the variation in these mandible shape trajectories to life-history traits and to the development of muscles and teeth will underline the importance of the development of these traits in the evolution of the mandible ontogenesis.

## 2 | MATERIALS AND METHODS

### 2.1 | Specimens

Specimens were selected from five different collections: the Royal Belgian Institute of Natural Sciences (IRSNB), the Natural History Museum Geneva (MHNG), the National Museum of Natural History Paris (MNHN), the Natural History Museum Basel (NMB) and the Biogéosciences Laboratory, Dijon (Table S1). *Mesocricetus auratus* (RjHan:AURA), *Meriones unguiculatus* (CrI:MON) and *Mus musculus* (BALB/c) are laboratory individuals raised at the University of

Burgundy (Project APAFIS#18405-2019011014262528) for which the age of each individual is known (7 days for juveniles). Juvenile specimens from Museum collections were carefully checked for their putative age with these following criteria about tooth eruption and ossification, which correspond to the observed characteristics made on laboratory 7-day-old juveniles. Molars' occlusal surface is just emerged from the bone and incisors are barely emerged as well. The ossification of mandibular processes is poor (presence of cartilage at the top of the postcondylar process) and the one of the cranium is incomplete (cartilage between the bones constituting the cranium). It results that a large number of registered juveniles were disregarded to keep only undoubtful early juveniles. The final data set for this study includes 105 hemimandibles attributed to 16 species: five for Myomorpha, eight for Hystricomorpha, two for Sciuromorpha, and *Oryctolagus cuniculus* (Lagomorpha) as the out-group species (Figure 1). Only one hemimandible per specimen was used, chosen by state of preservation. For the purpose of checking the effect of the age of juveniles, 27 additional specimens were also sampled and added as Data S1. They represented 15 days old juveniles of Myomorpha species raised in the laboratory and a few juveniles of *Microtus arvalis* older than one week.

Mandibles shorter than 5 cm in length were scanned by  $\mu$ CT scan (Bruker Skyscan 1174) and reconstructed using Avizo<sup>®</sup>9.2 (FEI systems). Those longer than 5 cm were scanned with a Shining 3D<sup>®</sup> Einscan Pro surface scanner. One specimen was processed on the two acquisition pipelines and digitized several times. Preliminary analysis identified no spurious variation in these replicates. Before

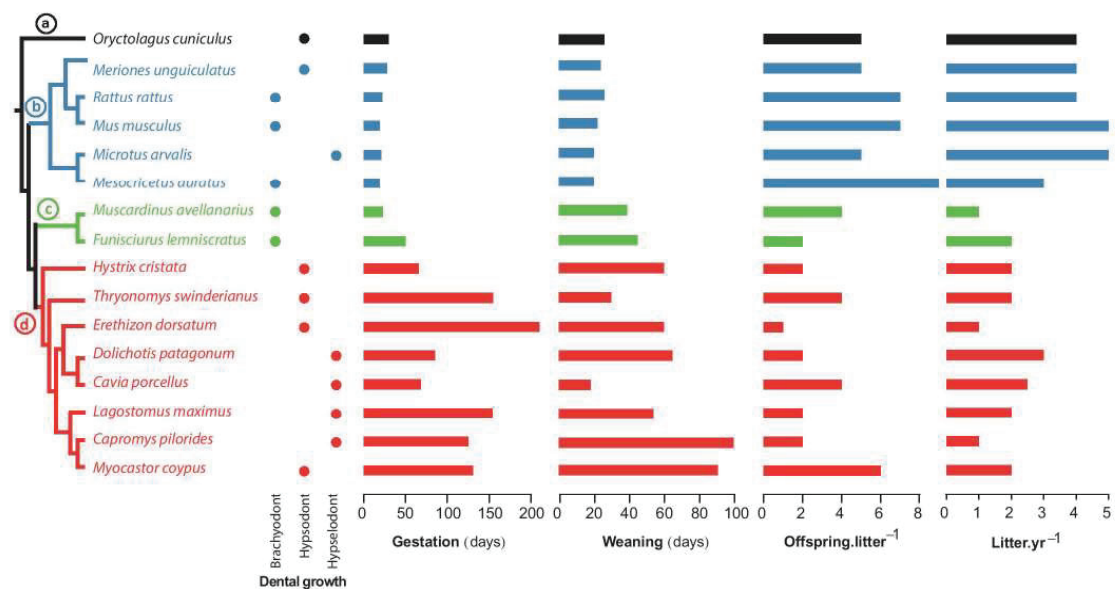


FIGURE 1 Summary of data on phylogeny, tooth growth (Ungar, 2010) and reproductive traits (gestational duration, weaning time and offspring by litter) for the species sampled for the study (Wilson et al., 2016, De Magalhaes & Costa, 2009). Colour code for outgroup and suborders: (a) Lagomorpha in black; (b) Myomorpha in blue; (c) Sciuromorpha in green; (d) Hystricomorpha in red

landmark digitization, 3D models were decimated to 200 000 faces, using the *Rvcg* R package 0.18 (Schlager, 2017).

## 2.2 | Life history

Data about dental development (Ungar, 2010), and ecology such as reproductive traits (De Magalhaes & Costa, 2009; Wilson et al., 2016), were gathered from the literature.

In summary (Figure 1), gestational duration varies considerably, three to nine times shorter for Myomorpha (19 to 22 days, median = 20), than for Hystricomorpha (66 to 210 days, median = 125). A similar difference is also observed for weaning time, which occurs in Myomorpha between 20 and 26 days after birth (median = 22), whereas it occurs from 18 to 100 days after birth (median = 60) in Hystricomorpha. The two suborders have a similar number of litters per year (a maximum of five), but on average Myomorpha have four litters per year, whereas Hystricomorpha have only two. About the skull structure, all species belonging to Myomorpha and Hystricomorpha are either myomorphous or hystricomorphous, respectively. Sciuromorpha species are either sciuromorphous (*Funisciurus lemniscatus*) or myomorphous (*Muscardinus avellanarius*). All species are sciurognaths except the Hystricomorpha species, which are hystricognaths.

## 2.3 | Landmarks and semilandmarks

Ten landmarks were digitized, together with 33 semilandmarks divided into three curves (with 4 on the coronoid process, 9 along the lunar notch and 10 between postcondylar and angular processes; Figure 2) using the *Digit3DLand* R package 0.1.3 (Laffont & Navarro, 2019). Semilandmarks were slid along their tangent by minimizing the bending energy and back-projected on the 3D curves (Gunz et al., 2005).

## 2.4 | Data analysis

### 2.4.1 | Procrustes alignment, checked for approximation and imbalance effects

Landmarks and sliding semilandmarks were superimposed using a full generalized Procrustes analysis (GPA) with the *Morpho* R package 2.8 (Schlager, 2017). Tangent space approximation of distances between specimens was checked against Riemannian distance, which has been shown to be generally accurate across studies encompassing a variety of taxa and taxonomic ranges (Klingenberg, 2020), including mammalian orders (Marcus & Hingst-Zaher, 2000). The reference shape on which landmark conformations are aligned is known to structure variation in the tangent space, thus determining any distortion of distances between individuals (Bookstein, 2016). As developmental stages and species were not equally sampled or

equally represented between clades, we also checked whether aligning landmark conformations on a weighted average rather than on the grand mean (the usual method) still provides consistent results. The average from each developmental stage of each clade (weighting species in the clade equally) was therefore used as reference shape in a new Procrustes superimposition. The angle between this weighted mean shape and the original mean shape was computed and compared to the angles observed between any two specimens. The Lagomorphs were aligned only as supplementary data.

### 2.4.2 | Developmental, phylogenetic-aligned and postnatal morphospaces

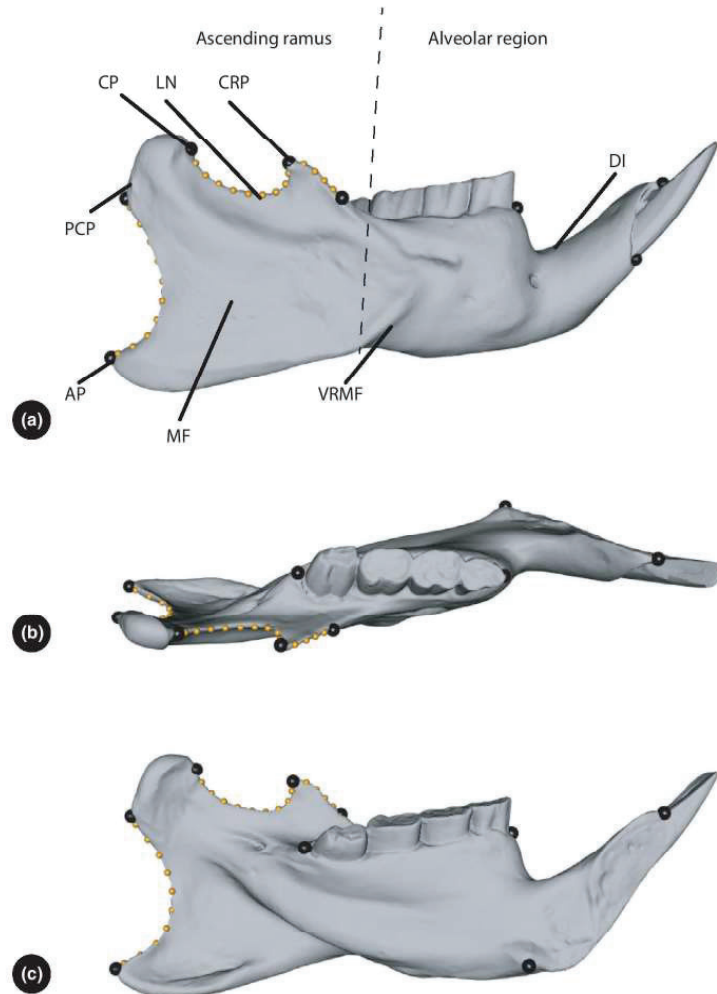
A developmental morphospace, the embedding of both juveniles and adults in the same morphospace (Eble et al., 2003), was obtained by applying principal component analysis (PCA) to the covariance matrix of the tangent coordinates. This morphospace maximizes shape variation in directions that describe either developmental changes, evolutionary changes or both simultaneously. To compare the developmental structuration of the morphospace and evolutionary divergences, a phylogenetically aligned morphospace was also computed based on the principal component ordination of the phylogenetic covariance matrix  $C$  (Collyer & Adams, 2021). The phylogenetic covariance matrix  $C$  was computed according to a Brownian-motion model of evolutionary divergence. This space (PaPCs) maximizes variation in directions that describe evolutionary divergences. This analysis was done with the *geomorph* R package 3.2.1 (Adams et al., 2016). To observe the structuration of the variation of the postnatal trajectories alone, a PCA was performed on the covariance matrix of the vectors  $z$  of differences between juvenile and adult shape averages  $y$  of each species. These vectors are the average shape changes occurring during postnatal growth. Scaling these vectors by the difference between juvenile and adult average sizes would have led to a rough estimate of allometric vectors. As Hystricomorpha species are much larger than other species, rescaling would have resulted in trivial size differences.

A tree pruned for the species present in the sample (Wilson et al., 2016) was built with the *ape* R package 5.3 (Paradis & Schliep, 2019) and was projected onto the different morphospaces, using the *phytools* R package 0.7-20 (Revell, 2012), to observe their phylogenetic structuration.

### 2.4.3 | Ancestral postnatal trajectories, common pattern of growth and evolutionary changes

The phylogenetic mean of postnatal trajectories was computed according to the generalized least-squares estimator  $\bar{z}_{pgls} = (1'C^{-1}1)^{-1}1'C^{-1}z$  (Revell, 2009; Rohlf, 2001), with  $z$  the vectors of shape changes between juveniles and adults and  $C$  the phylogenetic covariance matrix. This estimate corresponds to the value at

**FIGURE 2** Landmarks and semilandmarks on 3D mandibular surface. Black dots are manual 3D landmarks, and small yellow dots represent the semilandmark template. (AP, angular process; CP, condylar process; DI, diastema; CRP, coronoid process; LN, lunar notch; MF, masseter fossa; PCP, postcondylar process; VRMF, ventral ridge of masseter fossa). (a) labial view; (b) occlusal view; (c) lingual view



the root of the tree (Rohlf, 2001). The  $\mathbf{z}$  vectors correspond to postnatal shape changes,  $\bar{\mathbf{z}}_{pgls}$  estimates the ancestral pattern of shape changes during postnatal growth according to Brownian motion. Estimate of the postnatal trajectory for each suborder was computed as the least-squares (LS) means  $\hat{\mathbf{z}} = \mathbf{L}\beta$ , with  $\mathbf{L}$  the matrix corresponding to the linear contrast for the suborder, and  $\beta = (\mathbf{X}'\mathbf{C}^{-1}\mathbf{X})^{-1}\mathbf{X}'\mathbf{C}^{-1}\mathbf{z}$ , the phylogenetic generalized least-squares estimates of suborder differences.

To check the alignment of the principal directions of the morphospace (developmental or phylogenetically aligned) with the phylogenetic mean postnatal trajectory  $\bar{\mathbf{z}}_{pgls}$ , or with the suborder estimates of postnatal trajectories  $\hat{\mathbf{z}}$ , angles between these estimates and the shape features described by PCs were estimated as  $\theta = \cos^{-1}(\mathbf{v}_i \cdot \mathbf{v}_j)$  (Klingenberg, 1998; Zelditch et al., 2004), with the normalized vectors  $\mathbf{v}$  being either eigenvectors or normalized

trajectories to unit length. The probability that the angle between two random vectors is lower than the observed angle was estimated as the area of the cap of a hypersphere defined by this angle (Li, 2011) and computed with the *Morpho* R package 2.8 (Schlager, 2017). Approximation of standard errors on angles based on  $\hat{\beta}$  was computed based on the sampling distribution of  $\beta$  (Houle & Meyer, 2015; Meyer & Houle, 2013), and according to  $\mathbf{z}^* \sim N(\hat{\mathbf{z}}, \mathbf{S}_e \otimes \mathbf{L}(\mathbf{X}'\mathbf{C}^{-1}\mathbf{X})^{-1}\mathbf{L}')$ , where  $\mathbf{S}_e$  is the residual covariance matrix, and  $\otimes$  stands for the Kronecker product. Descriptive statistics on sampled angles were computed with the *circular* R package 0.4-93 (Agostinelli & Lund, 2017).

The angle between phylogenetically aligned variation (PaPCA) and the average directions of postnatal changes ( $\bar{\mathbf{z}}_{pgls}$  and  $\hat{\mathbf{z}}$ ) was measured as  $\delta_i = \cos^{-1}\left\{\left(\mathbf{v}_i' \mathbf{L} \mathbf{L}' \mathbf{v}_i\right)^{0.5}\right\}$  with  $\mathbf{L}_{3k \times q}$  the matrix of  $q$  eigenvectors

from the PaPCA, where  $q$  was set equal to half the divergence dimensionality ( $q = 7$ ) and  $v$  the normalized postnatal vectors (Krzanowski, 1979). To assess more formally the degree of independence between developmental trajectories and evolutionary divergences, a common spectral decomposition of the two matrices was performed (Krzanowski, 1979). This approach captures the overall similarity from the eigen decomposition of  $H = \sum_{i=1}^p L_i L_i^T$  where  $L$  is the matrix of the  $q$  first eigenvectors of either the divergences or the postnatal changes. The eigenvalues close to the maximum of  $p$  (here  $p = 2$ ) mean that the evolutionary or postnatal changes could be inferred from a linear combination of the eigenvectors of the other. Similarly to above, an angle  $\delta_i$  could be defined to estimate how similar an eigenvector of  $H$  is to the evolutionary or postnatal changes (Krzanowski, 1979).

#### 2.4.4 | Comparison of juvenile and adult disparities

Even if some evolutionary divergences arise in the directions of postnatal growth, adult disparity may or not increase compared with juvenile disparity as changes in the amount or direction could be compensated and finally most of the disparity could be established prenatally as suggested for Scuiridae (Zelditch et al., 2016). Disparity levels between developmental stages of Myomorpha and Hystricomorpha were calculated as the Procrustes variance, that is the sum of squared Euclidean distances in the tangent space between species means  $y$  and their average divided by the number of species in the group (Drake & Klingenberg, 2010; Zelditch et al., 2004). Bootstrapping of species means was used to estimate standard errors on disparity (Efron, 1979; Foote, 1994; Navarro, 2003). Disparities were also computed on a sequence including successive principal components (PCs) defining the developmental morphospace. This sequence was used to show how taxa spread over the morphospace as defined by the main patterns of shape differentiation among species and developmental stages. Comparison of disparity between the two suborders also assessed whether evolvability varies across anatomies and modes of development.

#### 2.4.5 | Evolution of postnatal trajectories

The degree of phylogenetic signal in the postnatal vectors  $z$  was assessed relative to their expectation given a Brownian evolution, using the multivariate version of the  $K$  statistics (Adams, 2014), with 10 000 simulations. The  $K_{\text{mult}}$  was computed with the *geomorph* R package 3.2.1 (Adams et al., 2016). This package also returns effect size as the z-score standardization of the  $K_{\text{mult}}$  statistics, given its distribution under the null obtained from simulation. For comparison, the phylogenetic signal was also computed separately for juvenile and for adult shapes.

To assess whether postnatal trajectories have evolved between suborders, the differences between suborder estimates  $\hat{z}$  with regard to their magnitude or direction of postnatal shape changes were computed. Standard errors on angles were approximated using  $z^*$

sampling as explained above. Evolutionary divergence in the magnitude of shape changes occurring after birth between the Myomorpha and Hystricomorpha was evaluated from the LS-means contrast of the Euclidean length of the suborder trajectories  $\|\hat{z}_{\text{myo}}\| - \|\hat{z}_{\text{hys}}\|$ , with a  $t$  test using approximate standard error based on  $z^*$  sampling and the residual degree of freedom of the linear model.

Approximately phylogeny-corrected postnatal changes were computed as  $z_c = D^{-1}z$  (Arnold, 1981; Schabender & Gotway, 2017), where  $z$  is the vector of shape changes between juveniles and adults of each species and  $D^{-1}$  is the inverse square root of the phylogenetic covariance matrix  $C$ . To obtain  $D^{-1}$ , the eigen decomposition of  $C$  was used as  $D^{-1} = UA^{-0.5}U^T$ , with  $U$  the matrix of eigenvectors, and  $A$  the diagonal matrix of eigenvalues of  $C$ . Their angles with the ancestral growth  $\bar{z}_{\text{pgls}}$  was measured to assess the degree of divergences from the root of the tree. The pairwise angles between these trajectories within suborders were computed to assess the remaining variation between species once Brownian divergence is factored in, variation that could have resulted from evolutionary divergence from other traits such as life-history traits. This question was evaluated more formally using a phylogenetic generalized least-squares analysis (pGLS) with the effects of tooth growth and reproductive traits on postnatal shape changes  $z$ . Considering the number of species sampled and differentiation between and within Myomorpha and Hystricomorpha, traits could be strongly aggregated (Adams & Collyer, 2018). Correlations between phylogeny and life-history traits were first checked using two-block partial least squares (Rohlf & Corti, 2000), following the approach of Adams and Collyer (2018). Because of the strong clustering of gestational and weaning duration and their resulting high correlation with phylogeny, they were pooled within suborders before being analysed. Significance of the Procrustes sum of squares was evaluated using 10 000 residual permutations with the *RRPP* R package 0.5.2 (Collyer & Adams, 2018). Residual permutations appear to control the family-wise error rate, even for small trees and for large isotropic dimensionalities, and to reach high power (Adams & Collyer, 2018; Collyer & Adams, 2018). Two points should, however, be noted: the sample size used here is smaller than the minimum size in these studies; the simulation scheme used by these authors did not acknowledge the peculiarities of isotropy in the tangent space where correlations between coordinates exist due to the Procrustes superimposition (Bookstein, 2016; Klingenberg, 2020). The family-wise error rate and power given the characteristics of the data (i.e. tree and mean shape) were computed for a continuous covariate, a three-state covariate and a binary classification. Covariates and shapes evolve according to a Brownian model and to Procrustes constraints on the tangent space. Simulation results are provided as supplementary materials.

#### 2.4.6 | Visualization of shape changes

Shape effects were visualized on two meshes, corresponding to the mean shape for Myomorpha, and then for Hystricomorpha, because of the considerable anatomical differences between the two suborders.

Meshes were deformed in relation to shape effect, using thin-plate spline with the *Morpho* R package 2.8 (Schlager, 2017). Deformations were either colourized in relation to the signed distance between the predicted and reference meshes or visualized as animated deformations, which are provided as supplementary movies.

### 3 | RESULTS

#### 3.1 | Checking tangent space approximation and imbalance effects

Correlation between Euclidean distances in the tangent space and Riemannian distances was very high ( $r = 0.999$ ), confirming the accuracy of the approximation. The mean shape of *Myomorpha* and *Hystricomorpha* was very similar to the mean shape based on weighted averages ( $\alpha = 2.55^\circ$ ), and angles between specimens were always larger than this angle, suggesting that the shape space was ideally projected for the sample studied and was not affected by the imbalance between the suborders. It should be recalled here that the *lagomorph* was aligned as supplementary data only.

#### 3.2 | Developmental and evolutionary patterns of shape changes

Variation is concentrated on the first two PCs, which account for 59.9% of the total shape variance (Figure 3a), with 90% for the first eight PCs. *Myomorpha* and *Hystricomorpha* are opposed on PC1, which accounts for 42.7% of shape variance. This pattern is expected, since mandible anatomy differs strongly between the two suborders. Developmental vectors (the arrows in Figure 3a) appear to be mainly orthogonal to this shape divergence and project consistently on PC2. In this 2D projection, these postnatal trajectories in *Myomorpha* appear to be oriented in similar directions, whereas the vectors of *Hystricomorpha* seem less consistent with this general trend. *Sciuromorpha* are placed close to *Myomorpha* and their developmental vectors seem to follow the same main direction. The special case of *Muscardinus*, which has a myomorphous skull structure but belongs to the *Sciuromorpha* suborder, does not seem to be more similar to the trajectories of *Myomorpha* species.

The PC2 axis seems to summarize a growth trajectory common among rodents. The phylogenetic mean of postnatal shape trajectory  $\bar{z}_{pgls}$ , which corresponds to the ancestral pattern of postnatal shape changes, is in close agreement with the shape changes described by PC2 ( $\alpha = 41.4^\circ$ ,  $p < 0.0001$ ). Suborder estimates  $\hat{z}$  of the postnatal trajectory are at  $31.1^\circ \pm 7.2$  of this common growth pattern described along PC2 for *Myomorpha*, at  $58.9^\circ \pm 14.9$  for *Hystricomorpha* and at  $49.6^\circ \pm 6.6$  for *Sciuromorpha*. These angles are more similar than expected between two random directions ( $p < 0.0001$ ). On average,  $47.3\% \pm 0.22$  of these vectors map onto PC2, with the remainder spread over all the other PCs. The estimation of the postnatal vectors and derived parameters seems robust

given the amount of change and species differences to the number of sampled juveniles (Figure S1). They may also be sensitive to variation in age of juveniles because of the nonlinearity of postnatal trajectories (Sheets & Zelditch, 2013). Nonetheless, the vectors are still describing a roughly similar direction in the shape space and for instance differences in angles with  $\bar{z}_{pgls}$  due to age variation are smaller than the observed angles (Table S2).

Postnatal shape changes described by the ancestral pattern of growth  $\bar{z}_{pgls}$  (Figure 3b,c; Movie S1) imply elongation of the condylar and postcondylar processes, with strong bending of the lunar notch. The angular process expands and subsides whereas the anterior part of the ventral ridge of the ramus retreats, increasing the ramus. The diastema elongates and flattens. The alveolar region is proportionally larger in the juvenile mandible, whereas in the adult mandible the alveolar region is of similar proportions to the ascending ramus.

The apparent orthogonality observed between the phylogenetic signal and the postnatal development on the first PCs of the developmental morphospace is actually weaker than supposed from the preceding. Whereas the first phylogeny-aligned component is clearly orthogonal to  $\bar{z}_{pgls}$  or to the suborder estimates  $\hat{z}$ , additional phylogeny-aligned components are more similar to some of these trajectories, implying that some divergences may have happen along similar directions than the postnatal development (Figure 4a). The overall angle with the *Hystricomorpha* estimate  $\hat{z}$  is larger (Figure 4a) and it could be noted the striking difference between suborder estimates on the second component (Figure 4b). These results suggest that the divergences in this suborder are somehow less related to its main pattern of postnatal changes. The overall congruence between evolutionary divergences and developmental directions is even stronger. Krzanowski's common subspace analysis shows that species divergences share some shape changes with the main patterns of postnatal changes. The first five eigenvalues  $\Delta$  of  $H$  range between 1.67 and 1.96 (for a maximum of 2) and the individual angles  $\delta$  between the eigenvectors of  $H$  and the postnatal or evolutionary matrices ranges from  $7.7^\circ$  and  $23.9^\circ$ .

#### 3.3 | Levels of adult and juvenile disparities

Given the levels of agreement between evolutionary changes and growth directions, an increase in disparity between juveniles and adults could be expected. However, such an increase is observed only in *Myomorpha* and is only marginal (Figure 4a, Table S3). On contrary in *Hystricomorpha*, disparity seems to be established in the early stages, as levels of disparity are similar in juveniles and in adults. Disparity in *Myomorpha* juveniles accumulates more slowly than for the other three clade  $\times$  age groups (Figure 4b). In particular, disparity based on the main patterns of differentiation between species and developmental stages (the first PCs) is much lower in juvenile than in adult *Myomorpha*, a pattern that is not observed in *Hystricomorpha*. This suggests that *Myomorpha* juveniles have a relatively undifferentiated mandible among species, given the broad pattern of differentiation of the mandible observed at the scale of the order.

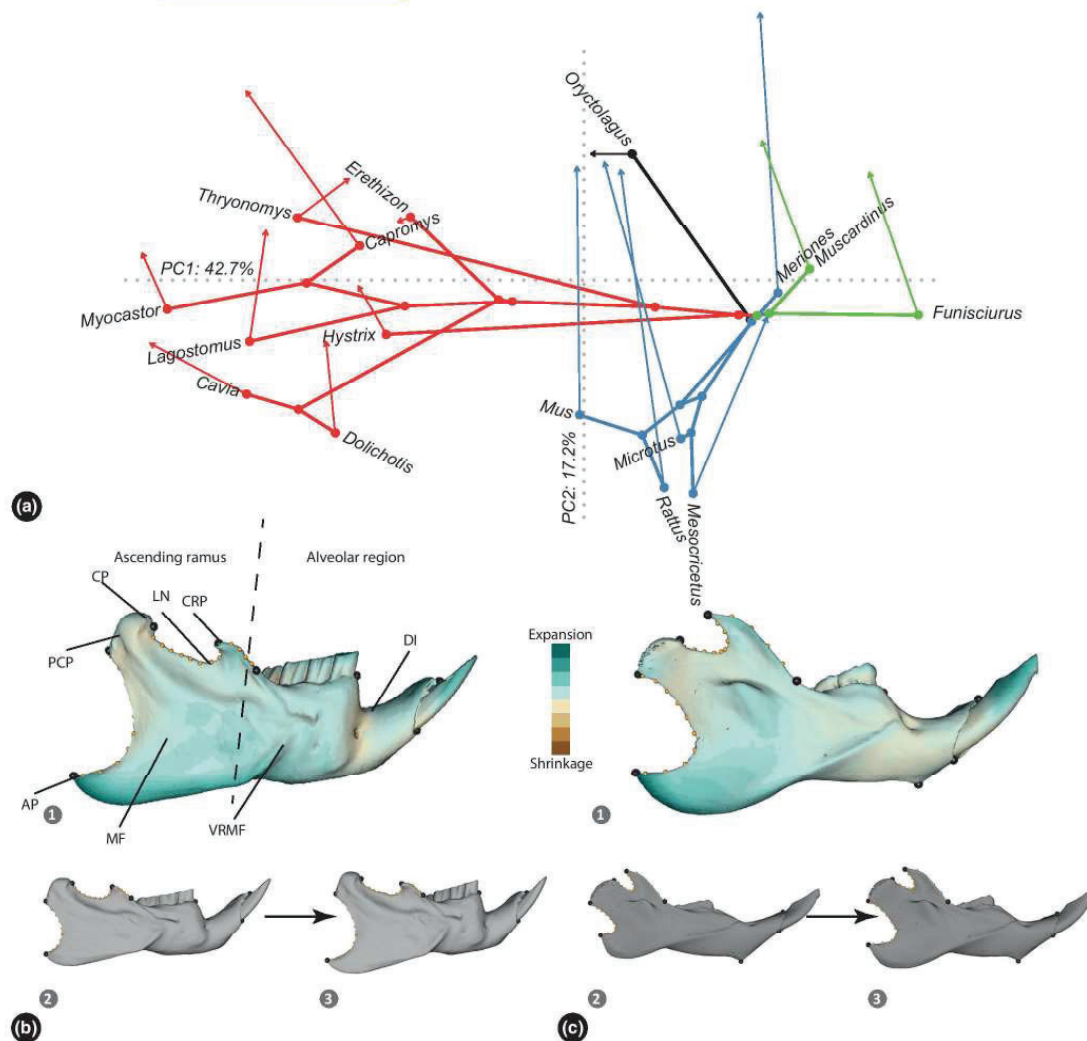


FIGURE 3 Developmental morphospace and shape changes associated with the phylogenetic mean postnatal trajectory. (a) Developmental morphospace where average juveniles of species are represented as the tip of the phylogenetic branches, postnatal trajectories are represented as arrows from the juvenile to adult shapes. Red is for Hystricomorpha species, blue for Myomorpha species, green for Sciuromorpha species and black for Lagomorpha; (b) Shape changes associated with the phylogenetic mean postnatal trajectory mapped on the Hystricomorpha mean shape (AP, angular process; CP, condylar process; DI, diastema; CRP, coronoid process; LN, lunar notch; MF, masseter fossa; PCP, postcondylar process; VRMF, ventral ridge of masseter fossa); (c) shape changes associated with the phylogenetic mean postnatal trajectory mapped on the Myomorpha mean shape. Green areas represent expansion from juvenile to adult shapes, whereas beige areas correspond to a compression effect. Grey shapes correspond to the juvenile mean shape (2) or to the modelling of adult mean shape (3) according to the juvenile mean shape plus the phylogenetic mean trajectory  $\bar{z}_{\text{reg}}$ . See also Movie S1 for dynamic shape changes

### 3.4 | Evolution of postnatal shape changes

The observed variation in postnatal shape trajectories (the arrows in Figure 3) appears consistent with a phylogenetic signal (Figure 5a–c). Species trajectories cluster within suborders both in direction and magnitude. The main pattern of changes shows an opposition

between larger postnatal shape changes on negative values of PC1 and smaller ones on positive values (Figure 5b). These variations agree with a pattern expected under Brownian divergence ( $K_{\text{mult}} = 0.42$ ,  $p = 0.04$ ), as was the case for the spreading of species in the developmental morphospace for both adults ( $K_{\text{mult}} = 0.91$ ,  $p < 1 \times 10^{-4}$ ) and juveniles ( $K_{\text{mult}} = 0.93$ ,  $p < 1 \times 10^{-4}$ ). However,

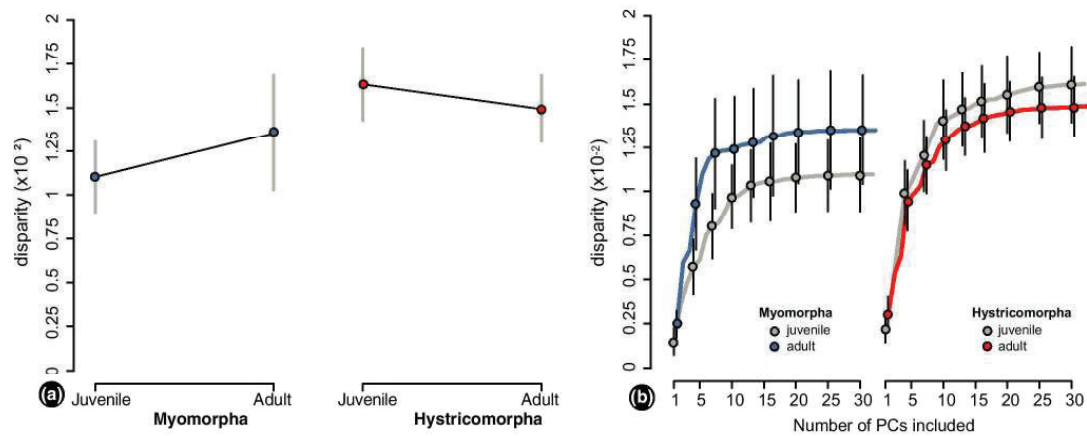


FIGURE 4 Developmental changes in disparity. (a) Comparison of levels of disparity between juveniles and adults within suborders. (b) Accumulation curves of juvenile and adult disparities along the principal components of the developmental morphospace. Blue is for Myomorpha and red is for Hystricomorpha

the effect size is much smaller for developmental trajectory than for shape ( $Z = 1.78$  versus 4.60 for adults and 4.96 for juveniles), suggesting a less neutral divergence and species-specific postnatal growth trajectories.

In agreement with this phylogenetic signal, the suborder trajectories  $\hat{z}$  of agree with the common growth pattern (Figure 5d). The deviation between these suborder estimates (Figure 5e) is  $54.7^\circ \pm 17.4^\circ$  (Myomorpha vs Hystricomorpha),  $37.1^\circ \pm 9.4^\circ$  (Myomorpha vs Sciuromorpha) and  $45.8^\circ \pm 15.1^\circ$  (Hystricomorpha vs Sciuromorpha). These angles are more similar than expected between two random directions ( $p < 0.0001$ ). These elements support a relative conservation of the main pattern of postnatal changes of the mandible in rodents. However, the magnitude of postnatal shape changes  $\|\hat{z}\|$  differs between Myomorpha and Hystricomorpha ( $t_{12} = 2.70$ ,  $p = 0.009$ ), with larger vectors in the latter (Figure 5f).

Once removed the expected patterns under Brownian divergence, the approximately phylogeny-corrected trajectories  $z_c$  still present important variation within and among suborders (Figure 5g). These angles between phylogeny-corrected vectors  $z_c$  are large, indicating species specificities and divergence of individual trajectories. For many species comparisons, this angle is still more similar than expected for random vectors. This evidences a relative conservation of the ancestral main pattern of growth.

To assess the influence of life-history traits and tooth growth on this remaining variation in trajectories, a phylogenetic generalized least squares was performed. Gestation time and duration of pre-weaning period were pooled within suborders prior to analysis as they present a very high correlation with deep node in the phylogeny (Figure 1). It appears that only type of tooth growth has an effect after controlling for Brownian expectation of evolutionary divergence (Table 1).

Simulations show that appropriate type I error is returned and adequate power could be obtained for large effects (Table S4 and Figure S2). Pairwise comparisons between types of tooth growth show that hypselodonty has a different effect from brachyodonty ( $d = 0.132$ ,  $Z = 3.36$ ,  $p = 0.002$ ) and hypsodonty ( $d = 0.117$ ,  $Z = 1.83$ ,  $p = 0.05$ ), whereas the effect of brachyodonty is similar to that of hypsodonty ( $d = 0.087$ ,  $Z = 0.934$ ,  $p = 0.17$ ).

Shape changes in relation to hypselodonty (Figure 6 and Movie S2) show an extension of the condylar process, which rises vertically and becomes thinner, and a thicker diastema, especially in its upper part. The molar area increases in volume, as does the anterior part of the ventral ridge of the masseter fossa. The alveolar region is more robust and extends further on the lingual side.

## 4 | DISCUSSION

### 4.1 | Conservation of the main patterns of growth and evolutionary divergences

Our main results highlight a general pattern of shape changes during postnatal development across Rodentia, with similar local bone growth. The mandible shape in juveniles is generally elongated and flattened, with relatively short processes. These processes later expand, increasing their relative height and thus enlarging the masseter fossa. This ontogenetic modification of the posterior part of the mandible, well described in laboratory mice (Swiderski & Zelditch, 2013), and observed in Sciuridae (Zelditch et al., 2016), is here shown to be conserved across the main clades of Rodentia. This pattern is undoubtedly related to the development of the muscular complex inserting on the mandible. As these muscles gain volume during growth, their contact surface with the bone must expand. Similarly, the different processes become

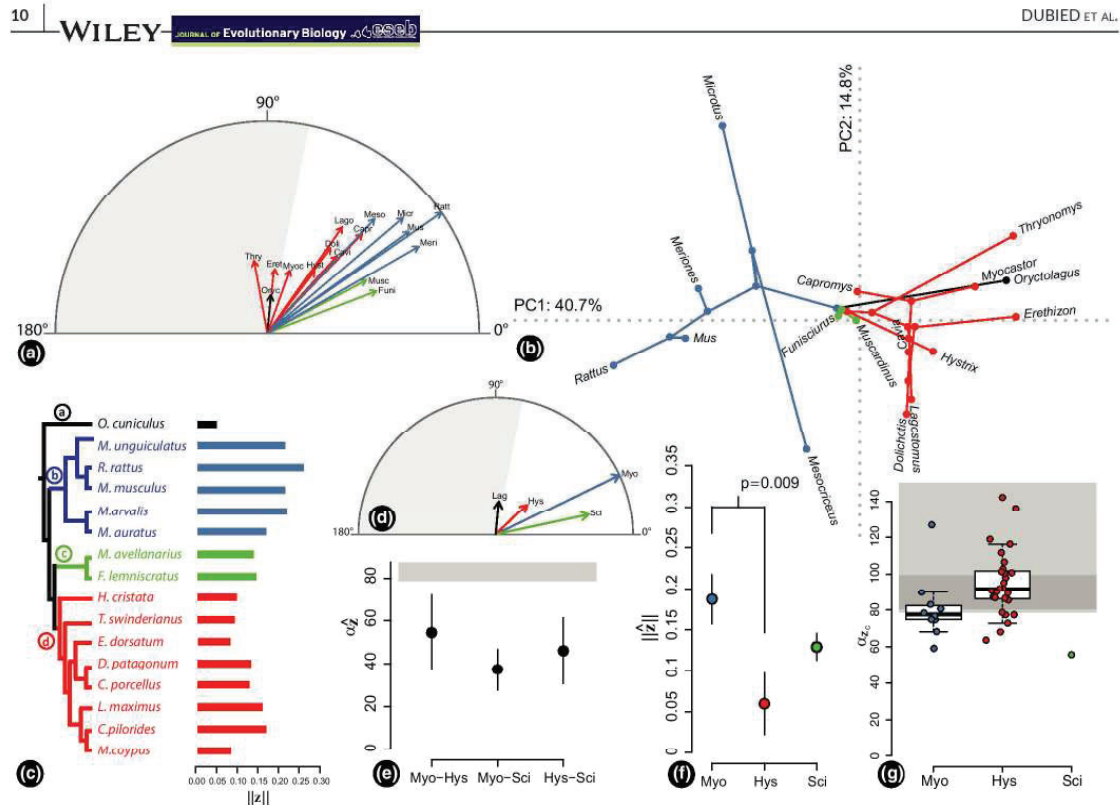


FIGURE 5 Variation of postnatal trajectories. (a) Angles between the postnatal trajectories of species ( $z$ ) and the phylogenetic mean ( $\bar{z}_{pgls}$ ). The lengths of the vectors are proportional to their norm; (b) the principal component ordination of the postnatal trajectories ( $z$ ) together with the projection of the phylogeny; (c) magnitude of postnatal shape changes; (d) angles between the estimates of suborder trajectories ( $\hat{z}$ ) and the common growth pattern  $\bar{z}_{pgls}$ ; (e) angles between the estimates of suborder trajectories ( $\hat{z}$ ); (f) magnitude of the suborder estimates of postnatal changes; (g) angles between  $z_c$  within suborders grey shading in panel (a, d, e) corresponds to the distribution of angles between random vectors with a probability > 0.05. See Figure 3 for colour scheme and species acronyms

more robust after weaning to support the attachment tension of the muscles. This musculoskeletal system articulates with the skull (cranium and mandible) to allow mastication, which will impose greater mechanical constraints at this life stage (Scott et al., 2014). This general pattern of growth appears orthogonal to the main shape divergence between suborders, which opposes the mandible shape of Hystricomorpha with the ones of Myomorpha and Sciuromorpha. This contrast corresponds to gross differences in anatomy, the mandibular structure of Tullberg (1899), opposing hystricognaths and sciurognaths based on the opposite orientation of the angular and condyloid processes.

Evolutionary divergences between species appear nonetheless much more related to the ontogenesis and its variation than expected from the orthogonality of their main directions, suggesting that developmental processes such as heterochrony could have played a role in species divergences. Based on the sampled species, Hystricomorpha exhibit developmental patterns that are much more genus-specific than those of Myomorpha species, where the

trajectories are more similar to the common developmental pattern. This difference seems to be mainly related to the difference in species divergence between suborders. Myomorpha have a common juvenile shape that diverges postnatally among subfamilies. In Hystricomorpha, beside the common juvenile pattern, the mandible shape of juveniles presents some species-specific features from the early stages, and the magnitude of postnatal shape changes is smaller. Hystricomorpha being not precisely age controlled and in smaller numbers compared with Myomorpha, variation observed in Hystricomorpha could be more biased by some age or sampling effects (Figure S1 and Table S2). These biases may partly explain some variation observed between the suborders. Nonetheless, the differences between suborders could also be explained by the vast differences between the ecological traits for each suborder (Wolff & Sherman, 2008), including reproductive strategy, gestation and weaning (acting directly on pup development), diet (leading to more or less mechanical stress on the masticatory apparatus) and taxonomic richness (reflecting the diversity

TABLE 1 Phylogenetic generalized least squares of postnatal trajectories

Source	df	SS	MS	$r^2$	F	Z	Pr(>F)
Gestation length	1	0.02228	0.022283	0.05460	1.0948	0.37464	0.3675
Weaning age	1	0.03433	0.034328	0.08411	1.6866	1.10556	0.1411
Litter per year	1	0.02846	0.028462	0.06974	1.3984	0.79606	0.2203
Tooth growth	2	0.08831	0.044156	0.21639	2.1695	1.94286	0.0252
Residuals	10	0.20353	0.20353	0.49871			

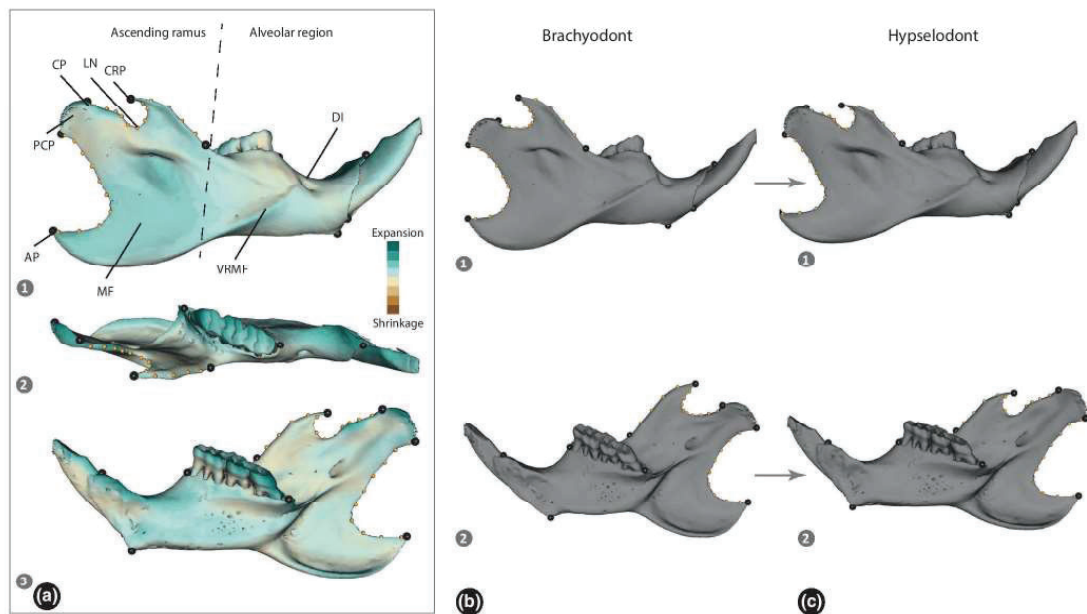


FIGURE 6 Shape changes associated with dental growth: brachyodont versus hypselodont. Effects are mapped on the mean shape of myomorph specimens. Green areas represent expansion from brachyodont to hypselodont shapes, whereas beige areas correspond to a compression effect. See also Movie S2 for dynamic shape changes. (AP, angular process; CP, condylar process; DI, diastema; CRP, coronoid process; LN, lunar notch; MF, masseter fossa; PCP, postcondylar process; VRMF, ventral ridge of masseter fossa). 1: Labial view; 2: upper view; 3: lingual view. Grey shapes correspond to the least-square estimates of the b, brachyodont or c, hypselodont shapes. 1: labial view; 2: lingual view

of a clade). Myomorpha newborns share common anatomical features, whereas the longer gestational period in Hystricomorpha allows longer in utero development, producing a skeletonized and differentiated organ (Huggett & Widdas, 1951). In this respect, the peculiarity of gerbils (*Meriones*) is revealing as this species has a longer gestation than other Myomorpha species and presents at seven days old a more differentiated juvenile mandible as the Hystricomorpha species.

This developmental difference between Myomorpha and Hystricomorpha suggests that juvenile disparity at birth is partly driven by timing differences in the skeletonization and differentiation processes in relation to variation in gestational duration. Therefore, the potential for plasticity after birth is likely to be different between the two suborders since the mandible at birth is not at the same state of ossification and differentiation.

## 4.2 | Evolution of postnatal trajectories

Variation in gestational length may explain changes in postnatal trajectories because it modifies the onset of the postnatal period. It could thus explain variation in magnitude of postnatal changes as juveniles could be more or less differentiated and skeletonized at birth. The observed differences in magnitude between suborders could be related to such factor. As developmental trajectories are strongly nonlinear (Green et al., 2017), variation in the onset of postnatal growth will affect the linear approximation of the postnatal trajectory leading to variation in angles in relation to differential duration of the gestation. Again, variation between suborders seems to be related to such an effect. However, once the expected effect of Brownian divergence was factored in, no effect of the gestational duration was observed to explain the residual differences

in postnatal shape changes. The separation between suborders is ancient and occurred during the Paleocene (Swanson et al., 2019). Deep-rooted phylogenetic signal strongly structures traits and aggregates them, as gestational length or weaning timing, within clades. These correlations potentially mask differences related to ecological traits.

The weaning period and dietary diversification occurring within this period could also play a role in the divergences of postnatal trajectories as different behaviours and feeding habits lead rodents to adapt their chewing movement. Rodents can gnaw with their incisors as well as chew with their cheek-teeth (Byrd, 1981; Cox et al., 2012; Hiiemäe & Ardran, 1968). These movements, acquired more or less rapidly during weaning, could induce new mechanical constraints and thus change the pattern of bone remodelling (Jacobs, 1984). Changes in the consistency of food are known to induce plasticity of the mandible, with a large effect on the angular and coronoid processes, modifying the correlation between the alveolar and muscle-bearing regions and their biomechanics (Anderson et al., 2014). In Myomorpha species, weaning is rapid and therefore mechanically brutal (Curley et al., 2009). This rapid upheaval in diet could explain the major changes observed in morphology. The feeding system must change from the sucking movement to active chewing in only a few days. In mice, bite force increases drastically in the days preceding weaning (Ginot et al., 2020). In the Hystricomorpha species, parental care is different, with long behavioural weaning and less brutal dietary weaning, over a much longer period (Wolff & Sherman, 2008). As the Hystricomorpha species, at least the ones sampled in this study, are born with a more differentiated shape and present postnatal shape changes of smaller magnitude during a longer period, dietary changes at weaning have likely less impact on the patterns of correlated bone remodelling. Guinea pigs (*Cavia*) have a short weaning timing of 18 days comparable to the one of the Myomorpha species but present nonetheless a magnitude and direction of postnatal trajectory similar to other Hystricomorpha species. As with gestation, no effect of the weaning period was observed to explain the residual differences in postnatal shape changes once the expected effect of Brownian divergence was factored in, but again weaning period timing is strongly aggregated within each clade.

Only tooth growth, especially molar hypselodonty, appears to produce a special signature on the postnatal shape changes of the mandible. Within Myomorpha, hypselodonty in arvicolines may explain the divergence of their postnatal trajectory, as their unrooted prismatic teeth strongly modify the dental alveolar region. A comparable effect of tooth growth has been shown on individual postnatal ontogenies in mice (Swiderski & Zelditch, 2013). During development, bone and teeth interact with each other and these interactions may explain important changes either in bone or in tooth. For instance, tooth-bone mechanical interaction explains the lateral offset of molar cusps during development, a repeated evolutionary innovation in the mammalian tooth pattern (Renvoisé et al., 2017). This interaction influences also the mandible shape as it is modified with arrested tooth development in mutant mice (Boughner et al.,

2018; Paradis et al., 2013). Thus, the bone must adapt to the dynamic process of tooth growth, which imposes new biomechanical stresses. This dynamic reconfiguration of bone strain imposes a new spatialization of bone formation and remodelling (Martínez-Vargas et al., 2017) that may have evolutionary outcomes in both tooth and bone shapes.

Our results suggest that evolutionary changes in the postnatal development of the mandible could be related to muscle and tooth development. The mandible responds dynamically to both the growth of the dental alveoli and the development of the masticatory muscles (Swiderski & Zelditch, 2013). The biomechanics of mastication functionally integrates the alveolar and ramus regions from their direct epigenetic interactions (Zelditch et al., 2008). Changes in environment (e.g. diet or behaviour) could induce changes in the spatialization of biomechanical strain and therefore of bone remodelling, because of the intricate relationship between the mandible and tooth and muscle growth. If tooth or muscle growth drives mandible plasticity, natural selection on these anatomical elements will induce correlated changes in the mandible via epigenetic interactions, which may in turn be subject to genetic accommodation (Uller et al., 2020; West-Eberhard, 2003). For example, at a smaller scale, the repeated dietary adaptation in mice observed following their invasion of sub-Antarctic islands seems to agree with a similar scenario, with mandible plasticity as the main process at the early stages of the invasion (Renaud et al., 2018).

### 4.3 | Comparison with the cranium

Despite a common pattern of postnatal changes in relation to muscle and tooth growth, mandibles are quite different between suborders suggesting that ontogeny did not constrained anatomical diversity. At its highest level (hystricognaths versus sciurognaths), this diversity occurs mainly in an orthogonal direction of the common postnatal growth pattern. This independence of anatomical diversity to developmental constraints was similarly observed for the cranium (Wilson, 2013; Wilson & Sánchez-Villagra, 2010). However, at a lower scale, the diversity of postnatal trajectories (i.e. variation in the magnitude of changes and angles) appears to be specific to the suborders. This observation contrasts with the constrained variation of allometric patterns observed on the cranium (Wilson, 2013; Wilson & Sánchez-Villagra, 2010). Within the head, the cranium is a composite unit composed of multiple bones, and this assemblage is constrained by the development of teeth (Renaud et al., 2009), facial muscles (Ravosa et al., 2008) and internal organs (i.e. the brain, Richtsmeier & Flaherty, 2013, or the olfactory and auditory organs, Barone, 1976). This complexity may explain the low skull disparity in relation to lineage diversification described in Rodentia (Alhajeri & Steppan, 2018), or in the adaptive radiation of some families (Maestri et al., 2017), or the relatively overlapping growth pattern of the skull observed among rodent clades (Wilson, 2013). The higher complexity of skull development is thought to reduce its dependence on muscle and tooth

development (Swiderski & Zelditch, 2013), and this difference in complexity probably explains the contrast observed between these two skeleton elements of the head.

## 5 | CONCLUSION

In conclusion, the main evolutionary and developmental patterns appear to be along orthogonal directions of the shape space. Beside these main patterns, most of the shape divergences arise along postnatal directions of growth. The filling of the morphospace varies between rodent suborders being mainly during the gestational period in Hystricomorpha and during the postnatal growth in Myomorpha. The postnatal trajectories of Myomorpha subfamilies are closer, but present a much stronger magnitude of changes over a shorter growth period. Among Hystricomorpha, part of the observed adult shape is set up prenatally, and most postnatal trajectories are genus-specific, which agrees with non-linear developmental trajectories over longer gestational periods. Juvenile mandibles present similarities among suborders, with a flattened shape. Mandible shape then diversifies during growth in relation to muscle and tooth development, with epigenetic interactions coordinating the changes in the alveolar and muscle-bearing regions. This functional integration by biomechanical interactions might have favoured evolutionary changes driven by developmental plasticity, but the importance of this process is likely to differ between rodent suborders.

## ACKNOWLEDGEMENTS

We are grateful to all the curators who allowed us to study their collections: Violaine Nicolas (National Natural History Museum Paris), Loïc Costeur (Natural History Museum Basel), Olivier Pauwels (Royal Belgian Institute of Natural Sciences) and Laurent Vallotton and Manuel Ruedi (Natural History Museum of Geneva). Mathilde Tissier (Hubert Curien Pluridisciplinary Institute) is also thanked for providing access to *Cricetus cricetus* specimens. We thank Lauriane Poloni (Biogéosciences) for help with CT scanning and Remi Laffont (Biogéosciences) for help in data curation. We are grateful to Philip Cox, Vincent Debat, Lionel Hautier and Miriam Leah Zelditch for helpful comments on early versions of the manuscript. We are also grateful to Carmela Chateau-Smith for English editing. The Gismo platform and morphOptics are acknowledged for providing access to 3D scanning. This research project was supported by the AP EPHE-2019.

## CONFLICT OF INTEREST

Authors declare no conflicts of interest.

## AUTHOR CONTRIBUTIONS

All authors contributed to the study design. MD collected species in museum and conducted the phenotyping. MD and NN analysed the data. All authors contributed with edits and comments to analyses and wrote the manuscript.

## PEER REVIEW

The peer review history for this article is available at <https://publons.com/publon/10.1111/jeb.13920>.

## DATA AVAILABILITY STATEMENT

The landmark data that support the findings of this study are openly available in Dryad at <https://doi.org/10.5061/dryad.70rxwdbz4>.

## ORCID

Morgane Dubied  <https://orcid.org/0000-0002-9304-2714>

Sophie Montuire  <https://orcid.org/0000-0002-5341-5344>

Nicolas Navarro  <https://orcid.org/0000-0001-5694-4201>

## REFERENCES

- Adams, D. (2014). A generalized K statistic for estimating phylogenetic signal from shape and other high-dimensional multivariate data. *Systematic Biology*, *63*, 685–697. <https://doi.org/10.1093/sysbio/syu030>
- Adams, D. C., & Collyer, M. L. (2018). Multivariate phylogenetic comparative methods: Evaluations, comparisons, and recommendations. *Systematic Biology*, *67*, 14–31. <https://doi.org/10.1093/sysbio/syx055>
- Adams, D. C., Collyer, M., Kaliontzopoulou, A., & Sherratt, E. (2016). *geomorph: Software for geometric morphometric analyses*. R Package.
- Agostinelli, C., & Lund, U. (2017). R package 'circular': Circular Statistics. R Package.
- Alberch, P. (1980). Ontogenesis and morphological diversification. *American Zoologist*, *20*, 653–667. <https://doi.org/10.1093/icb/20.4.653>
- Alberch, P. (1982). Developmental constraints in evolutionary processes. In J. T. Bonner (Ed.), *Evolution and development* (pp. 313–332). Springer.
- Alberch, P., Gould, S. J., Oster, G. F., & Wake, D. B. (1979). Size and shape in ontogeny and phylogeny. *Paleobiology*, 296–317. <https://doi.org/10.1017/S0094837300006588>
- Alhajeri, B. H., & Stepan, S. J. (2018). Disparity and evolutionary rate do not explain diversity patterns in Muroid rodents (Rodentia: Muroidea). *Evolutionary Biology*, *45*, 324–344. <https://doi.org/10.1007/s11692-018-9453-z>
- Álvarez, A., & Pérez, M. E. (2019). Deep changes in masticatory patterns and masseteric musculature configurations accompanied the eco-morphological evolution of cavioid rodents (Hystricognathi, Caviomorpha). *Mammalian Biology*, *96*, 53–60. <https://doi.org/10.1016/j.mambio.2019.03.009>
- Anderson, P. S., Renaud, S., & Rayfield, E. J. (2014). Adaptive plasticity in the mouse mandible. *BMC Evolutionary Biology*, *14*, 85. <https://doi.org/10.1186/1471-2148-14-85>
- Arnold, S. F. (1981). *The theory of linear models and multivariate analysis*. John Wiley & Sons, Inc.
- Arthur, W. (2001). Developmental drive: an important determinant of the direction of phenotypic evolution. *Evolution & Development*, *3*(4), 271–278. <https://doi.org/10.1046/j.1525-142x.2001.003004271.x>
- Atchley, W. R. (1993). Genetic and developmental aspects of variability in the mammalian mandible. *The Skull*, *1*, 207–247.
- Barone, R. (1976). *Anatomie comparée des mammifères domestiques*. Tome 1: ostéologie (2nd éd.). Vigot Frères.
- Bookstein, F. L. (2016). The inappropriate symmetries of multivariate statistical analysis in geometric morphometrics. *Evolutionary Biology*, *43*, 277–313. <https://doi.org/10.1007/s11692-016-9382-7>
- Boughner, J. C., van Eede, M. C., Spring, S., Yu, L. X., Rostampour, N., & Henkelman, R. M. (2018). P63 expression plays a role in

- developmental rate, embryo size, and local morphogenesis. *Developmental Dynamics*, 247, 779–787. <https://doi.org/10.1002/dvdy.24622>
- Brandt, J. F. (1855). *Beiträge zur nähern Kenntniss der Säugethiere Russlands* (Vol. 7). Kaiserl. Academ. d. Wiss.
- Byrd, K. E. (1981). Mandibular movement and muscle activity during mastication in the guinea pig (*Cavia porcellus*). *Journal of Morphology*, 170, 147–169. <https://doi.org/10.1002/jmor.1051700203>
- Cardini, A., & Thorington, R. W. Jr (2006). Postnatal ontogeny of marmot (Rodentia, Sciuridae) crania: allometric trajectories and species divergence. *Journal of Mammalogy*, 87(2), 201–215. <https://doi.org/10.1644/05-MAMM-A-242R1.1>
- Collyer, M. L., & Adams, D. C. (2018). RRPP: An R package for fitting linear models to high-dimensional data using residual randomization. *Methods in Ecology and Evolution*, 9, 1772–1779.
- Collyer, M. L., & Adams, D. C. (2021). Phylogenetically aligned component analysis. *Methods in Ecology and Evolution*, 12(2), 359–372. <https://doi.org/10.1111/2041-210X.13515>
- Cox, P. G., Rayfield, E. J., Fagan, M. J., Herrel, A., Pataky, T. C., & Jeffery, N. (2012). Functional evolution of the feeding system in rodents. *PLoS One*, 7, e36299. <https://doi.org/10.1371/journal.pone.0036299>
- Curley, J. P., Jordan, E. R., Swaney, W. T., Izraelit, A., Kammel, S., & Champagne, F. A. (2009). The Meaning of weaning: influence of the weaning period on behavioral development in mice. *Developmental Neuroscience*, 31, 318–331. <https://doi.org/10.1159/000216543>
- Darwin, C. (1859). *On the origin of species*. John Murray.
- Dibner, J. J., Richards, J. D., Kitchell, M. L., & Quiroz, M. A. (2007). Metabolic challenges and early bone development. *Journal of Applied Poultry Research*, 16, 126–137. <https://doi.org/10.1093/japr/16.1.126>
- Drake, A. G., & Klingenberg, C. P. (2010). Large-scale diversification of skull shape in domestic dogs: Disparity and modularity. *The American Naturalist*, 175, 289–301. <https://doi.org/10.1086/650372>
- Eble, G. J., Crutchfield, J. P., & Schuster, P. (2003). *Evolutionary dynamics: Exploring the interplay of selection, accident, neutrality, and function*. Oxford University Press.
- Efron, B. (1979). Bootstrap Methods: Another Look at the Jackknife. *The Annals of Statistics*, 7, 1–26. <https://doi.org/10.1214/aos/1176344552>
- Erwin, D. H. (2007). Disparity: Morphological pattern and developmental context. *Palaeontology*, 50, 57–73. <https://doi.org/10.1111/j.1475-4983.2006.00614.x>
- Foote, M. (1994). Morphological disparity in Ordovician-Devonian crinoids and the early saturation of morphological space. *Paleobiology*, 20, 320–344. <https://doi.org/10.1017/S009483730001280X>
- Fusco, G. (2008). *Evolving pathways: Key themes in evolutionary developmental biology*. Cambridge University Press.
- Gerber, S. (2014). Not all roads can be taken: Development induces anisotropic accessibility in morphospace. *Evolution & Development*, 16, 373–381. <https://doi.org/10.1111/ede.12098>
- Ginot, S., Hautier, L., Agret, S., & Claude, J. (2020). Decoupled ontogeny of in vivo bite force and mandible morphology reveals effects of weaning and sexual maturation in mice. *Biological Journal of the Linnean Society*, 129(3), 558–569. <https://doi.org/10.1093/biolinean/blz196>
- Gould, S. J. (1977). *Ontogeny and phylogeny*. Harvard University Press.
- Green, R. M., Fish, J. L., Young, N. M., Smith, F. J., Roberts, B., Dolan, K., Choi, I., Leach, C. L., Gordon, P., Cheverud, J. M., Roseman, C. C., Williams, T. J., Marcucio, R. S., & Hallgrímsson, B. (2017). Developmental nonlinearity drives phenotypic robustness. *Nature Communications*, 8(1), 1–12. <https://doi.org/10.1038/s41467-017-02037-7>
- Gunz, P., Mitteroecker, P., & Bookstein, F. L. (2005). Semilandmarks in three dimensions. In D. E. Slice (Ed.), *Modern morphometrics in physical anthropology* (pp. 73–98). Springer US.
- Hallgrímsson, B., Brown, J. J., Ford-Hutchinson, A. F., Sheets, H. D., Zelditch, M. L., & Jirik, F. R. (2006). The brachymorph mouse and the developmental-genetic basis for canalization and morphological integration. *Evolution & Development*, 8(1), 61–73. <https://doi.org/10.1111/j.1525-142X.2006.05075.x>
- Hallgrímsson, B., & Hall, B. K. (Eds.). (2011). *Epigenetics: Linking genotype and phenotype in development and evolution*. University of California Press.
- Hautier, L. (2010). Masticatory muscle architecture in the gundi *Ctenodactylus vali* (Mammalia, Rodentia). *Mammalia*, 74, 153–162. <https://doi.org/10.1515/mamm.2010.025>
- Hautier, L., Michaux, J., Marivaux, L., & Vianney-Liaud, M. (2008). Evolution of the zygomatic construction in Rodentia, as revealed by a geometric morphometric analysis of the mandible of Graphiurus (Rodentia, Gliridae). *Zoological Journal of the Linnean Society*, 154(4), 807–821.
- Herring, S. W. (2011). Muscle-bone interactions and the development of skeletal phenotype: Jaw muscles and the skull. In B. Hallgrímsson, & B. K. Hall (Eds.), *Epigenetics: Linking genotype and phenotype in development and evolution* (pp. 221–237). University of California Press.
- Hiimäe, K. M., & Ardran, G. M. (1968). A cinefluorographic study of mandibular movement during feeding in the rat (*Rattus norvegicus*). *Journal of Zoology*, 154, 139–154. <https://doi.org/10.1111/j.1469-7998.1968.tb01654.x>
- Houle, D., & Meyer, K. (2015). Estimating sampling error of evolutionary statistics based on genetic covariance matrices using maximum likelihood. *Journal of Evolutionary Biology*, 28(8), 1542–1549. <https://doi.org/10.1111/jeb.12674>
- Huggett, A. S. G., & Widdas, W. F. (1951). The relationship between mammalian foetal weight and conception age. *The Journal of Physiology*, 114, 306–317. <https://doi.org/10.1113/jphysiol.1951.sp004622>
- Jacobs, L. L. (1984). Rodentia: Extraordinary diversification of a morphologically distinctive and stereotyped order. *Series in Geology, Notes for Short Course*, 8, 155–166. <https://doi.org/10.1017/S027116480000944>
- Kavanagh, K. D., Shoval, O., Winslow, B. B., Alon, U., Leary, B. P., Kan, A., & Tabin, C. J. (2013). Developmental bias in the evolution of phalanges. *Proceedings of the National Academy of Sciences U S A*, 110(45), 18190–18195. <https://doi.org/10.1073/pnas.1315213110>
- Klingenberg, C. P. (1998). Heterochrony and allometry: The analysis of evolutionary change in ontogeny. *Biological Reviews*, 73, 79–123. <https://doi.org/10.1017/S000632319800512X>
- Klingenberg, C. P. (2020). Walking on Kendall's shape space: Understanding shape spaces and their coordinate systems. *Evolutionary Biology*, 47, 334–352. <https://doi.org/10.1007/s11692-020-09513-x>
- Klingenberg, C. P., & Navarro, N. (2012). Development of the mouse mandible: A model system for complex morphological structures. *Evolution of the House Mouse*, 135, 149.
- Krzanowski, W. J. (1979). Between-groups comparison of principal components. *Journal of the American Statistical Association*, 74(367), 703–707. <https://doi.org/10.1080/01621459.1979.10481674>
- Laffont, R., & Navarro, N. (2019). *Digitalization of 3D landmarks on mesh*. R Package.
- Li, S. (2011). Concise formulas for the area and volume of a hyperspherical cap. *Asian Journal of Mathematics and Statistics*, 4, 66–70. <https://doi.org/10.3923/ajms.2011.66.70>
- Lieberman, D. E. (2011). Epigenetic integration, complexity, and evolvability of the head: rethinking the functional matrix hypothesis. In B. Hallgrímsson, & B. K. Hall (Eds.), *Epigenetics: Linking genotype and phenotype in development and evolution* (pp. 271–289). University of California Press.
- Maestri, R., Monteiro, L. R., Fornel, R., Upham, N. S., Patterson, B. D., & de Freitas, T. R. O. (2017). The ecology of a continental evolutionary radiation: Is the radiation of sigmodontine rodents adaptive? *Evolution*, 71, 610–632. <https://doi.org/10.1111/evo.13155>

- Magalhães, J. P. D., & Costa, J. (2009). A database of vertebrate longevity records and their relation to other life-history traits. *Journal of Evolutionary Biology*, 22, 1770–1774. <https://doi.org/10.1111/j.1420-9101.2009.01783.x>
- Marcus, L., & Hingst-Zaher, E. (2000). Application of landmark morphometrics to skulls representing the orders of living mammals. *Hystrix, the Italian Journal of Mammalogy*, 11, 27–47.
- Martinez-Maza, C., Freidline, S. E., Strauss, A., & Nieto-Diaz, M. (2016). Bone growth dynamics of the facial skeleton and mandible in Gorilla gorilla and Pan troglodytes. *Evolutionary Biology*, 43(1), 60–80. <https://doi.org/10.1007/s11692-015-9350-7>
- Martinez-Vargas, J., Muñoz-Muñoz, F., Martínez-Maza, C., Molinero, A., & Ventura, J. (2017). Postnatal mandible growth in wild and laboratory mice: Differences revealed from bone remodeling patterns and geometric morphometrics. *Journal of Morphology*, 278, 1058–1074. <https://doi.org/10.1002/jmor.20694>
- Menegaz, R. A., & Ravosa, M. J. (2017). Ontogenetic and functional modularity in the rodent mandible. *Zoology*, 124, 61–72. <https://doi.org/10.1016/j.zool.2017.05.009>
- Meyer, K., & Houle, D. (2013, October). *Sampling based approximation of confidence intervals for functions of genetic covariance matrices*. In Proceedings of Association for the Advancement of Animal Breeding and Genetics (Vol. 20, pp. 523–526).
- Mitteroecker, P., & Bookstein, F. (2009). The Ontogenetic trajectory of the phenotypic covariance matrix, with examples from craniofacial shape in rats and humans. *Evolution*, 63, 727–737. <https://doi.org/10.1111/j.1558-5646.2008.00587.x>
- Navarro, N. (2003). MDA: A MATLAB-based program for morphospace-disparity analysis. *Computers & Geosciences*, 29, 655–664. [https://doi.org/10.1016/S0098-3004\(03\)00043-8](https://doi.org/10.1016/S0098-3004(03)00043-8)
- Nijhout, H. F., & Emlen, D. J. (1998). Competition among body parts in the development and evolution of insect morphology. *Proceedings of the National Academy of Sciences U S A*, 95, 3685–3689. <https://doi.org/10.1073/pnas.95.7.3685>
- Nowak, R. M., & Walker, E. P. (1999). *Walker's mammals of the world* (Vol. 1). JHU press.
- Olsen, B. R., Reginato, A. M., & Wang, W. (2000). Bone development. *Annual Review of Cell and Developmental Biology*, 16, 191–220. <https://doi.org/10.1146/annurev.cellbio.16.1.191>
- Paradis, E., & Schliep, K. (2019). ape 5.0: An environment for modern phylogenetics and evolutionary analyses in R. *Bioinformatics*, 35, 526–528. <https://doi.org/10.1093/bioinformatics/bty633>
- Paradis, M. R., Raj, M. T., & Boughner, J. C. (2013). Jaw growth in the absence of teeth: the developmental morphology of edentulous mandibles using the p63 mouse mutant. *Evolution & Development*, 15(4), 268–279. <https://doi.org/10.1111/ede.12026>
- Ravosa, M. J., López, E. K., Menegaz, R. A., Stock, S. R., Stack, M. S., & Hamrick, M. W. (2008). Using "Mighty Mouse" to understand masticatory plasticity: Myostatin-deficient mice and musculoskeletal function. *Integrative and Comparative Biology*, 48, 345–359. <https://doi.org/10.1093/icb/icn050>
- Renaud, S., Auffray, J.-C., & de la Porte, S. (2010). Epigenetic effects on the mouse mandible: COMMON features and discrepancies in remodeling due to muscular dystrophy and response to food consistency. *BMC Evolutionary Biology*, 10, 28. <https://doi.org/10.1186/1471-2148-10-28>
- Renaud, S., Ledevin, R., Pisanu, B., Chapuis, J. L., Quillfeldt, P., & Hardouin, E. A. (2010). Divergent in shape and convergent in function: Adaptive evolution of the mandible in Sub-Antarctic mice. *Evolution*, 72(4), 878–892. <https://doi.org/10.1111/evo.13467>
- Renaud, S., Pantalacci, S., Quééré, J.-P., Laudet, V., & Auffray, J.-C. (2009). Developmental constraints revealed by co-variation within and among molar rows in two murine rodents. *Evolution & Development*, 11, 590–602. <https://doi.org/10.1111/j.1525-142X.2009.00365.x>
- Renvoisé, E., Kavanagh, K. D., Lazzari, V., Häkkinen, T. J., Rice, R., Pantalacci, S., Salazar-Ciudad, I., & Jernvall, J. (2017). Mechanical constraint from growing jaw facilitates mammalian dental diversity. *Proceedings of the National Academy of Sciences U S A*, 114, 9403–9408. <https://doi.org/10.1073/pnas.1707410114>
- Renvoisé, E., & Montuire, S. (2015). Developmental mechanisms in the evolution of phenotypic traits in rodent teeth. In P. G. C. In, & L. Hautier (Eds.), *Evolution of the Rodents: Advances in phylogeny, functional morphology and development* (pp. 478–509). Cambridge University Press.
- Revell, L. J. (2009). Size-correction and principal components for interspecific comparative studies. *Evolution*, 63(12), 3258–3268. <https://doi.org/10.1111/j.1558-5646.2009.00804.x>
- Revell, L. J. (2012). phytools: an R package for phylogenetic comparative biology (and other things): Phytools: R package. *Methods in Ecology and Evolution*, 3, 217–223. <https://doi.org/10.1111/j.2041-210X.2011.00169.x>
- Richtsmeier, J. T., & Flaherty, K. (2013). Hand in glove: Brain and skull in development and dysmorphogenesis. *Acta Neuropathologica*, 125, 469–489. <https://doi.org/10.1007/s00401-013-1104-y>
- Rohlf, F. J. (2001). Comparative methods for the analysis of continuous variables: Geometric interpretations. *Evolution*, 55(11), 2143–2160. <https://doi.org/10.1111/j.0014-3820.2001.tb00731.x>
- Rohlf, F. J., & Corti, M. (2000). Use of two-block partial least-squares to study covariation in shape. *Systematic Biology*, 49, 740–753. <https://doi.org/10.1080/106351500750049806>
- Salazar-Ciudad, I. (2021). Why call it developmental bias when it is just development? *Biology Direct*, 16, 1–13. <https://doi.org/10.1186/s13062-020-00289-w>
- Schabenberger, O., & Gotway, C. A. (2017). *Statistical methods for spatial data analysis*. CRC Press.
- Schlager, S. (2017). Chapter 9 - Morpho and Rvcg - Shape analysis in R: R-Packages for geometric morphometrics, shape analysis and surface manipulations. In G. Zheng, S. Li, & G. Székely (Eds.), *Statistical shape and deformation analysis* (pp. 217–256). Academic Press.
- Scott, J. E., McAbee, K. R., Eastman, M. M., & Ravosa, M. J. (2014). Teaching an old jaw new tricks: Diet-induced plasticity in a model organism from weaning to adulthood. *Journal of Experimental Biology*, 217, 4099–4107. <https://doi.org/10.1242/jeb.111708>
- Sheets, H. D., & Zelditch, M. L. (2013). Studying ontogenetic trajectories using resampling methods and landmark data. *Hystrix, the Italian Journal of Mammalogy*, 24(1), 67–73.
- Simpson, G. G. (1945). The principles of classification and a classification of Mammals. *Bulletin of the American Museum of Natural History*, 85, 16–350.
- Smith, J. M., Burian, R., Kauffman, S., Alberch, P., Campbell, J., Goodwin, B., Lande, R., Raup, D., & Wolpert, L. (1985). Developmental constraints and evolution: A perspective from the Mountain Lake conference on development and evolution. *The Quarterly Review of Biology*, 60(3), 265–287. <https://doi.org/10.1086/414425>
- Swanson, M. T., Oliveros, C. H., & Esselstyn, J. A. (2019). A phylogenomic rodent tree reveals the repeated evolution of masseter architectures. *Proceedings of the Royal Society B: Biological Sciences U S A*, 286, 20190672.
- Swiderski, D. L., & Zelditch, M. L. (2013). The complex ontogenetic trajectory of mandibular shape in a laboratory mouse. *Journal of Anatomy*, 223, 568–580. <https://doi.org/10.1111/joa.12118>
- Tullberg, T. (1899). *Ueber das System der Nagethiere: eine phylogenetische Studie*. Akademische Buchdruckerei.
- Uller, T., Feiner, N., Radersma, R., Jackson, I. S. C., & Rago, A. (2020). Developmental plasticity and evolutionary explanations. *Evolution & Development*, 22, 47–55. <https://doi.org/10.1111/ede.12314>
- Uller, T., Moczek, A. P., Watson, R. A., Brakefield, P. M., & Laland, K. N. (2018). Developmental bias and evolution: A regulatory network perspective. *Genetics*, 209(4), 949–966. <https://doi.org/10.1534/genetics.118.300995>
- Ungar, P. S. (2010). *Mammal teeth: origin, evolution, and diversity*. JHU Press.

- Webster, M., & Zelditch, M. L. (2005). Evolutionary modifications of ontogeny: Heterochrony and beyond. *Paleobiology*, 31(3), 354–372.
- West-Eberhard, M. J. (2003). *Developmental Plasticity and evolution*. Oxford University Press.
- Wilson, D. E., Mittermeier, R. A., Ruff, S., Martínez-Vilalta, A., & Cavallini, P. (Eds.) (2016). *Handbook of the mammals of the world: lagomorphs and rodents I*. Lynx Edicions.
- Wilson, L. A. B. (2013). Allometric disparity in rodent evolution. *Ecology and Evolution*, 3, 971–984. <https://doi.org/10.1002/ece3.521>
- Wilson, L. A. B., & Sánchez-Villagra, M. R. (2010). Diversity trends and their ontogenetic basis: An exploration of allometric disparity in rodents. *Proceedings of the Royal Society B: Biological Sciences*, 277, 1227–1234.
- Wolff, J. O., & Sherman, P. W. (2008). *Rodent societies: An ecological and evolutionary perspective*. University of Chicago Press.
- Wood, A. E. (1965). Grades and clades among rodents. *Evolution*, 19, 115–130. <https://doi.org/10.1111/j.1558-5646.1965.tb01696.x>
- Young, R. L., & Badyaev, A. V. (2007). Evolution of ontogeny: Linking epigenetic remodeling and genetic adaptation in skeletal structures. *Integrative and Comparative Biology*, 47, 234–244. <https://doi.org/10.1093/icb/icm025>
- Zelditch, M. L., Calamari, Z. T., & Swiderski, D. L. (2016). Disparate postnatal ontogenies do not add to the shape disparity of infants. *Evolutionary Biology*, 43, 188–207. <https://doi.org/10.1007/s11692-016-9370-y>
- Zelditch, M. L., Sheets, H. D., & Fink, W. L. (2003). The ontogenetic dynamics of shape disparity. *Paleobiology*, 29, 139–156. [https://doi.org/10.1666/0094-8373\(2003\)029<0139:TODOSD>2.0.CO;2](https://doi.org/10.1666/0094-8373(2003)029<0139:TODOSD>2.0.CO;2)
- Zelditch, M. L., & Swiderski, D. L. (2011). Epigenetic interactions: The developmental route to functional integration. In B. Hallgrímsson, & B. K. Hall (Eds.), *Epigenetics: Linking genotype and phenotype in development and evolution* (pp. 290–316). University of California Press.
- Zelditch, M. L., Swiderski, D. L., Sheets, H. D., & Fink, W. L. (2004). Chapter 14 - Morphometrics and systematics. In M. L. Zelditch, D. L. Swiderski, H. D. Sheets, & W. L. Fink (Eds.) *Geometric morphometrics for biologists* (pp. 363–381). Academic Press.
- Zelditch, M. L., Wood, A. R., Bonett, R. M., & Swiderski, D. L. (2008). Modularity of the rodent mandible: Integrating bones, muscles, and teeth. *Evolution & Development*, 10, 756–768. <https://doi.org/10.1111/j.1525-142X.2008.00290.x>

#### SUPPORTING INFORMATION

Additional supporting information may be found online in the Supporting Information section.

**How to cite this article:** Dubied, M., Montuire, S., & Navarro, N. (2021). Commonalities and evolutionary divergences of mandible shape ontogenies in rodents. *Journal of Evolutionary Biology*, 00, 1–16. <https://doi.org/10.1111/jeb.13920>





## Chapter 3 – Ontogenetic changes and plasticity across Myomorpha: experimental design



In the previous chapter, ontogenetic shape change of the mandible was observed at a large taxonomic scale but with only two stages. As the ontogenetic trajectories are non-linear, it was therefore essential to provide information on the change in morphology during growth at a finer scale. The most feasible solution was therefore to breed on model organisms whose traits are well known in the literature. The vast majority of the laboratory-raised rodents are Myomorpha (except Guinea pig), which was also a very positive point, as these are the ones in which I was able to observe the greatest magnitude of change between the two stages studied. This is why three species of Myomorpha over the four classic Myomorpha models (the fourth being Rat) were selected in order to describe the morphological changes between birth and adulthood (sexual maturity) through weaning. Thus, the following chapters of this manuscript will focus on a much smaller taxonomic scale but at a finer resolution along the growth path to be placed, this time, from the point of view of developmental processes.

As development involves various tissues, I have sought to follow bone growth, muscle growth and morphological change. It was therefore necessary to test various ways of monitoring tissue changes. For bone, I tried to follow the growth quantitatively with fluorochrome markings and qualitatively with the observation of bone formation/resorption structures by SEM observation. For muscle, I tried to follow the evolution of the quantity of proteins composing the muscle fiber (actin/myosin) by Rt-qPCR. Finally, morphological changes were monitored by geometric morphometrics.

### 3.1 Experimental design

Three different species were bred (Fig 3.1), the mouse (*Mus musculus*: BALB/c), the golden hamster (*Mesocricetus auratus*: RjHan:AURA) and the Mongolian gerbil (*Meriones unguiculatus*: Crl:MON). These animals were bred in the central animal facility of the University of Burgundy (Dijon) and were the subject of a project application reviewed by the ethical committee (Project APAFIS#18405-2019011014262528).

Depending on the species, the number of mothers and offspring varies. Gravid mice and hamsters were obtained from registered suppliers (University of Burgundy facility for mice and Janvier Labs for hamsters), while for gerbils two males and five females (Charles River) were needed in order to carry out matings at the central animal facility. For the mice, six pregnant dams were received and gave birth to litters ranging from four to seven pups. For hamsters, six pregnant dams gave litters ranging from seven to thirteen pups. Five female gerbils were mated with two males, resulting in litters of five to nine pups. The total sample size was therefore forty mice, sixty-one hamsters and forty-two gerbils. Details of the specimens can be found in Annexe 2.

One individual per litter was sacrificed at 7 and 14 day old. After weaning, at 21 days for mice and hamsters or 30 days for the gerbils, the remaining individuals were divided into two groups with different diets. The first group was fed with pellets (Safe® A04) to match the conventional diet. The second group was fed pellets that were transformed into soft food by dipping in

water. The pellets were moistened for 6h in the fridge to obtain a slurry to represent a less mechanically demanding diet. Individuals were collected at 35 and 63 days. Moms were used as 100 days control and so were only fed with conventional food.

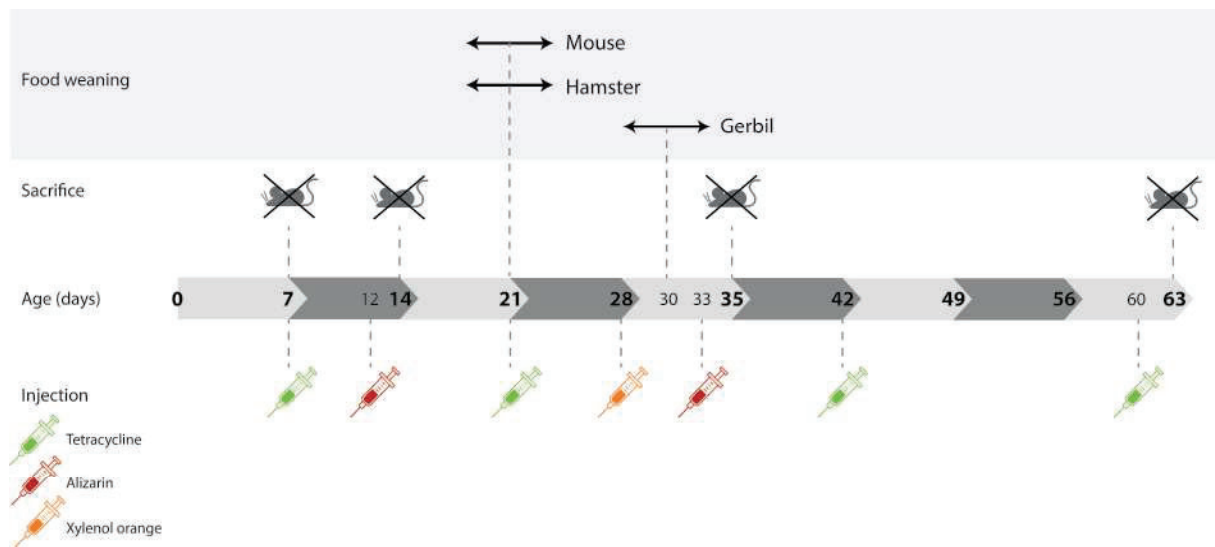


Figure 3.1. Experimental design.

## 3.2 Fluorochromes study

### 3.2.1 Material and methods

Three different fluorochromes were selected in order to be able to recognize the different markers more easily (Table 3.1). These different markers were chosen for their suitability for administration by injection and their dosages are well known in the literature. Three different colors of fluorescence were chosen in order to easily recognize the stages of bone development at the time of microscopic observation.

Tetracycline ( $C_{22}H_{24}N_2O_8$ ) is classically used as a bacteriostatic antibiotic (Chopra & Roberts, 2001). It is also a yellow dye that binds to developing bones and teeth by clumping with calcium on the ossification front (Puranen, 1966). Its molecular weight is 444.44 g/mol.

Alizarin ( $C_{14}H_8O_4$ ) is a red dye from the madder root. It binds to bone during its formation by chelating calcium (Myers, 1968). Its molecular weight is the lowest of the three fluorochromes used at 342.253 g/mol.

Xylenol orange ( $C_{31}H_{32}N_2O_{15}S$ ) is a dye of the triarylmethan family (Horobon, 2020). It is the most molecularly heavy fluorochrome of the three with 760.59 g/mol.

Product	Classic use	Fluorescence color	Dosage for injections	Excitation Emission	Supplier
<b>Tetracycline</b> $C_{22}H_{24}N_2O_8$	Bacteriostatic antibiotic	Green	30 mg/kg Piemontese <i>et al.</i> 2017	390 nm 560 nm	Alfa Aesar™
<b>Alizarin</b> $C_{14}H_8O_4$	Dye	Red	30 mg/kg Pautke <i>et al.</i> 2005	530-560 nm 645 nm	Alfa Aesar™
<b>Xylenol orange</b> $C_{31}H_{32}N_2O_{13}S$	Dye Antioxidant	Orange	90 mg/kg Pautke <i>et al.</i> 2005	546 nm 580 nm	Acros Organics™

**Table 3.1.** Properties and dosage of administered fluorochromes.

These products are in powder form and were mixed with PBS (Fisher Bioreagents) as advised by the European Directive 2010/63/EU for injection. As recommended by the same directive, individuals were injected at 0.02mL of solution per g of animal, intraperitoneally using 25G 0.5mm x 16mm needles (BD Microlance™ 3).

During development, bone undergoes multiple pulses of mineralization and remodeling, in response to various stimuli as hormone fluctuation or mechanical constraint (Kovar *et al.*, 2011). These episodes can be labelled by polychrome labelling (Pautke *et al.* 2005). Polychrome fluorescent labelling is a standard technique used classically to characterize the growth of the bone (Harris, 1960, Frost *et al.* 1969, Lee *et al.* 2003). The principle consists in using calcium-binding fluorochromes which settle in the sites of mineralization. By injecting several fluorochromes (different colors) in intra-peritoneal injection, the sequence of bone growth can be observed. As I aimed to characterize the pattern and timing of mandible growth during postnatal development, I tried to inject these fluorochromes during growth at specific ages, in order to see preferred sites of bone growth and their evolution.

The specimens used in the first instance were as follows (Table 3.2):

Species	Specimen	Litter	Age (Days)	Sex	Food
<b>Mouse</b>	M-E-15J	E	15	-	-
	M-AFH-1	A	35	Female	Hard
	M-BFH-1	B	63	Female	Hard
	M-EFS-1	E	35	Female	Soft
	M-EFS-2	E	63	Female	Soft
<b>Hamster</b>	H-C1MH-1	C1	35	Male	Hard
<b>Gerbil</b>	G-KMH-1	K	35	Male	Hard

**Table 3.2.** Pilot specimens used for fluorochromes observations.

Once the skulls were recovered, they were embedded in LR White resin (Sigma-Aldrich), vacuum bagged for 24 hours and cured for 12 hours at 40°C. Once the plots were formed, they were sawn with a microtome (Leica SP 1600) to a thickness of 300 µm. This thickness was chosen after testing in order to ensure the integrity of the section while allowing its observation. Throughout the process, the samples were kept in a dark box between two manipulations in order to preserve the fluorescence of the fluorochromes.

Observations of these slides were carried out at Ifsttar (Institut français des sciences et technologies des transports, de l'aménagement et des réseaux), on a ZEISS Axio Scope SIP microscope. Several excitation beams were tested (DAPI, GFP, RFP, YFP) and only the use of the DAPI filter allowed the observation of the three fluorochromes.

In light of the results obtained on the pilot specimens (described below) and taking into account the time required to prepare the samples, it was decided to limit the observation analysis to the sole pilot individuals.

The results were uneven across sections and specimens. On most sections, tetracycline markings are visible but discontinuous. Alizarin markings are only visible on some sections (Fig. 3.2 A-B) and no xylene orange markings are visible. Therefore, growth rates could not be estimated from the obtained sections and images.

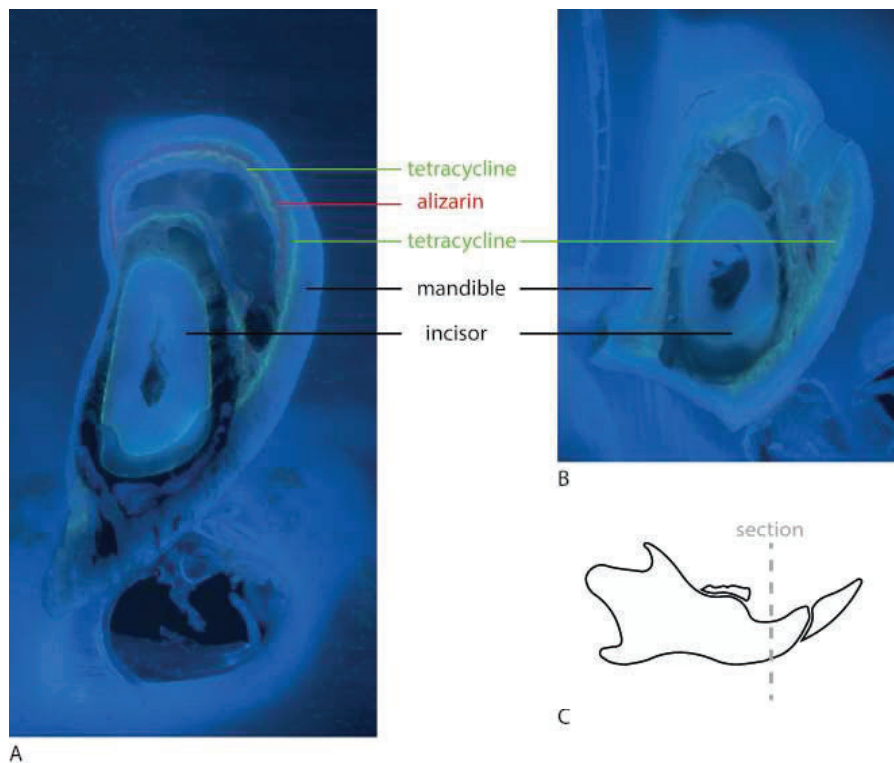


**Figure 3.2.** Section of the right hemi-mandible, observed by fluorescence microscopy, of individuals. A) G-KMH-1. B) M-EFS-2. C) position of the section in the mandible.

### 3.2.2 *Why it probably did not work*

There are several likely explanations for the negative results. Firstly, the individuals were injected intraperitoneally (IP). This means that they were injected into the peritoneum, which is the semi-permeable membrane lining the viscera and abdominal wall (Lichtenstein, 2011). It extends above the blood and lymphatic capillary beds, so fluids injected into this cavity can be rapidly re-absorbed (Baek *et al.*, 2015). This type of injection is easier to perform than an intravenous injection in small organisms but also has some disadvantages such as risks of intra-intestinal injection, which poses little risk to the animals but limits the uptake of fluorochromes. There are also some risks of peritonitis, hemorrhage secondary to blood vessel perforation or accidental organ trauma (Guarnieri, 2016), which are dangerous for the animal's condition, but none of the above-mentioned pathologies has been observed. There is therefore a risk that the injected products have been poorly administered, resulting in poor absorption of the fluorochromes, especially given the high incidence of poor injection even among experienced practitioners, failure rate is reported to be of the order of 10-20 % (Gaines Das & North 2007). Such failure rates suggest that treatment by IP must be monitored by ultrasound scan to validate the administration especially in design with longitudinal treatments as it was used here.

Secondly, although great care was taken to keep the specimens in a dark environment, the entire sawing process had to be carried out in daylight, which could alter the fluorescence ability of the fluorochromes attached to the bone. This step can take up to a full day for a block, which is not necessarily negligible. In order to test this hypothesis, a small portion of the three fluorochromes has been exposed to daylight for one month. The lower intensity of fluorescence observed is the tetracycline one which is well visible on our specimens, this effect seems not to explain the poor observation of alizarin and the absence of xylenol.

Thirdly, the individuals had to be kept in a freezer while waiting to be cleaned by the dermestid beetles. Fluorochromes are usually stored at room temperature for tetracycline and alizarin, at 5°C for xylenol orange. This waiting stage could therefore have deteriorated the fluorochromes. Tetracycline is highly resistant to freezing (Okombe *et al.* 2017). To test this factor, a small portion of the products were kept at -20° during one month. In this case too, the lower intensity of fluorescence observed is the tetracycline one. This factor does not seem to explain my observations.

Finally, xylenol orange has a much higher molecular weight than the other two molecules used. Thus, it is less easily assimilated, which could be the reason for its absence in the observed tissues.

	Control	After one month congelation	After one month at daylight
<b>Tetracycline</b>	1802 ± 4	1650 ± 2	1328 ± 4
<b>Alizarin</b>	2103 ± 3	2017 ± 2	1704 ± 2
<b>Orange xylenol</b>	1900 ± 4	1709 ± 3	1331 ± 1

**Table 3.3.** Fluorescence intensity measured in  $\mu\text{W}/\text{cm}^2$  on the three different fluorochromes in different configurations of conservation: a control one, after on month spent in a freezer at 20°C, after one month at the daylight.

### 3.2.3 If it had worked

The succession of different colored markings at specific ages was intended to be able to recognize sites of greater or lesser ossification. Indeed, the interval between two markings would have made it possible to measure the rate of bone growth over a given period of time. The initial idea was to be able to digitally mark the ossification fronts (fluorescent lines) and then reconstruct a model to visualize the ossification accelerations at given locations in 3D. It would then have been possible to compare these data with the results obtained on the scans presented in chapter 4 to see if the areas of deformation and growth of the mandible were directly consistent with bone remodeling.

### 3.3 Bone microstructure

Adult morphology results from multiple and complex processes including bone growth and remodeling. The bone must accommodate to enable the growth of the individual both allometrically and functionally. The bone is formed and resorbed multiple times by specialized cells coordinated to respond to the extension of bone, but also to different movement undergone by the different skeletal elements between them and/or with the soft tissues (e.g., relocation, primary and secondary displacements, and rotations, Freidline *et al.* 2017). It therefore seemed appropriate to try to document this bone remodeling on our specimen. In this way, we could have mapped the areas of bone resorption and formation. Subsequently it would have been possible to compare the arrangement of these histological remodeling zones with the ones observed on 3D models.

A mandible and a skull of a 15-day-old mouse was observed using SEM to explore the surface of the bone (Figure 3.3). The age of the specimen was chosen because at this stage, the skull undergoes a strong growth. We compared the structures observed to the one seen in the literature (Martinez-Maza *et al.* 2010, 2015).

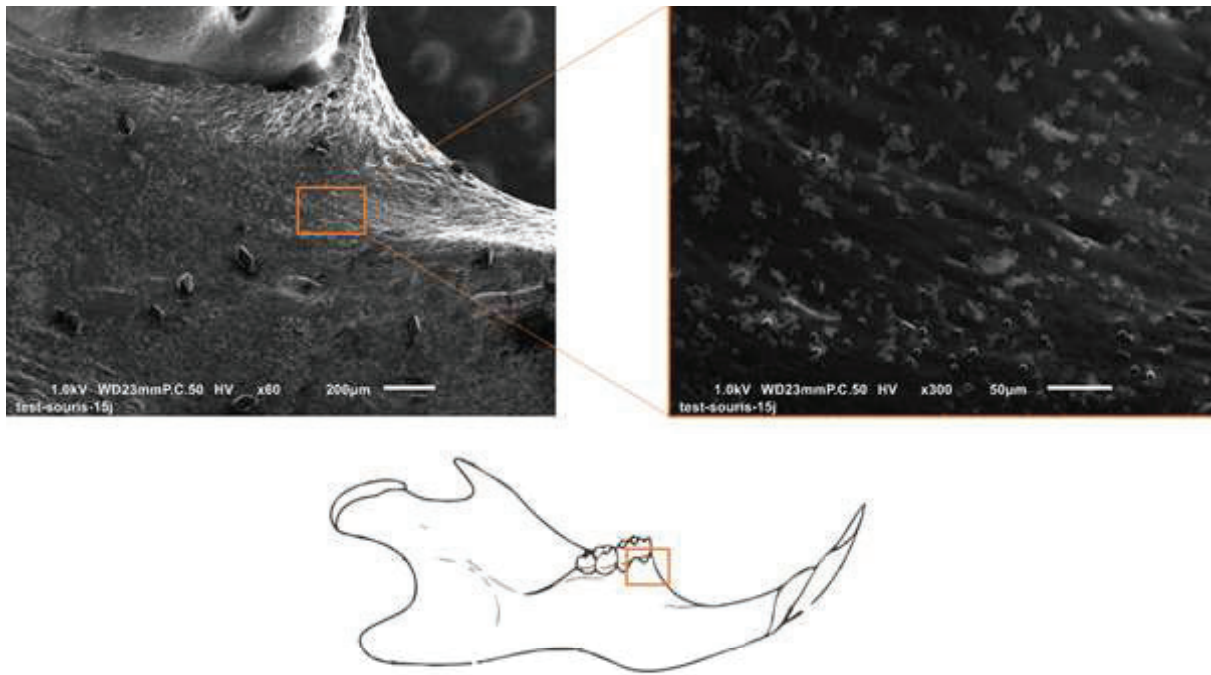


**Figure 3.3.** SEM observation of test specimen.

Unfortunately, the structures were very difficult to assess to resorption or formation. Indeed, the benchmarks present in the literature have been developed on other groups. It would have been necessary to develop our own repository to apply to our specimens, which was not possible during this work. This is why I have abandoned these observations for this thesis work in order to focus on geometric morphometrics.

### 3.4 Myosin study

#### 3.4.1 Material and methods

During development, the various tissues must coordinate to obtain a functional masticatory apparatus (McNeill 2000). The growth of muscles is thus as important as that of the bone, especially the masseteric complex as it is the one involved in structuring the craniofacial complex. The contraction of a single muscle fiber involves the motor unit within each myofibril, called the sarcomere. The sarcomere is composed of two types of filaments: the actin and the myosin protein filaments. The myosin filaments show a greater variety than the actin filaments. The plasticity of the muscle fibers is linked to the isoform diversity of the myosin heavy chain (MHC) which is determinant in the contractile properties of the muscle (Mahdavi *et al.* 1986). The MHC isoforms preferentially expressed in masseter muscles are MHC-IIa (MyH2) and MHC-IIb (MyH4) associated to the actin (Mahdavi *et al.* 1986). Heterogeneity in muscle structure allows adaptability to different developmental (Monemi *et al.* 1996, Raadsheer *et al.* 1996) and functional demands (Auluck *et al.*, 2005) during postnatal development. As muscle development is linked to the functioning of the masticatory apparatus, I wanted to test whether the expression of these two myosin isoforms (Myh2 and Myh4) and actin were expressed in the same way in the two food groups on mouse specimens (Table 3.3), as the primers for this species were already available.

Specimen	Age	Sex	Food	Litter
M-AFH-1	35	F	Hard	A
M-G1FH-1	35	F	Hard	G
M-BMH-1	35	M	Hard	B
M-DMH-1	35	M	Hard	D
M-EMH-1	35	M	Hard	E
M-BFH-1	63	F	Hard	B
M-DFH-1	63	F	Hard	D
M-G2FH-1	63	F	Hard	G
M-JFH-1	63	F	Hard	J
M-AMH-1	63	M	Hard	A
M-EMH-2	63	M	Hard	E
M-Mom-A	100	F	Hard	A
M-Mom-B	100	F	Hard	B
M-Mom-D	100	F	Hard	D
M-Mom-E	100	F	Hard	E
M-Mom-G	100	F	Hard	G
M-Mom-J	100	F	Hard	J

Specimen	Age	Sex	Food	Litter
M-EFS-1	35	F	Soft	E
M-G2FS-1	35	F	Soft	G
M-G2FS-2	35	F	Soft	G
M-G2FS-3	35	F	Soft	G
M-EFS-2	63	F	Soft	E
M-EFS-3	63	F	Soft	E
M-G2FS-4	63	F	Soft	G
M-G2FS-5	63	F	Soft	G
M-JFS-1	63	F	Soft	J
M-JFS-2	63	F	Soft	J
M-JFS-3	63	F	Soft	J
M-G2MS-1	63	M	Soft	G
M-JMS-1	63	M	Soft	J
M-JMS-2	63	M	Soft	J
M-JMS-3	63	M	Soft	J

**Table 3.3.** Specimens used for myosin study.

Masseter biopsies were taken immediately after death and stored in RNAlater solution (Invitrogen) at  $-20^{\circ}\text{C}$ . The expression of myosin and actin in the masseter biopsies was assayed by RT-qPCR. Total RNA was extracted from masseter biopsies with Trizol® (Ambion by life technologies) and quantified by optical density at 260 nm using NanoDrop 2000 (Thermo Scientific). RNA was transcribed into complementary DNA (cDNA) using Moloney murine leukemia virus (M-MLV) reverse transcriptase, random primers ( $0.5 \mu\text{g}/\mu\text{g}$  RNA, Promega) and recombinant RNasin® Plus RNase Inhibitor (Promega). The qPCR was then carried out in 96-well plates in order to quantify the cDNAs using a Master mix PowerUp™ SYBR™ Green (Applied biosystems). mRNA expression was determined using the  $2^{-\Delta\text{Ct}}$  method after GAPDH ( $\Delta\text{Ct}$ ) subtraction. The sense and antisense primers used (Eurogentec) are listed in table 3.4.

Primer (mouse)	Forward	Reverse
MHC-IIa (MyH2)	3' CTCGTTTGCCAGTAAGGGTCT 5'	3' CCCCAGAAAACGGCCATCTC 5'
MHC-IIb (MyH4)	3' TGGGAAATGGAAAGAGGACC 5'	3' GACCATGACTATGCCAGCCC 5'
Actine	3' GGCACCACACCTTCTACAATGAGC 5'	3' CGACCAGAGGCATACAGGGACAG 5'
GAPDH	3' CACTACCGTACCTGACACCA 5'	3' ATGTCGTTGTCCCACCACCT 5'

**Table 3.4.** Sequences of primer used for myosin, actine and GAPDH genes.

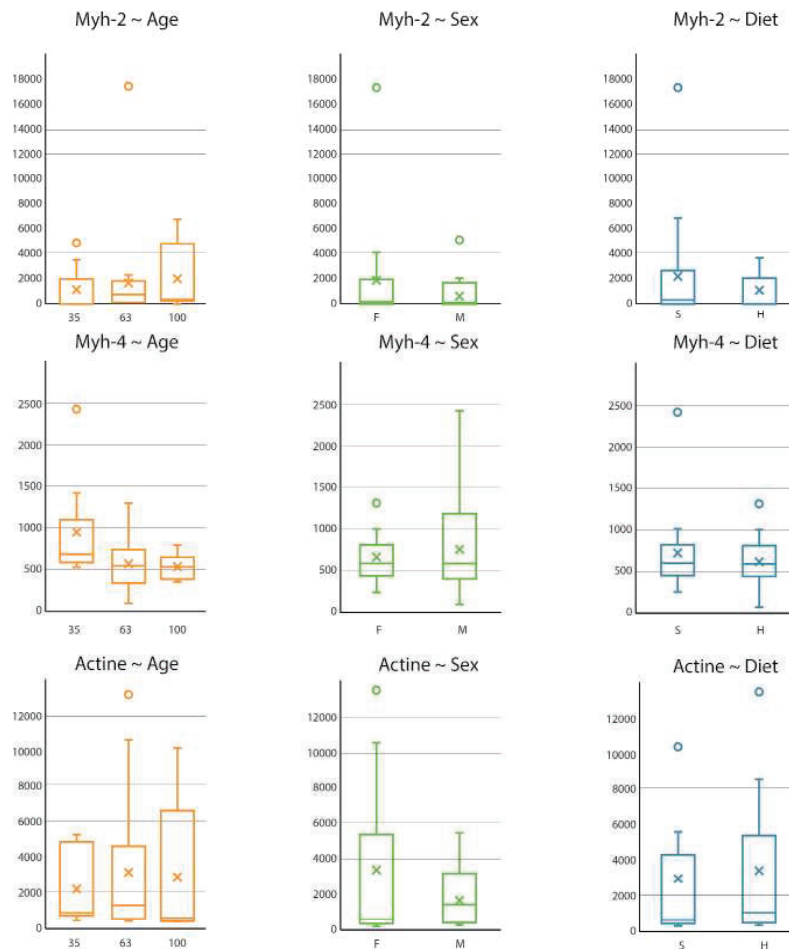


**Figure 3.4.** Quantification of the different genes depending on the age, the sex or the diet.

### 3.4.2 Why it probably did not work

Unfortunately, the housekeeping gene (GAPDH) primer mix turned out to be contaminated, so normalized results are not reliable. In addition, we cannot normalize the amount of myosin by actin since this protein also enters into the composition of the muscle fiber. The amount of RNA extracted from the samples was not sufficient to make replicas, so it is not possible to perform new analysis on these biopsies.

### 3.4.3 If it had worked

It was expected that the amount of myosin and actin expressed would be lower in specimens that had been fed a soft diet. If this had been the case, this could have meant that the production of the proteins that make up the muscle fibers has a close link with the mechanical load applied to these same muscles. Thus, this production would not be entirely linked to protein signaling triggered during development.

If no difference had been observed between the different diet groups, it would have meant that the mechanical constraint does not modify the quality of the muscle fibers during development. The role of mechanical strain will be more discussed in chapter 5.

### 3.5 Acquisition of 3D models and landmarks

Bones were cleaned using dermestid beetles except those of 7-day-old juveniles, the skull being poorly ossified and likely be too damaged by the insects. The cranium and mandibles were scanned by  $\mu$ CT scan (Bruker Skyscan 1174) at 50kV and 800  $\mu$ A (exposition of 5000ms for the 7-day-old specimens, 3000ms for the others). They were then reconstructed using AvizoR9.2 (FEI systems).

On the mandibles, fourteen landmarks were digitized using Digit3DLand R package 0.1.3 (Laffont & Navarro 2019), together with 22 curve semilandmarks along five distinct curves (with two semilandmarks on the coronoid process curve, three along the two lunar notch curves, seven on the curve between postcondylar and angular processes, and ten on the masseter ridge). An atlas was created from a mouse specimen with the PseudoLMGenerator module of the SlicerMorph package (Rolfe *et al.* 2021) on 3D Slicer 4.11 (Fedorov *et al.* 2012), with five patches of surface semi-landmarks totalizing 256 semi-landmarks (Fig. 3.5). This atlas was transferred on all models using the ProjectSemiLM module. Curve and surface semilandmarks were then slid along their tangent by minimizing the bending energy and back-projected on the 3D surfaces (Gunz *et al.* 2005) using the Morpho R package 2.9 (Schlager 2017).

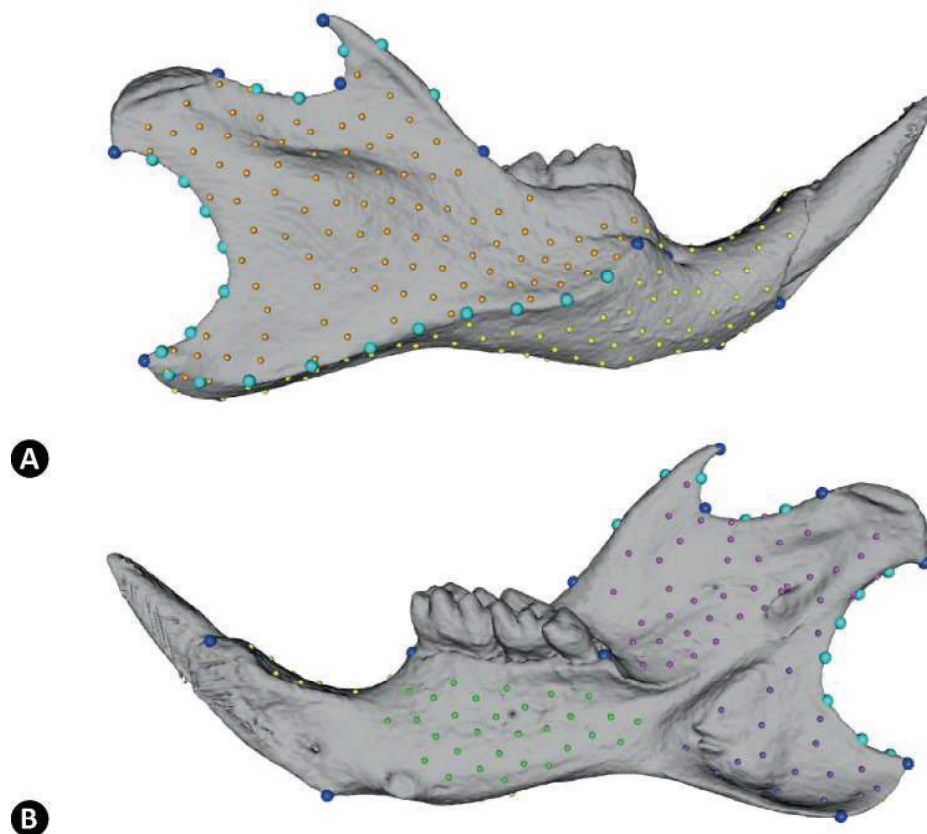


**Figure 3.5.** Landmarking on the mandible, dark blue dots are landmarks, light blue dots are curves landmarks, orange, yellow, pink, purple and green dots are patch-landmarks. A) in lateral external view. B) in lateral internal view.

For skulls, 44 landmarks were digitized using Digit3DLand, 34 of them correspond to one side (left) of paired landmarks (Fig 3.6A). The right side was obtained using a mirroring procedure. The 3D surfaces were mirrored according to their major axes. The 10 unpaired landmarks were used to choose the mirror axis as the one minimizing the distance to the origin. The paired landmarks were then predicted using the ALPACA module of SlicerMorph (Porto *et al.* 2021, Rolfe *et al.* 2021). The mirror surfaces and mirrored left landmarks were used as references. The original surfaces were non-rigidly aligned to the mirror ones according to the default parameters and the right landmarks were predicted after projection into the original surfaces (Fig 3.6B).

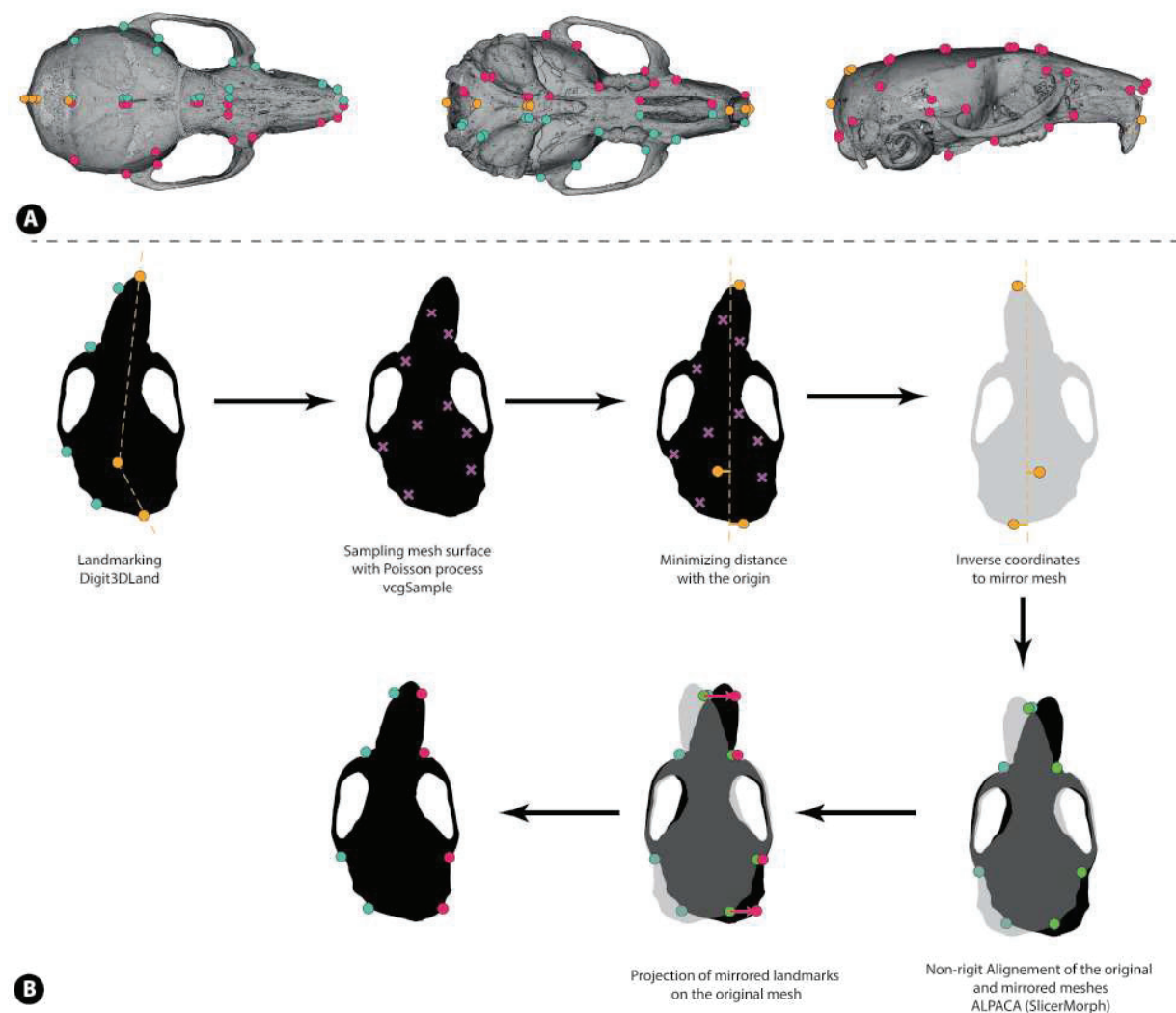


**Figure 3.6.** Skull landmarkings. A) From the left to the right, in upper view, lower view, lateral view; yellow dots are unpaired landmarks, blue dots are paired landmarks, red dots are mirrored landmarks. B) Pipeline used to mirror paired landmarks on skulls.

A pilot study to evaluate this pipeline was done on a set of 28 mice from a AJxB6 backcross (28 day old, Maga et al 2015). These mice were digitize at 55 landmarks from which 23 were paired landmarks and 9 unpaired. The non-rigid alignment using the coherent point drift algorithm was done on  $\alpha$  and  $\beta$  values ranging from 1 to 10 to evaluate the variation in landmarking according to

the deformation process. The root mean squared error (RMSE) between the predicted right landmarks and the original ones was computed as the Euclidean distance between the two landmark conformations standardized by the original centroid size. This RMSE ranges from 0.02 to 0.033. After merging the original left side and the predicted right side, the individuals were also superimposed using a generalized full Procrustes analysis with bilateral symmetry (Klingenberg *et al.* 2002). The principal components analysis on the symmetric component shows a homogeneity of the predictions but some systematic bias compared to the manual shapes. This bias has been well recognized in the first attempts of automatic landmarking (Devine *et al.* 2020, Navarro & Maga 2016, Percival *et al.* 2019), but here, the Procrustes distance between the median of the predicted symmetric shapes and the manual shape is always lower than between two individuals.

## References

- AULUCK, A., MUDERA, V., HUNT, N. P., and LEWIS, M. P. A three-dimensional in vitro model system to study the adaptation of craniofacial skeletal muscle following mechanostimulation. *European journal of oral sciences*, 2005, vol. 113, no 3, p. 218-224.
- BAEK, J. M., KWAK, S. C., KIM, J.-Y., AHN, S.-J., JUN, H. Y., YOON, K.-H., LEE, M. S., and OH, J. Evaluation of a novel technique for intraperitoneal injections in mice. *Lab Animal*, 2015, vol. 44, no 11, p. 440-444.
- CHOPRA, I., and ROBERTS, M. Tetracycline antibiotics: mode of action, applications, molecular biology, and epidemiology of bacterial resistance. *Microbiology and molecular biology reviews*, 2001, vol. 65, no 2, p. 232-260.
- DEVINE, J., APONTE, J. D., KATZ, D. C., LIU, W., LO VERCIO, L. D., FORKET, N. D., MARCUCIO, R., PERCIVAL, C. J., and HALLGRIMSSON, B. A registration and deep learning approach to automated landmark detection for geometric morphometrics. *Evolutionary biology*, 2020, vol. 47, no 3, p. 246-259.
- FEDOROV, A., BEICHEL, R., KALPATHY-CRAMER, J., FINET, J., FILLION-ROBIN, J.-C., PUJOL, S., BAUER, C., JENNINGS, D., FENNESSY, F., SONKA, M., BUATTI, J., AYLWARD, S., MILLER, J. V., PIEPER, S., and KIKINIS, R. 3D Slicer as an image computing platform for the Quantitative Imaging Network. *Magnetic resonance imaging*, 2012, vol. 30, no 9, p. 1323-1341.
- FREIDLINE, S. E., MARTINEZ-MAZA, C., GUNZ, P., and HUBLIN, J.-J. Exploring modern human facial growth at the micro-and macroscopic levels. *Building bones: Bone formation and development in anthropology*, 2017, p. 104-127.
- FROST, H. M. Tetracycline-based histological analysis of bone remodeling. *Calcified tissue research*, 1969, vol. 3, no 1, p. 211-237.
- GAINES DAS, R. and NORTH, D. Implications of experimental technique for analysis and interpretation of data from animal experiments: outliers and increased variability resulting from failure of intraperitoneal injection procedures. *Laboratory animals*, 2007, vol. 41, no 3, p. 312-320.
- GUARNIERI, M. Considering the risks and safety of intraperitoneal injections. *Lab Animal*, 2016, vol. 45, no 4, p. 131-131.
- HARRIS, W. H. A microscopic method of determining rates of bone growth. *Nature*, 1960, vol. 188, no 4755, p. 1038-1039.
- HOROBIN, R. W. Hydroxy triarylmethanes. In : *Conn's Biological Stains*. Taylor & Francis, 2020. p. 203-217.
- KOVAR, J. L., XU, X., DRANEY, D., CUPP, A., SIMPSON, M. A., and OLIVE, D. M.. Near-infrared-labeled tetracycline derivative is an effective marker of bone deposition in mice. *Analytical biochemistry*, 2011, vol. 416, no 2, p. 167-173.
- KLINGENBERG, C. P., BARLUENGA, M., and MEYER, A. Shape analysis of symmetric structures: quantifying variation among individuals and asymmetry. *Evolution*, 2002, vol. 56, no 10, p. 1909-1920.

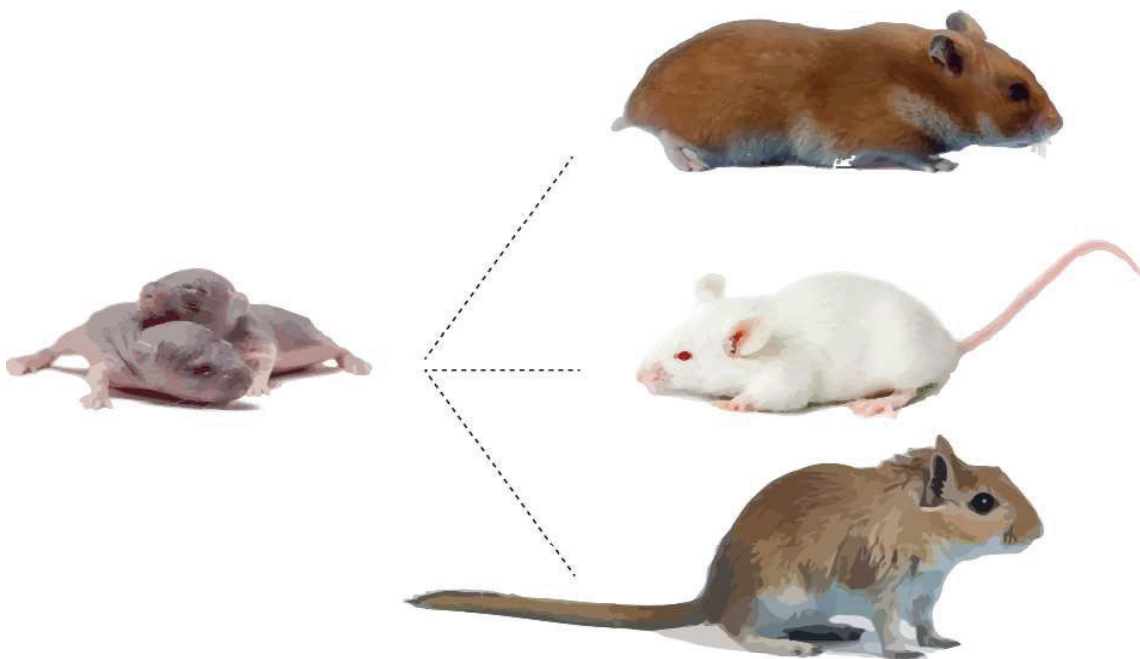
- LAFFONT, R., and NAVARRO, N. Digit3Dland : Digitalization of 3D landmarks on mesh. R package, 2019.
- LEE, J. B., KURODA, S., SHICHINOHE, H., IKEDA, J., SEKI, T., HIDA, K., TADA, M., SAWADA, K.-I., and IWASAKI, Y. Migration and differentiation of nuclear fluorescence-labeled bone marrow stromal cells after transplantation into cerebral infarct and spinal cord injury in mice. *Neuropathology*, 2003, vol. 23, no 3, p. 169-180.
- LICHTENSTEIN, D. A. *L'échographie corps entier chez le patient critique*. Springer Paris, 2012.
- MAHDAVI, V., STREHLER, E. E., PERIASAMY, M., WIECZOREK, D. F., IZUMO, S., and NADAL-GINARD, B. Sarcomeric myosin heavy chain gene family: organization and pattern of expression. *Medicine and Science in Sports and Exercise*, 1986, vol. 18, no 3, p. 299-308.
- MARTINEZ-MAZA, C., FREIDLIN, S. E., STRAUSS, A., and NIETO-DIAZ, M. Bone growth dynamics of the facial skeleton and mandible in Gorilla gorilla and Pan troglodytes. *Evolutionary Biology*, 2016, vol. 43, no 1, p. 60-80.
- MARTINEZ-MAZA, C., ROSAS, A., and NIETO-DIAZ, M. Brief communication: Identification of bone formation and resorption surfaces by reflected light microscopy. *American journal of physical anthropology*, 2010, vol. 143, no 2, p. 313-320.
- MCNEILL, C. Occlusion: what it is and what it is not. *Journal of the California Dental Association*, 2000, vol. 28, no 10, p. 748-758.
- MONEMI, M., ERIKSSON, P.-O., DUBAIL, I., BUTLER-BROWNE, G. S., and THORNELL, L.-E. Fetal myosin heavy chain increases in the human masseter muscle during aging. *FEBS letters*, 1996, vol. 386, no 1, p. 87-90.
- MYERS, H. M. Alizarin and tetracycline binding by bone mineral. *American Journal of Physical Anthropology*, 1968, vol. 29, no 2, p. 179-182.
- OKOMBE, E. V., LUBOYA, L. R., NZUZI, M. G., and PONGOMBO, S. C. Detection des residus d'antibiotiques dans les denrees alimentaires d'origine animale commercialisees a lubumbashi en Republique Democratique du Congo. *Agronomie Africaine*, 2017, vol. 29, no 3, p. 207-216.
- PAUTKE, C., TISCHER, T., VOGT, S., HACZEK, C., DEPPE, H., NEFF, A., HORCH, H.-H., SCHIERKER, M. and KOLK, A. New advances in fluorochrome sequential labelling of teeth using seven different fluorochromes and spectral image analysis. *Journal of anatomy*, 2007, vol. 210, no 1, p. 117-121.
- PERCIVAL, C. J., DEVINE, J., DARWIN, B. C., LIU, W., VAN EEDE, m., HENKELMAN, R. M., and HALLGRIMSSON, B. The effect of automated landmark identification on morphometric analyses. *Journal of anatomy*, 2019, vol. 234, no 6, p. 917-935.
- PIEMONTESE, M., ALMEIDA, M., ROBLING, A. G., KIM, H.-N., XIONG, J., THOSTENSON, J. D., WEINSTEIN, R. S., MANOLAGAS, S. C., O'BRIEN, C. A., and JILKA, R. L. Old age causes de novo intracortical bone remodeling and porosity in mice. *JCI insight*, 2017, vol. 2, no 17.
- PORTO, A., ROLFE, S., et MAGA, A. M. ALPACA: A fast and accurate computer vision approach for automated landmarking of three-dimensional biological structures. *Methods in Ecology and Evolution*, 2021, vol. 12, no 11, p. 2129-2144.

- PURANEN, J. Reorganization of fresh and preserved bone transplants: an experimental study in rabbits using tetracycline labelling. *Acta Orthopaedica Scandinavica*, 1966, vol. 37, no sup92, p. 3-77.
- RAADSHEER, M. C., KILIARIDIS, S., VAN EIJDEN, T. M. G. J., VAN GINKEL, F. C., and PRAHL-ANDERSEN, B. Masseter muscle thickness in growing individuals and its relation to facial morphology. *Archives of oral biology*, 1996, vol. 41, no 4, p. 323-332.
- ROLFE, S., PIEPER, S., PORTO, A., DIAMOND, K., WINCHESTER, J., SHAN, S., KIRVESLAHTI, H., BOYER, D., SUMMERS, A, and MAGA, A. M. SlicerMorph: An open and extensible platform to retrieve, visualize and analyse 3D morphology. *Methods in Ecology and Evolution*, 2021, vol. 12, no 10, p. 1816-1825.
- SCHLAGER, S. Morpho and Rvcg—shape analysis in R: R-packages for geometric morphometrics, shape analysis and surface manipulations. In : *Statistical shape and deformation analysis*. Academic Press, 2017. p. 217-256.





## Chapter 4 – Postnatal development of the craniofacial complex



## Chapter 4 - Postnatal development of the craniofacial complex

The aim of this chapter is to study the two constitutive units of the cranium, the skull and the mandible, to compare their timing and rate of development during the postnatal stages. To this end, the postnatal trajectories of three model species, the hamster, the mouse and the gerbil, are followed on both the mandible and the skull. The monitoring of shape changes during postnatal development has never been documented taking into account the whole craniofacial complex to my knowledge. Furthermore, this monitoring is realized by comparing three phylogenetically close species in order to compare the plastic behavior of these bone structures at both intra- and inter-specific levels.

The two units being very closely related since they are anatomically linked and has to maintain functions, one would expect the skull and the mandible to follow similar timing and rate of development. Nevertheless, these two elements are not totally constrained by the same tissue interactions and therefore should not present the same developmental constraints (Richtsmeier *et al.* 2006). Thus, it is conceivable that these two structures could show different timing in ontogeny on the condition that they remain sufficiently integrated to maintain some efficiency in their common functions.

The first part of this chapter is composed of the study of mandible shape ontogeny, which was accepted to Royal Society Open Science on March 21th, 2022. The second part refers to the study conducted on the skull, completing the data for the entire craniofacial complex. The third part will discuss the morphological integration of these two anatomical structures.

### 4.1 Functional constraints channel mandible shape ontogenies

ROYAL SOCIETY  
OPEN SCIENCE

royalsocietypublishing.org/journal/rsos

Research



**Cite this article:** Dubied M, Montuire S, Navarro N. 2022 Functional constraints channel mandible shape ontogenies in rodents. *R. Soc. Open Sci.* **9**: 220352.

<https://doi.org/10.1098/rsos.220352>

Received: 21 March 2022

Accepted: 31 August 2022

**Subject Category:**

Organismal and evolutionary biology

**Subject Areas:**

evolution

**Keywords:**

geometric morphometrics, mandible shape, ontogeny, rodent

**Authors for correspondence:**

Morgane Dubied

e-mail: [morgane.dubied@u-bourgogne.fr](mailto:morgane.dubied@u-bourgogne.fr)

Sophie Montuire

e-mail: [sophie.montuire@ephe.psl.eu](mailto:sophie.montuire@ephe.psl.eu)

Nicolas Navarro

e-mail: [nicolas.navarro@ephe.psl.eu](mailto:nicolas.navarro@ephe.psl.eu)

Electronic supplementary material is available online at <https://doi.org/10.6084/m9.figshare.c.6250547>.

THE ROYAL SOCIETY  
PUBLISHING

# Functional constraints channel mandible shape ontogenies in rodents

Morgane Dubied<sup>1</sup>, Sophie Montuire<sup>1,2</sup> and Nicolas Navarro<sup>1,2</sup>

<sup>1</sup>Biogéosciences, UMR 6282 CNRS, EPHE, Université Bourgogne Franche-Comté, 6 bd Gabriel, 21000 Dijon, France

<sup>2</sup>EPHE, PSL University, 75014 Paris, France

MD, 0000-0002-9304-2714; SM, 0000-0002-5341-5344; NN, 0000-0001-5694-4201

In mammals, postnatal growth plays an essential role in the acquisition of the adult shape. During this period, the mandible undergoes many changing functional constraints, leading to spatialization of bone formation and remodelling to accommodate various dietary and behavioural changes. The interactions between the bone, muscles and teeth drive this developmental plasticity, which, in turn, could lead to convergences in the developmental processes constraining the directionality of ontogenies, their evolution and thus the adult shape variation. To test the importance of the interactions between tissues in shaping the ontogenetic trajectories, we compared the mandible shape at five postnatal stages on three rodents: the house mouse, the Mongolian gerbil and the golden hamster, using geometric morphometrics. After an early shape differentiation, by both longer gestation and allometric scaling in gerbils or early divergence of postnatal ontogeny in hamsters in comparison with the mouse, the ontogenetic trajectories appear more similar around weaning. The changes in muscle load associated with new food processing and new behaviours at weaning seem to impose similar physical constraints on the mandible, driving the convergences of the ontogeny at that stage despite an early anatomical differentiation. Nonetheless, mice present a rather different timing compared with gerbils or hamsters.

## 1. Introduction

Variation in time and space of developmental processes within an anatomical context will influence the mapping from genotypes to phenotypes [1–5]. Through ontogeny, mechanical forces in relation to cell properties are fundamental in shaping and remodelling tissues [6–9]. The physical constraints experienced by

© 2022 The Authors. Published by the Royal Society under the terms of the Creative Commons Attribution License <http://creativecommons.org/licenses/by/4.0/>, which permits unrestricted use, provided the original author and source are credited.

a growing organism could be similar across a certain range of anatomical contexts, and then may structure in a comparable way the phenotypic variation in influencing the spatialization of the underlying developmental processes. For example, during mammalian postnatal growth, major biomechanical changes in response to diet shift at weaning [10] influence the spatialization of bone remodelling [11–13]. Indeed, changes in muscle strain led to convergences in the developmental processes imposing some directionality in the ontogenetic trajectories despite a relatively diversified anatomical context [14], and constraining, as a consequence, the evolution of ontogenies and the adult shape variation [15]. However, early shape differentiation may have a profound effect on the directionality and intensity of shape changes through ontogenies. For instance, early functional requirements of the jaw or the forelimbs in relation to precocious suckling or crawling in marsupials have constrained the rate of shape evolution and disparity in comparison with eutherians [16–19].

The rodent mandible undergoes major modifications on its posterior part in order to accommodate the growth of masticatory muscles during the postnatal development [20]. These muscle–bone interactions constrain the main direction of shape changes in the mandible ontogeny across a wide range of rodent species [14,21]. Several functional and behavioural factors could affect one or the other component of these interactions. For example, suckling, gnawing and chewing movements have different functional requirements [22] and different diets will imply a different distribution of stresses [23]. Behaviours in relation to siblings or conspecifics (fights for example, [24]) will also have functional demands on the jaws through biting [25]. Changes in the timing and rates of these physical stresses should therefore be associated with shape changes through their modulation by muscle–bone interactions. This mechanism is well studied on adult shape covariation with changes in muscle anatomy and diet [26–28] or in context of ecological radiation [29,30], and it appears to lead to indirect responses of the mandible shape to the various sources of natural and sexual selections [31,32]. Much less is known on how this mechanism constrains ontogeny. A good model system for testing the importance of these interactions in shaping the ontogenies is the major functional shift affecting the mechanical stresses arising at weaning, which recomposes the field of physical constraints applied to the mandible in relation to the changes in muscle load associated with new food processing as well as new behaviours.

In this study, we focus on three rodents belonging to the suborder Myomorpha (the house mouse, Mongolian gerbil and golden hamster), and using geometric morphometrics, we compared the ontogenetic trajectories of the mandible shape at five postnatal stages. In Myomorpha, weaning is early and abrupt, as it occurs over a very short period of time, forcing the mandible to adapt rapidly to the chewing movement. If functional constraints arising at weaning channel the developmental trajectories, changes affecting the shape ontogenies should be similar across the three species despite their early shape divergence. Otherwise, shape differentiation inherited from differences of gestational length or pre-weaning divergence of ontogenies could provide enough variation in the anatomical context to condition the effect of functional constraints in different ways.

## 2. Material and methods

### 2.1. Breeding design and three-dimensional imaging

The specimens were bred in the central animal facility of the University of Burgundy (Project APAFIS#18405-2019011014262528). Six gravid females of mice (*Mus musculus*) were obtained from an internal breeding colony of Balb/c inbred strain at the University of Burgundy. Six gravid females of golden hamsters (*Mesocricetus auratus*) were obtained from the inbred colony of Janvier labs (RjHan: AURA). Gerbils (*Meriones unguiculatus*) were bred from breeding pairs (five females and two males) obtained from Charles River (RjTub:MON). In this study, at least one specimen per family was sacrificed at 7, 14, 35 and 63 days. The 100-day stage is represented by the mothers and, for gerbils, also by the fathers. Skeletons were cleaned using dermestid beetles. After removing broken specimens, 88 mandibles were scanned by  $\mu$ CT scan (Bruker Skyscan 1174) and reconstructed using Avizo® 9.2 (FEI systems). Before landmark digitization, three-dimensional models were decimated to 200 000 faces, using the Rvcg R package 0.18 [33]. Six specimens per species in average represent each stage.

### 2.2. Three-dimensional landmarks and semilandmarks collection

Fourteen landmarks were digitized, together with 22 curve semilandmarks along five distinct curves (with two semilandmarks on the coronoid process curve, three along the two lunar notch curves,

seven on the curve between postcondylar and angular processes, and 10 on the masseter ridge; electronic supplementary material, figure S1). Digitization was done within the Digit3Dland R package 0.1.3 [34]. An atlas was created with five patches of surface semilandmarks totalizing 256 semilandmarks, from a mouse specimen with the PseudoLMGenerator module of the SlicerMorph package [35] on 3D Slicer 4.11 [36]. This atlas was transferred on all models using the ProjectSemiLM module. Curve and surface semilandmarks were then slid along their tangent by minimizing the bending energy and back-projected on the three-dimensional surfaces [37] using the Morpho R package 2.9 [33].

### 2.3. Statistical shape analysis

A full generalized Procrustes analysis (GPA) was performed using the Morpho R package [33]. Procrustes-aligned coordinates were projected on the tangent space at the mean shape and a principal component analysis was performed. Postnatal developmental trajectories were modelled from the expected marginal means of each developmental stage per species estimated from a multivariate linear model according to  $\hat{z} = L\beta$ , with  $L$  the design matrix corresponding to the linear contrasts for the different stages of species, and  $\beta$ , the least-square estimates of shape differences. Significance of the Procrustes sum of squares was evaluated using 1000 residual permutations with the RPP R package 0.5.2 [38]. To check for allometry, an additional model with the effect of the log of the centroid size per species was estimated. The associated regression score [39], which corresponds to the most correlated shape variable to the allometric vectors, was computed.

Ontogenetic trajectories were parallel transported (PT) prior to analysis in order to remove the influences of inter-group shape differences on the shape changes along the trajectories [40]. To do so, and after checking if the variation is small enough, we used the linear shift algorithm, which provides a Euclidean approximation of the PT [41]. Briefly, as ontogenetic trajectories are defined based on discrete postnatal stages, we superimposed the 7-day-old expected marginal means ( $\hat{z}_{a=7}$ ) of each species using a generalized Procrustes analysis without scaling to obtain a common reference ( $\bar{z}_{a=7}$ ). We then superimposed the expected marginal means of all stages on this reference via ordinary Procrustes analysis using the deformetrics R package [42]. Finally, we added the tangent residual of each individual from the linear model to the transported mean of the group to which it belongs ( $\hat{z}_{a=j}^{\text{tr}}$ ) to obtain transported individual values. In other words, we translated the shapes into a common space, centred on the 7-day-old common mean shape. The least-square estimates of shape differences  $\beta$  were updated accordingly  $\beta^{\text{tr}} = L^{-1}\hat{z}^{\text{tr}}$ . Expected marginal means of growth vectors were then obtained from the linear contrast between two successive stages as  $\hat{v} = (L_{a=j} - L_{a=j-1})\beta^{\text{tr}}$ .

### 2.4. Ontogenetic trajectory analysis

To assess the similarity of growth vectors between species, angles between a similar developmental stage  $i$  of two different species,  $j$  and  $k$ , were computed as  $\theta = \cos^{-1}(v_{a=i,j} \cdot v_{a=i,k})$  with the growth vectors  $\hat{v}$  normalized to unit length [43,44]. To assess whether the amount of shape changes between each stage was similar across species, the magnitude of the growth vector between two developmental stages was computed as the norm of the vector. Stepwise magnitude of the trajectories was computed as the sum of the vector norms, which represents the total shape change since birth. The magnitude of each step was further normalized by the growth length in days to allow comparison across growth periods. Approximation of standard errors on magnitudes and angles were computed based on the sampling distribution of  $\beta^{\text{tr}}$  [14,29,45], and according to  $v^* \sim N(\hat{v}, S_e \otimes (L_{a=j} - L_{a=j-1})(X'X)^{-1}(L_{a=j} - L_{a=j-1})')$ , where  $S_e$  is the residual covariance matrix, and  $\otimes$  stands for the Kronecker product. Descriptive statistics on sampled angles were computed with the *circular* R package 0.4-93 [46]. Pairwise differences between trajectories in term of path distances, angles and shapes were evaluated using 1000 permutations [47].

The influence of weaning on the direction of growth was inferred by comparing the trajectory during weaning (14–35 days) with the trajectories immediately before (7–14 days) and after (35–63 days). These changes were computed as the angle ( $\alpha$ ) between these trajectories. As before, standard errors on these angles were computed based on the sampling distribution of  $\beta^{\text{tr}}$ .

Shape changes along the trajectories ( $\hat{v}$ ) were visualized from the common reference ( $\bar{z}_{a=7}$ ). Meshes were deformed using thin plate splines and distances between corresponding vertices were reported as colour on the mesh modelling the end of the trajectory between two developmental stages. These visualizations were computed with the Morpho R package [33].

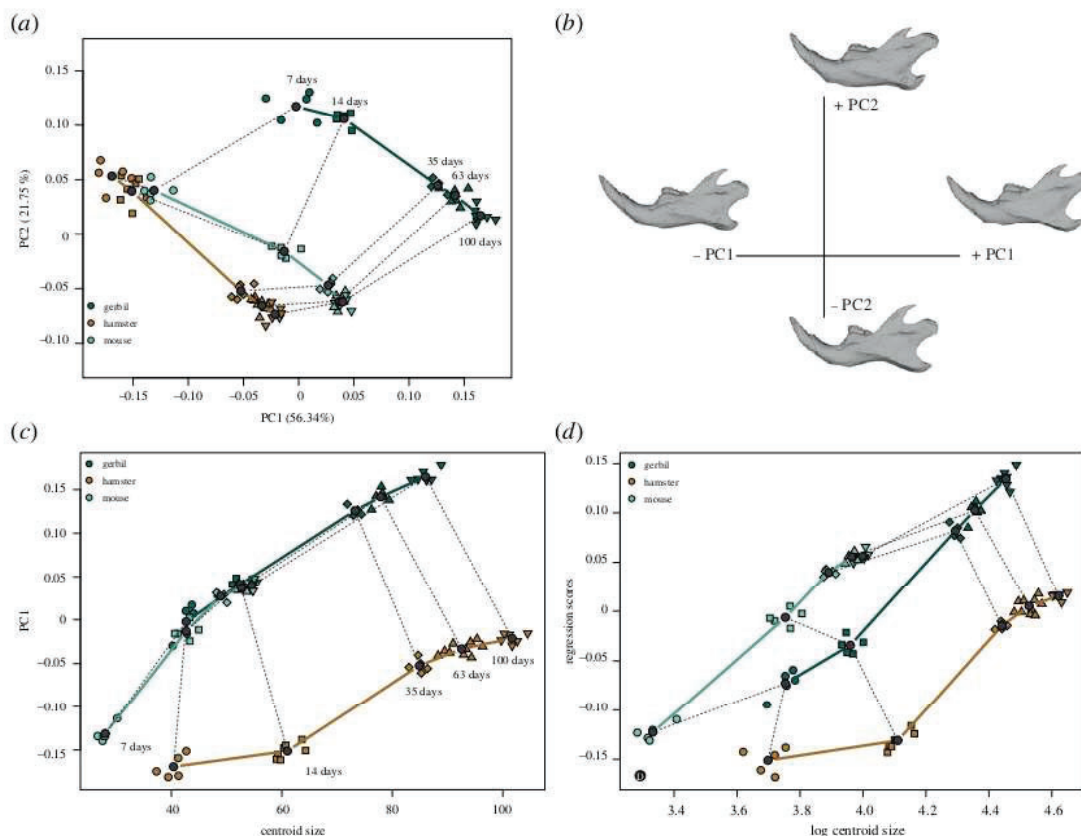


**Figure 1.** Shape variation of the mandible along the postnatal trajectories. (a) First two principal components (PC) of the variation in mandible shapes across ages and taxa. (b) Shape changes in relation to PCs based on a mouse reference mesh. (c) Relationship between PC1 scores and centroid sizes. (d) Regression scores of the allometric model. Dark grey dots represent expected marginal means computed for each age by species group. Dotted lines match equivalent ages across species. Ages are given in days after birth.

### 3. Results

#### 3.1. Allometry and shape variation between species

The first two components of the principal component analysis (PCA) account for 78.09% of the total shape variance (figure 1*a*). Within species  $\times$  age variances are much smaller than the ontogenetic variances (electronic supplementary material, table S1), which spread on the two first components. The 7-day-old hamsters and mice are grouped together with the 14-day-old hamsters in the morphospace. Gerbils appear more distant on these first two components in relation to an important shape difference of the 7-day-old juveniles. PC1 is highly related to the allometric vectors (about  $37^\circ$  for gerbils and mice and  $46^\circ$  for hamsters), and corresponds to shape changes with an elongation of the processes, an expansion of all the masseteric fossa, associated with a compression and straightening of the diastema (figure 1*b*). The shape difference of gerbils compared with mice is mainly related to allometry as the 7-day-old gerbils cluster with the 14-day-old mice on PC1 for a similar size (figure 1*c*). Some non-allometric differences remain, as the regression scores of the two species do not overlap (figure 1*d*).

#### 3.2. Postnatal developmental trajectories

After accounting for shape differences between species using parallel transport, the 7-day-old juveniles are grouped together by design (figure 2*a*), and the trajectories of the two murids (gerbils and mice) traced similar paths, separating from the cricetid (hamsters) on PC2. Thus, gerbils and mice share similar patterns of ontogenetic shape changes (i.e. similar anatomical parts of the mandible are modified in a similar way), whereas hamsters show shape changes along their ontogenetic trajectory

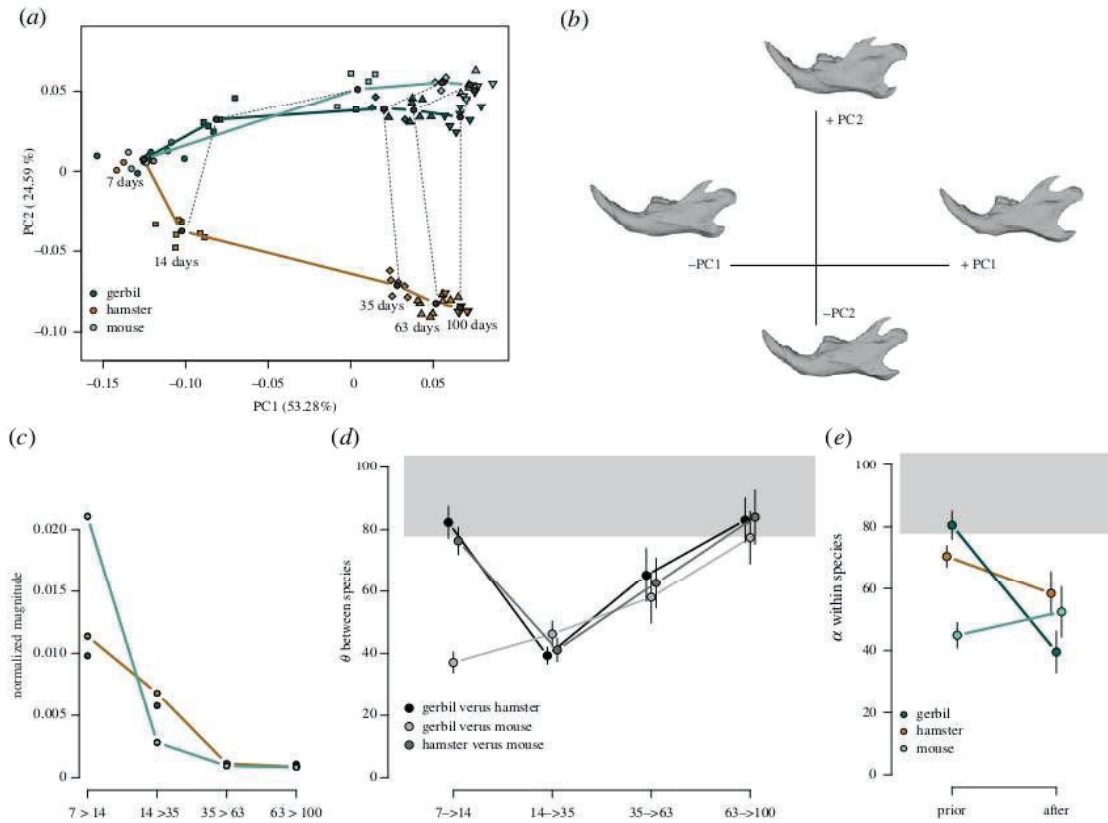


**Figure 2.** Analyses of postnatal trajectories after parallel transport on the common reference (average of the expected marginal means at 7 days). (a) First two parallel transported principal components (PC). (b) Shape changes in relation to parallel transported PCs based on mouse reference mesh. (c) Magnitude (in Procrustes unit per days) of the growth vectors of shape changes between two consecutive developmental stages normalized by the age differences. (d) Angles between growth vectors of two species at the same developmental interval. (e) Angles between the 14–35 days vector and the 7–14 days (prior) or the 35–63 days (after) growth vectors for each species. Error bars represent sampled standard errors.

different from the two other species (i.e. different parts of the mandible are modified or similar ones but in a different manner). The two murids tend towards an adult shape with a wide masseteric fossa whose ventral ridge is very marked, a short coronoid process, a wide condylar process, as well as a shortened and well-verticalized diastema. Cricetids differentiate during development by acquiring a more horizontalized mandible with a less extensive masseteric fossa than in murids, as well as highly developed angular and coronoid processes, deepening the lunar and the posterior notch. The diastema is more flat and more elongated (figure 2*b*). Description of ontogenetic shape changes per species is available in electronic supplementary material, figure S2.

Overall, the amount of shape changes along the ontogeny is similar between species (path distances equal to  $0.26 \pm 0.01$  for gerbils and mice and  $0.28 \pm 0.01$  for hamsters, electronic supplementary material, table S2). By contrast, the timing of these changes differs between species. A striking pattern is the amount of shape changes in mice between 7 and 14 days compared with the two other species (figure 2*c*). When hamsters and gerbils show a similar rate of shape changes (0.011 and 0.009 per day, respectively), in mice, however, this portion of the trajectory is twice as high (0.021 per day). Rate of shape changes decreases drastically in mice (0.002 per day) between 14 and 35 days, while it stays about threefold higher in hamsters (0.006 per day) and gerbils (0.005 per day). From 35 days, whatever the species, the trajectories show minimal rates (between 0.0009 and 0.002 per day). Thus, whereas hamsters and gerbils have comparable rates of shape changes all along their ontogenetic trajectories (rates that seem to drop linearly until 35 days old), the mice show a different shape of their trajectory (electronic supplementary material, table S3) with a very condensed and rapid shape ontogeny.

As suggested above (figure 2*a*), gerbils and mice share quite similar directions of shape changes along their ontogenies (starting with an angle of  $37^\circ$ ), accumulating progressively more differences (figure 2*d*). The average directions of these two trajectories have an angle of  $33.6^\circ$ , but again with a timing shift

between these two species. On the contrary, the hamsters have in the first step a very different direction of shape changes (forming an angle of  $82.30^\circ$  with the gerbils and  $76.39^\circ$  with the mice). However, from 14 days old, the directions of shape changes in hamsters are much more similar to the two other species, with a minimal angle for the shape changes arising between 14 and 35 days ( $\theta = 39.28^\circ$  with the gerbils and  $\theta = 46.20^\circ$  with the mice). At this stage, the shape trajectories are in the direction of the common pattern of growth (transported PC1) with angles ranging from  $23.7^\circ$  for hamsters to  $33^\circ$  for gerbils ( $30.5^\circ$  for mice,  $p < 0.001$ ), and correspond to the enlargement of the ascending ramus (figure 2b). Differences in directions between the hamsters and the two murids accumulate afterwards. The average directions of the three trajectories differ (electronic supplementary material, table S2) but with an angle on average of  $36.7^\circ$  much smaller than expected between two random vectors ( $p < 0.0001$ ).

The directions of shape changes (figure 2e) arising within species prior (7–14 days) to the weaning phase (14–35 days) are quite different to the trajectory during weaning in both the hamsters ( $80.5^\circ$ ) and the gerbils ( $70.5^\circ$ ). On the contrary, the directions after weaning (35–63 days) are much more similar to the weaning phase with angles varying from  $39.5^\circ$  in hamsters to  $58.4^\circ$  in gerbils. In mice, the pattern of differences is more stable with an angle of about  $50^\circ$ , but again, in mice, the ramus enlargement is more precocious in the postnatal growth.

## 4. Discussion

Our result supports a shape differentiation of early young gerbils partly by allometric scaling compared with mice. Gerbils have a longer gestation of 7 days compared with the other two species [48]. This particularity modifies the onset of postnatal period [49] and explains an already differentiated mandible at birth [50]. After birth, gerbils present a similar general trajectory than the two other species but shifted according to this initial offset. Hamsters and mice, despite a large size difference at birth, share a common mandible shape in the first stage of the postnatal growth.

A common pattern of morphological changes during the postnatal development in the three rodent species studied was observed. This pattern is partly related to the allometry. Indeed, the mandible of juveniles presents small processes that will later develop, allowing the growth of the masseteric fossa. In addition, the diastema, which is initially long and flat, will gradually deepen to allow the incisor to become vertical. This repatterning highlights the strong modification of the posterior part of the mandible during early stages of the postnatal growth. Such changes of the mandible have already been observed in mice [20], in the Sciuridae [21] as well as at a larger scale in the Myomorpha and Hystricomorpha [14]. This geometrical re-spatialization is likely to go hand in hand with the development of the masseter muscles, which allow articulation between the skull and the mandible. The posterior part of the mandible develops to accommodate and resist the pressure induced by the activation of these muscles, allowing the transition from sucking to chewing movement during weaning [51].

The amount of shape change occurring throughout the ontogeny is similar across species according to the similar growth duration and despite very different body mass [52]. However, the timing of these changes, i.e. the relative contribution of each stage to the total amount, differs greatly in mice compared with the two others. In gerbils and hamsters, this timing is quite well conserved with most of the changes occurring equally between 7 and 35 days. In hamsters, the first signs of chewing and masseter muscle action are only observed at 14 days [53], and around 16 days in gerbils [54]. Thereby, the mandible of the mouse undergoes major changes from the first stage (7–14 days). Indeed, it has already been shown that the bite force of mouse juveniles increases well before food weaning [55], which may explain early bone remodelling [56]. Early competition among pups and lower parental care in mice [10,57,58] may explain this acceleration of shape development and the correlated functional changes in mice compared with the two other species.

Gerbils and mice share quite similar directions of shape changes along their ontogenetic trajectories, meaning that similar anatomical parts of the mandible are modified in a similar way, and progressively diverge through the ontogeny. The hamsters have, in the first step, a very different direction of shape changes that seems supported by an important growth of the coronoid process. This differentiation is consistent with the known divergences of the mandibular movement during chewing. It contrasts the mouse and gerbil, which chew with a propalinal motion [59–62], to the hamster, which exhibits an oblique motion [59,61]. Anatomical constraints on the jaw movements appear to be established at an early age and may therefore also influence sucking movements. This early onset of specific movements could in turn influence bone growth as human-induced changes do [60]. However, movements may not be strictly constrained and, for instance, propalinal movements have been

observed in hamsters to adapt their chewing to seed processing [63]. Ontogenetic data on the acquisition process of movement types are therefore needed to reach any robust conclusion but are not yet documented to our knowledge.

After these early anatomical differences, the ontogenetic trajectories of the three species become more similar between 14 and 35 days. This channelling of the ontogenetic variation corresponds to shape changes in the direction of the main pattern of changes (parallel transported PC1), which appears to be related to the expansion of the ascending ramus. The transition of mandible movement between sucking and chewing occurs at around 21 days for mice and hamsters [64,65] and 30 days for gerbils [48]. This transition implies new mechanical constraints on the bone [66], which may explain the convergence of the directions of change at this stage between the three species. If the early divergence of the trajectories relates to the movement acquisition, then their convergence at weaning is probably more related to the functional load of the mandible by muscles than to the movements themselves. Reduction in muscle mass or activity by the use of soft diet, surgical intervention or in the case of muscular dystrophy led to smaller condyle and reduction in the height of the ramus [67] in agreement with the observed pattern of shape changes.

In mice, the directions of shape changes before and after weaning are just as different from the changes that occur during the weaning phase. Indeed, the intense shape changes occurring before 14 days in this species may explain this similarity. In hamsters and gerbils, the directions of shape changes within species prior to the weaning are quite different to the trajectory during weaning. As expected, if the mechanical forces induced by mastication influence growth [68,69], the directions after weaning are much more similar to the direction of shape changes during the weaning phase for these two species than the prior-weaning trajectories. Thus, in hamsters and gerbils, the weaning period seems to have a significant impact on shape ontogeny in implying similar local bone growth in relation to the functional constraints. The mechanical stresses of occlusion and masticatory function during this period implied an adaptive response of the bone both in term of anatomy [10] and structure [60,70]. Changes in feeding behaviour are associated with changes in social behaviour (behavioural weaning) with the mother and other juveniles [61,62,71]. Fighting or playing with siblings for example [24] will also contribute to the total physical stress applied to the mandible and therefore will contribute to the effect of bone loading on shape changes occurring at this period. This bone response at both structural and anatomical levels could allow an indirect response to some potential selection arising at this stage among siblings and conspecifics. This indirect process may then have driven some mandibular shape divergences over time.

## 5. Conclusion

Throughout the postnatal ontogeny, similar shape changes, with an increase in the posterior part of the bone and a straightening of the diastema, are observed across the three rodent species. Nonetheless, mice present very different timing compared with the gerbils or the hamsters. The mouse mandible undergoes most of its changes just before weaning, thus inducing little shape modifications during and especially after this event, which may be related to the early increase of bite force observed in the literature. On the other hand, the longer gestational period of the gerbil seems to condition a time-shifted trajectory and a mandibular shape divergence partly by allometric scaling in comparison with the mouse. After an early shape divergence between subfamilies, muscular loading and other mechanical stresses arising around weaning drive similarly the ontogenetic shape changes in both gerbils and hamsters, consistent with the earlier changes observed in mice.

**Ethics.** Breeding of animals used in this study complies with all local guidelines and was conducted in compliance with Université de Bourgogne Animal Care and Use Committee protocol APAFIS#18405-2019011014262528.

**Data accessibility.** Data are available at the Dryad Digital Repository (<https://doi.org/10.5061/dryad.ffbg79cx3>) [72]. All analytical codes are available in R packages or open software Slicer.

The data are provided in electronic supplementary material [73].

**Authors' contributions.** M.D.: conceptualization, data curation, formal analysis, investigation, methodology, writing—original draft, writing—review and editing; S.M.: conceptualization, funding acquisition, investigation, supervision, writing—original draft, writing—review and editing; N.N.: conceptualization, formal analysis, funding acquisition, investigation, methodology, software, supervision, writing—original draft, writing—review and editing.

All authors gave final approval for publication and agreed to be held accountable for the work performed therein.

**Conflict of interest declaration.** We declare we have no competing interests.

**Funding.** This research project was supported by the AP EPHE-2019 to S.M. and N.N.

**Acknowledgements.** We thank the Centre of Zootechnie of the Université de Bourgogne for animal husbandry. We are grateful to Lauriane Poloni (Biogéosciences) for help with CT scanning, and Remi Laffont (Biogéosciences) for help in data curation. The Gismo platform is acknowledged for providing access to 3D scanning. We also thank P. David Polly for his constructive comments on the manuscript.

## References

- Debat V, David P. 2001 Mapping phenotypes: canalization, plasticity and developmental stability. *Trends Ecol. Evol.* **16**, 555–561. (doi:10.1016/S0169-5347(01)02266-2)
- Alberch P. 1982 Developmental constraints in evolutionary processes. In *Evolution and development* (ed. JT Bonner), pp. 313–332. Dahlem Workshop Reports. Berlin, Germany: Springer.
- Salazar-Ciudad I, Jemvall J, Newman SA. 2003 Mechanisms of pattern formation in development and evolution. *Development* **130**, 2027–2037. (doi:10.1242/dev.00425)
- Milocco L, Salazar-Ciudad I. 2020 Is evolution predictable? Quantitative genetics under complex genotype-phenotype maps. *Evolution* **74**, 230–244. (doi:10.1111/evo.13907)
- Hallgrímsson B, Mio W, Marcucio RS, Spritz R. 2014 Let's face it—complex traits are just not that simple. *PLoS Genet.* **10**, e1004724. (doi:10.1371/journal.pgen.1004724)
- Lecuit T, Lenne PF. 2007 Cell surface mechanics and the control of cell shape, tissue patterns and morphogenesis. *Nat. Rev. Mol. Cell Biol.* **8**, 633–644. (doi:10.1038/nrm2222)
- Salazar-Ciudad I, Jemvall J. 2010 A computational model of teeth and the developmental origins of morphological variation. *Nature* **464**, 583–586. (doi:10.1038/nature08838)
- Valet M, Siggia ED, Brivanlou AH. 2022 Mechanical regulation of early vertebrate embryogenesis. *Nat. Rev. Mol. Cell Biol.* **23**, 169–184. (doi:10.1038/s41580-021-00424-z)
- Thompson WR, Rubin CT, Rubin J. 2012 Mechanical regulation of signaling pathways in bone. *Gene* **503**, 179–193. (doi:10.1016/j.gene.2012.04.076)
- Curley JP, Jordan ER, Swaney WT, Izraelit A, Kammel S, Champagne FA. 2009 The meaning of weaning: influence of the weaning period on behavioral development in mice. *Dev. Neurosci.* **31**, 318–331. (doi:10.1159/000216543)
- Herring SW. 2011 *Muscle–bone interactions and the development of skeletal phenotype: jaw muscles and the skull*, pp. 771–737. Berkeley, CA: University of California Press.
- Zelditch ML, Swiderski DL. 2011 Epigenetic interactions: the developmental route to functional integration. In *Epigenetics linking genotype and phenotype in development and evolution* (eds B Hallgrímsson, BK Hall), pp. 290–316. Oakland, CA: University of California Press.
- Zelditch ML, Wood AR, Bonett RM, Swiderski DL. 2008 Modularity of the rodent mandible: integrating bones, muscles, and teeth. *Evol. Dev.* **10**, 756–768. (doi:10.1111/j.1525-142X.2008.00290.x)
- Dubied M, Montuire S, Navarro N. 2021 Commonalities and evolutionary divergences of mandible shape ontogenies in rodents. *J. Evol. Biol.* **34**, 1637–1652. (doi:10.1111/jeb.13920)
- Hallgrímsson B, Hall BK. 2011 *Epigenetics: linking genotype and phenotype in development and evolution*, p. 468. Berkeley, CA: University of California Press.
- Fabre AC, Dowling C, Portela Miguez R, Fernandez V, Noirault E, Goswami A. 2021 Functional constraints during development limit jaw shape evolution in marsupials. *Proc. R. Soc. B* **288**, 20210319. (doi:10.1098/rspb.2021.0319)
- Goswami A, Randau M, Polly PD, Weisbecker V, Bennett CV, Hautier L, Sánchez-Villagra MR. 2016 Do developmental constraints and high integration limit the evolution of the marsupial oral apparatus? *Integr. Comp. Biol.* **56**, 404–415. (doi:10.1093/icb/icw039)
- Conith AJ, Meagher MA, Dumont ER. 2022 The influence of divergent reproductive strategies in shaping modularity and morphological evolution in mammalian jaws. *J. Evol. Biol.* **35**, 164–179. (doi:10.1111/jeb.13944)
- Sears KE. 2009 Differences in the timing of prechondrogenic limb development in mammals: the marsupial–placental dichotomy resolved. *Evolution* **63**, 2193–2200. (doi:10.1111/j.1558-5646.2009.00690.x)
- Swiderski DL, Zelditch ML. 2013 The complex ontogenetic trajectory of mandibular shape in a laboratory mouse. *J. Anat.* **223**, 568–580. (doi:10.1111/joa.12118)
- Zelditch ML, Calamari ZT, Swiderski DL. 2016 Disparate postnatal ontogenies do not add to the shape disparity of infants. *Evol. Biol.* **43**, 188–207. (doi:10.1007/s11692-016-9370-y)
- Herring SW. 1985 The ontogeny of mammalian mastication. *Am. Zool.* **25**, 339–350. (doi:10.1093/icb/25.2.339)
- Thomson JJ. 1991 Cranial strength in relation to estimated biting forces in some mammals. *Can. J. Zool.* **69**, 2326–2333. (doi:10.1139/z91-327)
- Wolff JO, Sherman PW. 2008 *Rodent societies: an ecological and evolutionary perspective*, p. 627. Berkeley, CA: University of Chicago Press.
- Blanchard RJ, Hebert MA, Ferrari P, Palanza P, Figueira R, Blanchard DC, Parmigiani S. 1998 Defensive behaviors in wild and laboratory (Swiss) mice: the mouse defense test battery. *Physiol. Behav.* **65**, 201–209. (doi:10.1016/S0031-9384(98)00012-2)
- Brassard C, Merlin M, Mondhôte-Leroy E, Guintard C, Barrat J, Callou C, Cornette R, Herrel A. 2020 How does masticatory muscle architecture covary with mandibular shape in domestic dogs? *Evol. Biol.* **47**, 133–151. (doi:10.1007/s11692-020-09499-6)
- Fabre AC, Perry JMG, Hartstone-Rose A, Lowie A, Boens A, Dumont M. 2018 Do muscles constrain skull shape evolution in strepsirrhines? *Anat. Rec.* **301**, 291–310. (doi:10.1002/ar.23712)
- Spassov A, Toro-Ibacache V, Krautwald M, Brinkmeier H, Kupczik K. 2017 Congenital muscle dystrophy and diet consistency affect mouse skull shape differently. *J. Anat.* **231**, 736–748. (doi:10.1111/joa.12664)
- Missagia RV, Patterson BD, Kentzel D, Perini FA. 2021 Insectivory leads to functional convergence in a group of Neotropical rodents. *J. Evol. Biol.* **34**, 391–402. (doi:10.1111/jeb.13748)
- Maestri R, Patterson BD, Fornel R, Monteiro LR, De Freitas TRO. 2016 Diet, bite force and skull morphology in the generalist rodent morphotype. *J. Evol. Biol.* **29**, 2191–2204. (doi:10.1111/jeb.12937)
- Klingenberg CP, Leamy LJ. 2001 Quantitative genetics of geometric shape in the mouse mandible. *Evolution* **55**, 2342–2352. (doi:10.1111/j.0014-3820.2001.tb00747.x)
- Klingenberg CP, Navarro N. 2012 Development of the mouse mandible: a model system for complex morphological structures. In *Evolution of the house mouse* (eds M Macholán, SJE Baird, J Piálek). Cambridge, UK: Cambridge University Press.
- Schlager S. 2017 Morpho and Rvcg – shape analysis in R: R-packages for geometric morphometrics, shape analysis and surface manipulations. In *Statistical shape and deformation analysis* (eds G Zheng, S Li, G Székely), pp. 217–256. New York, NY: Academic Press.
- Laffont R, Navarro N. 2019 *Digitalization of 3D landmarks on mesh*. Dijon, France: R Package.
- Rolfe S, Davis C, Maga M. 2021 Comparing semi-landmarking approaches for analyzing three-dimensional cranial morphology. *Am. J. Phys. Anthropol.* **175**, 227–237. (doi:10.1002/ajpa.24214)
- Fedorov A, et al. 2012 3D Slicer as an image computing platform for the Quantitative Imaging Network. *Magn. Reson. Imaging* **30**, 1323–1341. (doi:10.1016/j.mri.2012.05.001)
- Gunz P, Mitteroecker P, Bookstein FL. 2005 Semilandmarks in three dimensions. In *Modern morphometrics in physical anthropology* (ed. DE Slice), pp. 73–98. Developments in Primatology: Progress and Prospects. Boston, MA: Springer US.
- Collyer ML, Adams DC. 2018 RRRP: an R package for fitting linear models to high-dimensional data using residual randomization.

- Methods Ecol. Evol.* **9**, 1772–1779. (doi:10.1111/2041-210X.13029)
39. Drake AG, Klingenberg CP. 2010 Large-scale diversification of skull shape in domestic dogs: disparity and modularity. *Am. Nat.* **175**, 289–301. (doi:10.1086/650372)
  40. Piras P, Teresi L, Traversetti L, Varano V, Gabriele S, Kotsakis T, Raia P, Puddu PE, Scalici M. 2016 The conceptual framework of ontogenetic trajectories: parallel transport allows the recognition and visualization of pure deformation patterns. *Evol. Dev.* **18**, 182–200. (doi:10.1111/ede.12186)
  41. Piras P, Evangelista A, Gabriele S, Nardinocchi P, Teresi L, Torromeo C, Schiariti M, Varano V, Puddu PE. 2014 4D-analysis of left ventricular heart cycle using Procrustes motion analysis. *PLoS ONE* **9**, e86896. (doi:10.1371/journal.pone.0086896)
  42. Piras P et al. 2021 *Deformetrics: R functions for shape analysis*. Rome, Italy: R Package.
  43. Klingenberg CP. 1998 Heterochrony and allometry: the analysis of evolutionary change in ontogeny. *Biol. Rev.* **73**, 79–123. (doi:10.1017/S000632319800512X)
  44. Zelditch ML, Lundrigan BL, Garland Jr T. 2004 Developmental regulation of skull morphology. I. Ontogenetic dynamics of variance. *Evol. Dev.* **6**, 194–206.
  45. Houle D, Meyer K. 2015 Estimating sampling error of evolutionary statistics based on genetic covariance matrices using maximum likelihood. *J. Evol. Biol.* **28**, 1542–1549. (doi:10.1111/jeb.12674)
  46. Agostinelli C, Lund U. 2017 *R package 'circular': circular statistics*. Venice, Italy: R package.
  47. Adams DC, Collyer ML. 2009 A general framework for the analysis of phenotypic trajectories in evolutionary studies. *Evol. Int. J. Org. Evol.* **63**, 1143–1154. (doi:10.1111/j.1558-5646.2009.00649.x)
  48. Norris M, Adams C. 1972 Mortality from birth to weaning in the Mongolian gerbil, *Meriones unguiculatus*. *Lab. Anim.* **6**, 49–53. (doi:10.1258/002367772781082703)
  49. Green RM, et al. 2017 Developmental nonlinearity drives phenotypic robustness. *Nat. Commun.* **8**, 1970. (doi:10.1038/s41467-017-02037-7)
  50. Huggett ASG, Widdas WF. 1951 The relationship between mammalian foetal weight and conception age. *J. Physiol.* **114**, 306–317. (doi:10.1113/jphysiol.1951.sp004622)
  51. Scott JE, Mcabee KR, Eastman MM, Ravosa MJ. 2014 Teaching an old jaw new tricks: diet-induced plasticity in a model organism from weaning to adulthood. *J. Exp. Biol.* **217**, 4099–4107. (doi:10.1242/jeb.111708)
  52. De Magalhães JP, Costa J. 2009 A database of vertebrate longevity records and their relation to other life-history traits. *J. Evol. Biol.* **22**, 1770–1774. (doi:10.1111/j.1420-9101.2009.01783.x)
  53. Lakars TC, Herring SW. 1980 Ontogeny of oral function in hamsters (*Mesocricetus auratus*). *J. Morphol.* **165**, 237–254. (doi:10.1002/jmor.1051650303)
  54. Kaplan H, Hyland SO. 1972 Behavioural development in the Mongolian gerbil (*Meriones unguiculatus*). *Anim. Behav.* **20**, 147–154. (doi:10.1016/S0003-3472(72)80185-4)
  55. Ginot S, Hautier L, Agret S, Claude J. 2020 Decoupled ontogeny of *in vivo* bite force and mandible morphology reveals effects of weaning and sexual maturation in mice. *Biol. J. Linn. Soc.* **129**, 558–569. (doi:10.1093/biolinnean/blz196)
  56. Martínez-Maza C, Montes L, Lamrous H, Ventura J, Cubo J. 2012 Postnatal histomorphogenesis of the mandible in the house mouse. *J. Anat.* **220**, 472–483. (doi:10.1111/j.1469-7580.2012.01488.x)
  57. González-Mariscal G, Poindron P. 2002 Parental care in mammals: immediate internal and sensory factors of control. In *Hormones, brain and behavior* (eds DW Pfaff, AP Arnold, SE Fahrbach, AM Etgen, RT Rubin), pp. 215–298. San Diego, CA: Academic Press.
  58. Weber EM, Olsson IAS. 2008 Maternal behaviour in *Mus musculus* sp.: an ethological review. *Appl. Anim. Behav. Sci.* **114**, 1–22. (doi:10.1016/j.applanim.2008.06.006)
  59. Charles C, Jaeger JJ, Michaux J, Viriot L. 2007 Dental microwear in relation to changes in the direction of mastication during the evolution of Myodonta (Rodentia, Mammalia). *Naturwissenschaften* **94**, 71–75. (doi:10.1007/s00114-006-0161-7)
  60. Nakamura A, Zeredo JL, Utsumi D, Fujishita A, Koga Y, Yoshida N. 2013 Influence of malocclusion on the development of masticatory function and mandibular growth. *Angle Orthod.* **83**, 749–757. (doi:10.2319/083012-698.1)
  61. Tiphaine C, Yaowalak C, Cyril C, Helder G-R, Jacques M, Paul T, Monique V-L, Laurent V, Vincent L. 2013 Correlated changes in occlusal pattern and diet in stem Murinae during the onset of the radiation of old world rats and mice. *Evolution.* **67**, 3323–3338. (doi:10.1111/evo.12172)
  62. Butler PM. 1985 Homology of cusps and crests, and their bearing on assessments of rodent phylogeny. In *Evolutionary relationships among rodents* (eds WP Luckett, J-L Hartenberger), pp. 381–401. New York, NY: Plenum.
  63. Gomiak GC. 1977 Feeding in golden hamsters, *Mesocricetus auratus*. *J. Morphol.* **154**, 427–458. (doi:10.1002/jmor.1051540305)
  64. Damian I, Ramírez JM. 1994 Influence of timing of post-weaning isolation on play fighting and serious aggression in the male golden hamster (*Mesocricetus auratus*). *Aggress. Behav.* **20**, 115–122. (doi:10.1002/1098-2337(1994)20:2<115::AID-AB2480200204>3.0.CO;2-J)
  65. Kikusui T, Takeuchi Y, Mori Y. 2004 Early weaning induces anxiety and aggression in adult mice. *Physiol. Behav.* **81**, 37–42. (doi:10.1016/j.physbeh.2003.12.016)
  66. Jacobs LL. 1984 Rodentia: extraordinary diversification of a morphologically distinctive and stereotyped order. *Ser. Geol. Notes Short Course* **8**, 155–166. (doi:10.1017/S0271164800000944)
  67. Buvinic S, Balanta-Melo J, Kupczik K, Vásquez W, Beato C, Toro-Ibacache V. 2021 Muscle-bone crosstalk in the masticatory system: from biomechanical to molecular interactions. *Front. Endocrinol.* **11**, 606947. (doi:10.3389/fendo.2020.606947)
  68. Martínez-Maza C, Freidline SE, Strauss A, Nieto-Diaz M. 2016 Bone growth dynamics of the facial skeleton and mandible in *Gorilla gorilla* and *Pan troglodytes*. *Evol. Biol.* **43**, 60–80. (doi:10.1007/s11692-015-9350-7)
  69. Renaud S, Auffray JC, De La Porte S. 2010 Epigenetic effects on the mouse mandible: common features and discrepancies in remodeling due to muscular dystrophy and response to food consistency. *BMC Evol. Biol.* **10**, 28. (doi:10.1186/1471-2148-10-28)
  70. Martínez-Vargas J, Muñoz-Muñoz F, Martínez-Maza C, Molinero A, Ventura J. 2017 Postnatal mandible growth in wild and laboratory mice: differences revealed from bone remodeling patterns and geometric morphometrics. *J. Morphol.* **278**, 1058–1074. (doi:10.1002/jmor.20694)
  71. Nichita I, Şereş M, Coman C. 2010 Maternal behaviour on golden hamster (*Mesocricetus auratus*). *Lucr. Stiinfice Med. Vet.* **43**, 335–340.
  72. Dubied M, Montuire S, Navarro N. 2022 Data from: Functional constraints channel mandible shape ontogenies in rodents. Dryad Digital Repository. (doi:10.5061/dryad.fbg79cx3)
  73. Dubied M, Montuire S, Navarro N. 2022 Functional constraints channel mandible shape ontogenies in rodents. Figshare. (doi:10.6084/m9.figshare.c.6250547)

### 4.2 Skull postnatal development

The development of the skull has mainly been studied in model organisms such as the mouse or the rat, in order to understand the processes of ossification and suturing of the different bones that make up the skull. These studies have mainly focused on the protein and mineralization processes of the bone (Holleville *et al.* 2003, Martinez-abadias *et al.* 2013, Motch Perrine *et al.* 2014, Percival and Richtsmeier 2013, Wan and Cao 2005). They have mostly monitored the prenatal stages (Barbeito-Andrés *et al.* 2016), pathological cases (Motch Perrine *et al.* 2017), or growth of individual bones and not of the whole cranium shape (Maga 2016).

The morphological description of the structures in formation is mostly done by histological images (Lee *et al.* 2015), as it is quite difficult to obtain clean and resolved tomographic images of these very young stages (prenatal and first postnatal days, as cartilage is more difficult to capture with X-rays than bone). However, thanks to advances in X-ray tomography, it is becoming increasingly possible to obtain 3D models of young and therefore not fully ossified stages. These protocols need a substantial preparation time, like DiceCT (Diffusible iodine-based contrast-enhanced Computed Tomography) which requires several days of sample processing before scanning (Callahan *et al.* 2021), often longer scanning times under high energy intensity. Last but not least, these protocols require a real expertise together with an important segmentation time in order to differentiate the different structures, which could look very alike (Cox 2020), sometimes it even needs the help of deep learning pipeline (Zheng *et al.* 2022). That is why for this study, it was preferred to still clean the bones before scanning for adult specimens and to treat only young specimens with ethanol.

#### 4.2.1 Material and methods

The ontogenetic study of the skull used the same material and methods that were used for the mandible in the ROS manuscript. Here, for the skull, only landmarks were applied (Fig 3.5-6), which does not allow a description of the shape change as precise as for the mandible where semi-landmark patches were applied. It was not possible to place patches, as the skulls of the younger stages were not fully sutured. This is a current limitation on skull studies (Toussaint *et al.* 2021), and the skull was mapped with a significant number of landmarks spread as much as possible over the whole unit.

#### 4.2.2 Results

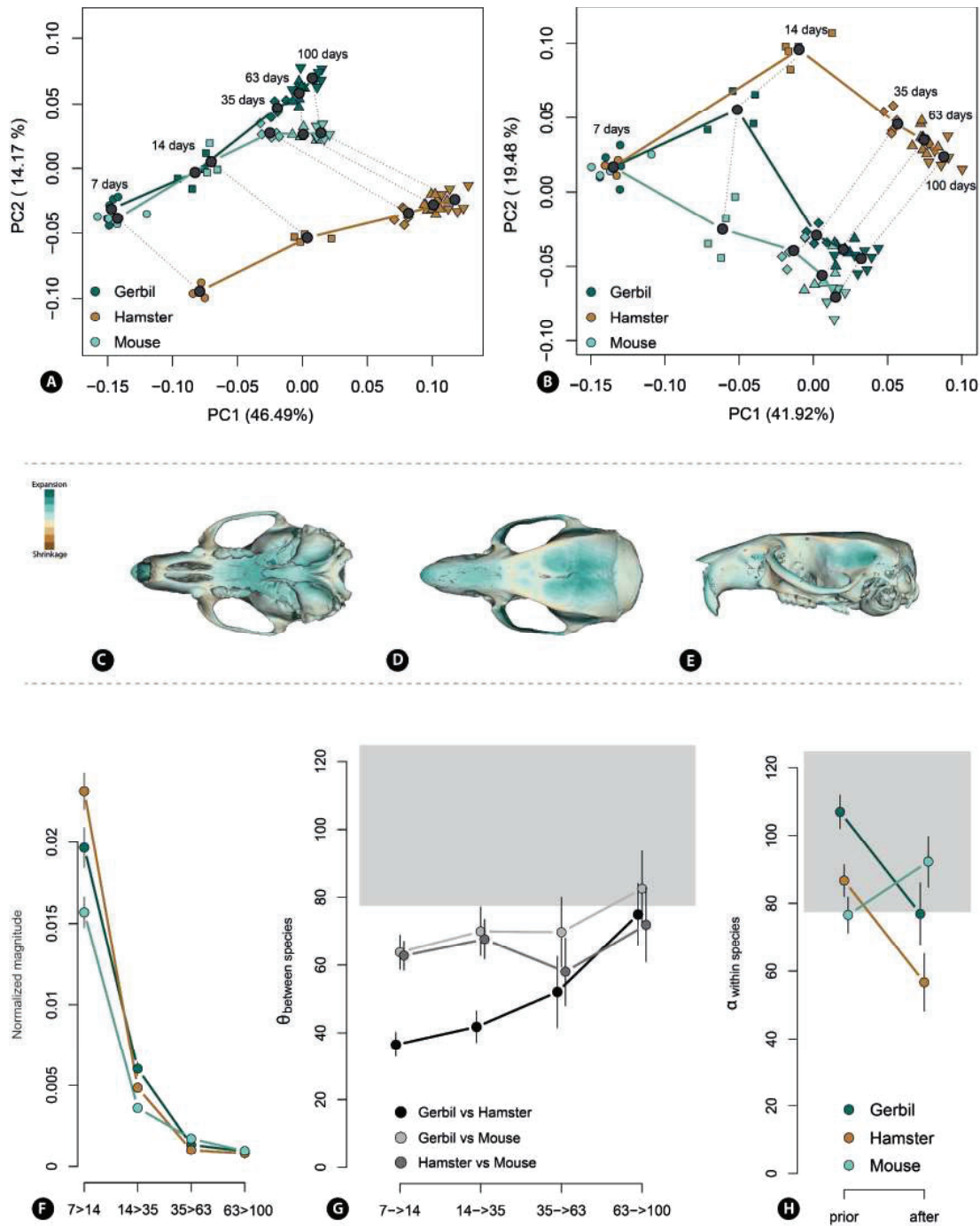


**Figure 4.1.** A) First two principal components (PC) of the variation in the skull shape across ages and taxa. B-C-D-E) Analyses of postnatal trajectories after parallel transport on the common reference average of the expected marginal means at 7 days). B) First two parallel transported principal components (PC). C-E) Shape changes of the skull along PC2 after parallel transport; C) in lower view; D) in upper view; E) in lateral view. F) Magnitude (in Procrustes unit per day) of the growth vectors of shape changes between two consecutive developmental stages normalized by the age difference. G) Angles between growth vectors of two species at the same developmental interval. H) Angles between the 14-35 days vector and the 7-14 days (prior) or the 35-63 days (after) growth vectors of each species. Error bars represent sampled standard errors.

The first two components of the PCA cumulates 60.7% of the total shape variance (Fig. 4.1 A). The gerbil and mouse trajectories stay close in the 7-day-old and 14-day-old stages and then diverge gradually. The hamster trajectory appears more distant on the two first components in relation to an important shape difference from the first stage.

After accounting for shape differences between species using parallel transport, the 7-day-old juveniles are grouped together by construction (Fig.4.1 B). Between 7 and 14 days, gerbil and hamster's trajectories are pretty close. The 14-day-old stages are spread along PC2 separating the trajectories of the three species. The trajectories of the two murids (gerbils and mice) are getting closer from the third stage and are separated on PC2 with the cricetid trajectory (hamsters). Shape changes along PC2 correspond to an extension of the palatine and basisphenoid (Fig 4.1 C) in inferior view. In superior view (Fig.4.1 D), development is marked by the expansion of the parietal and the nasal. In lateral view (Fig 4.1 E), one can see the development of the squamosal.

The amount of shape changes along the ontogeny is similar between the three species (path distance equal to  $0.33 \pm 0.08$  for gerbil and hamster,  $0.27 \pm 0.01$  for mouse). The timing of these changes is also similar with a maximum between 7-day-old and 14-day-old and then a progressive decrease until 63 day-old (Fig 4.1 F). At the first stage rate of shape changes is comprised between 0.023 for hamsters and 0.015 for mouse, this rate is then divided by five for gerbil and hamster, by three for mouse at the second stage. At the third stage (35 to 63-day-old), this rate is significantly reduced ( $0.0010$  for hamster to  $0.0017$  for mouse) and tends to  $0.00088 (\pm 0.00007)$  at the fourth stage.

Gerbils and hamsters share similar directions of shape changes (Fig 4.1 G), starting with an angle of  $36^\circ$  and then accumulate differences progressively. Mice present a different direction from the first stage (with a  $\theta$  of  $63.9^\circ$  with gerbils and  $62.7^\circ$  with hamsters). At the third stage, mouse and hamster's trajectories are getting slightly closer ( $58^\circ$ ) which is close to the  $\theta$  at the same stage for gerbils and hamsters ( $52^\circ$ ). In general, the three trajectories are quite different since 35-day-old.

The directions of shape changes (Fig 4.1 H) within species prior (7 to 14 days) to the weaning phase (14 to 35 days) are different to the trajectory during weaning for all three species, more for gerbils ( $\alpha = 107^\circ$ ) than for hamsters ( $\alpha = 86^\circ$ ) and mice ( $\alpha = 76^\circ$ ). On the contrary, the directions after weaning (35 to 63 days) are more similar for gerbils ( $\alpha = 76^\circ$ ) and hamsters ( $\alpha = 56^\circ$ ) than for mice ( $\alpha = 92^\circ$ ).

### 4.2.3 Discussion

Our results show that skull shape appears to be subfamily dependent from the start, with murids and cricetids being distant in the first two components (PCA). No general pattern emerges from the fact that these shapes are already partly established at the first stage. Weaning does not seem to have a significant impact on the change in skull shape, the development of which finally takes place quite early in the postnatal ontogeny.

The skull and mandible therefore do not behave in the same plastic way during postnatal development. Indeed, they do not respond to the same constraints. The mandible develops at the same time as the teeth and muscles. The skull, for its part, must also synchronize its growth with that of the brain and the various sensory organs it contains (Richtsmeier *et al.* 2006). This hypothesis is supported by the anatomical regions modified during development. The expansion of the parietal may be linked to the brain growth. The nasal undergoes an extension to allow the occlusion of the incisors with those of the mandible as well as the development of the entire olfactory region. The modification of the squamosal region is certainly linked to the accommodation with the growth of masseter muscles and the expansion of mandible's processes.

Furthermore, it seems that the changes undergone by the two units do not occur with the same timing. Indeed, the trajectory shift visible on the gerbil mandible, due partly to allometric effect, is not present in the skull. On the other hand, the large amount of shape changes present in the first stage (7 to 14 days) of the mouse mandible is not observed in the skull. There is thus a certain desynchronization between the developmental rates of the mandible and the skull.

### 4.3 Covariation between the skull and the mandible

After looking independently at the skull and the mandible, the question of their integration within the craniofacial complex arises. Thus, it is proposed in this section to look at the covariation of these two units. The methods of analysis of covariation gain in performance with large samples. It has been chosen here to look at this signal not by species but rather by combining them to obtain a *Myomorpha* signal.

#### 4.3.1 *Material and methods*

To study the morphological integration of the skull and the mandible, a partial least-squares analysis (PLS) was performed with the Morpho R package 2.9 (Schlager 2017). The per-species per-age sample sizes are too small to allow to get good estimates of the covariance matrices for these 15 groups (species  $\times$  age groups) considering that integration metrics (rv-coefficient, etc) could be very sensible to small sample sizes (Fruciano *et al.* 2013). Therefore, the sample was pooled according to the expected marginal means of the species  $\times$  age groups, and the covariation between the two anatomical units was studied on this pooled sample of 81 individuals. It means that the observed patterns of covariation correspond to the main pattern of integration conserved along the ontogeny and across all species.

#### 4.3.2 *Results*

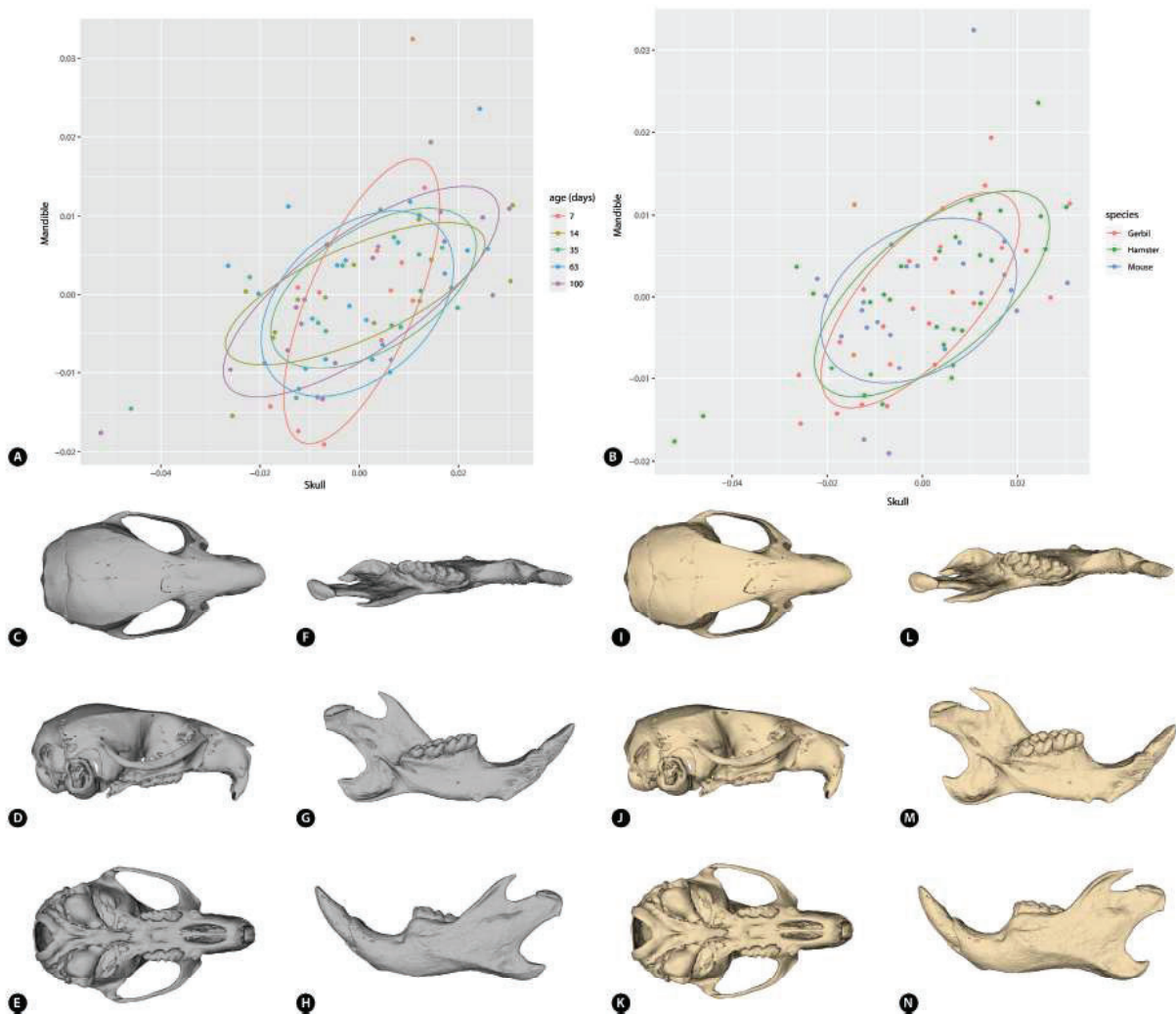


**Figure 4.2.** Main pattern of covariation between the mandible and the skull. A) First PLS axes. Individuals are colored according to their age. Ellipses correspond to 68% of the data ( $1\sigma$ ). B) First PLS axes. Individuals are colored according to their species. C-H) Skull and mandible shape corresponding to the negative values of PLS axes according to the ages. I-N) Skull and mandible shape corresponding to the positive values of PLS axes according to the ages. C & I) Skull in dorsal view. D & J) Skull in lateral view. E & K) Skull in ventral view. F & L) Mandible in dorsal view. G & M) Mandible in lateral internal view. H & N) Mandible in lateral external view.

The skull and the mandible appear to covariate slightly ( $R_v = 0.22, p = 0.004$ ). The main pattern as represented by the first PLS axes (Fig. 4.2) accounts for 22.2% of the total squared cross-covariance ( $r = 0.59, p = 0.31$ ). This pattern appears roughly consistent during the ontogeny and across species according to the age-based ellipses which are about the same. Two additional PLSs explain more than 10% of the covariation (PLS2 = 18.3%,  $r = 0.56, p = 0.03$ , PLS3 = 11.5%,  $r = 0.52, p = 0.09$ ) and four additional present a percentage higher than 5%.

The most remarkable anatomical differences between negative and positive values of the first PLS axes as a function of age are described in the following table.

Negative values		Positive values	
Mandible	Skull	Mandible	Skull
Coronoid process short and verticalized	Post-orbital apophysis of the squamosal arriving posteroanteriorly at the level of the middle jugal	Coronoid process long and thrown backwards	Post-orbital apophysis of the squamosal positioned posteriorly
Condylar process long and verticalized	Posterior part of the zygomatic apophysis of the squamosal raised	Condylar process shorter than the coronoid process	Posterior part of the zygomatic apophysis of the squamosal horizontalized
Angular process poorly developed on its internal part		Angular process well developed in the internal direction	

**Table 4.1.** Main anatomical differences along the first PLS axes as function of age.

#### 4.3.3 Discussion

The two units composing the craniofacial complex seem to slightly covariate. Indeed, the covariance is spread over several PLS axes, meaning that the pattern of covariation depends on many factors. However, although slight, covariation patterns emerge between the skull and the mandible, regardless of species or age. Indeed, throughout development and as feeding and behavioral changes occur, the craniofacial complex must remain functional. Without this cohesion between the two units, the animal would limit its chances of individual survival, especially in a wild context (Blackett 2015, Miller 2019, Sainsbury *et al.* 2004). The covariation of the different structure is essential to maintain appropriate size and shape across ontogeny and ranges of phenotypic variations (Hallgrímsson *et al.* 2007). It has been observed that mutation on cartilage synthesis gene can alter covariance in mouse's skull by increasing the variance in cartilage formation and so the variance in brachymorph phenotype (Hallgrímsson *et al.* 2009). Thus, while covariation may be altered by changes in the development of a single tissue type, this covariation may be more sensitive if several structures are considered as they have to coordinate to maintain a functional craniofacial complex. It has also been proposed that the growth of the different parts of the skull does not necessarily take place in a coordinated manner, but that this process can occur via compensatory interactions that correct locally disproportionate growth (Zelditch *et al.* 2006). Shape is thus actively regulated by developmental plasticity of the bone. Thus potentially allowing accommodation to the various internal or external factors regulating and/or forcing bone remodeling. The shape is therefore both canalized and rapidly adaptable to any change.

### 4.4 Conclusions

After birth, mandible and skull are modified with different timing. The mandible seems to be sensitive to different factors as gestational time, weaning but is also partly phylogeny dependent. After an early shape divergence between subfamilies, changes seem to be driven by muscular loading and other mechanical stresses arising around weaning. The skull, on its part, shows also an early shape divergence between subfamilies but does not undergo major changes during weaning. This unit is constrained by more tissues interactions than the mandible and must therefore follows a different development in terms of timing, although these two units must interconnect to ensure the viability of the individual. Nevertheless, the skull and the mandible covariate slightly throughout development, which is consistent with the need to maintain a functional head.

## References

- BARBEITO-ANDRÉS, J., GONZALEZ, P. N., and HALLGRÍMSSON, B. Prenatal development of skull and brain in a mouse model of growth restriction. *Revista argentina de antropología biológica*, 2016, vol. 18, no 1, p. 0-0.
- BLACKETT, Tiffany. Squirrels—an overview of common clinical presentations and important diseases. *Companion Animal*, 2015, vol. 20, no 10, p. 583-588.
- CALLAHAN, S., CROWE-RIDDELL, J. M., NAGESAN, R. S., GRAY, J. A., RABOSKY, A. R. D. A guide for optimal iodine staining and high-throughput diceCT scanning in snakes. *Ecology and evolution*, 2021, vol. 11, no 17, p. 11587-11603.
- COX, Timothy C. Microcomputed tomography of craniofacial mineralized tissue: A practical user's guide to study planning and generating quality data. *Bone*, 2020, vol. 137, p. 115408.
- FRUCIANO, C., FRANCHINI, P., and MEYER, A. Resampling-based approaches to study variation in morphological modularity. *PLoS One*, 2013, vol. 8, no 7, p. e69376.
- HALLGRÍMSSON, B., JAMNICZKY, H., YOUNG, N. M., ROLIAN, C., PARSONS, T. E., BOUGHNER, J. C., and MARCUCIO, R. S. Deciphering the palimpsest: studying the relationship between morphological integration and phenotypic covariation. *Evolutionary biology*, 2009, vol. 36, no 4, p. 355-376.
- HALLGRÍMSSON, B., LIEBERMAN, D. E., YOUNG, N. M., PARSONS, T., and WAT, S. Evolution of covariance in the mammalian skull. In: *Tinkering: The Microevolution of Development: Novartis Foundation Symposium 284*. Chichester, UK: John Wiley & Sons, Ltd, 2006. p. 164-190.
- HOLLEVILLE, N., QUILHAC, A., BONTOUX, M., and MONSORO-BURQ A.-H. BMP signals regulate Dlx5 during early avian skull development. *Developmental biology*, 2003, vol. 257, no 1, p. 177-189.
- LEE, C., RICHTSMEIER, J. T., and KRAFT, R. H. A computational analysis of bone formation in the cranial vault in the mouse. *Frontiers in bioengineering and biotechnology*, 2015, vol. 3, p. 24.
- MAGA, M. A. Postnatal development of the craniofacial skeleton in male C57BL/6J mice. *Journal of the American Association for Laboratory Animal Science*, 2016, vol. 55, no 2, p. 131-136.
- MARTÍNEZ-ABADÍAS, N., MOTCH, S. M., PANKRATZ, T. L., WANG, Y., ALDRIDGE, K., JABS, E. W., and RICHTSMEIER, J. T. Tissue-specific responses to aberrant FGF signaling in complex head phenotypes. *Developmental Dynamics*, 2013, vol. 242, no 1, p. 80-94.
- MILLER, Erica A. Natural History and Medical Management of Squirrels and Other Rodents. *Medical Management of Wildlife Species: A Guide for Practitioners*, 2019, p. 167-184.
- MOTCH PERRINE, S. M., STECKO, T., NEUBERGER, T., JABS, E. W., RYAN, T. M., and RICHTSMEIER, J. T. Integration of brain and skull in prenatal mouse models of Apert and Crouzon syndromes. *Frontiers in human neuroscience*, 2017, vol. 11, p. 369.
- MOTCH PERRINE, S. M., COLE, T. M., MARTÍNEZ-ABADÍAS, N., ALDRIDGE, K., JABS, E., and RICHTSMEIER, J. T. Craniofacial divergence by distinct prenatal growth patterns in Fgfr2 mutant mice. *BMC developmental biology*, 2014, vol. 14, no 1, p. 1-17.
- PERCIVAL, C. J. and RICHTSMEIER, J. T. Angiogenesis and intramembranous osteogenesis. *Developmental Dynamics*, 2013, vol. 242, no 8, p. 909-922.
- RICHTSMEIER, J. T., ALDRIDGE, K., DELEON, V. B., PANCHAL, J., KANE, A. A., MARSH, J. L., YAN, P., and COLE, T. M. Phenotypic integration of neurocranium and brain. *Journal of Experimental Zoology Part B: Molecular and Developmental Evolution*, 2006, vol. 306, no 4, p. 360-378.

## Chapter 4 - Postnatal development of the craniofacial complex

- SAINSBURY, A. W., KOUNTOURI, A., DUBOULAY, G., and KERTESZ, P. Oral disease in free-living red squirrels (*Sciurus vulgaris*) in the United Kingdom. *Journal of Wildlife Diseases*, 2004, vol. 40, no 2, p. 185-196.
- SCHLAGER, S. Morpho and Rvcg—shape analysis in R: R-packages for geometric morphometrics, shape analysis and surface manipulations. In: *Statistical shape and deformation analysis*. Academic Press, 2017. p. 217-256.
- TOUSSAINT, N., REDHEAD, Y., VIDAL-GARCÍA, M., LO VERCIO, L., LIU, W., FISHER, E. M. C., HALLGRIMSSON, B., TYBULEWICZ, V. L. J., SCHNABEL, J. A., and GREEN, J. B. A. A landmark-free morphometrics pipeline for high-resolution phenotyping: application to a mouse model of Down syndrome. *Development*, 2021, vol. 148, no 18, p. dev188631.
- WAN, M., and CAO, X. BMP signaling in skeletal development. *Biochemical and biophysical research communications*, 2005, vol. 328, no 3, p. 651-657.
- ZELDITCH, M. L., MEZEY, J., SHEETS, H. D., LUDRIGAN, B. L., and GARLAND Jr, T. Developmental regulation of skull morphology II: ontogenetic dynamics of covariance. *Evolution & development*, 2006, vol. 8, no 1, p. 46-60.
- ZHENG, H., MOTCH PERRINE, S. M., PITIRRI, M. K., KAWAZAKI, K., WANG, C., RICHTS-MEIER, J. T., and CHEN, D. Z. Cartilage segmentation in high-resolution 3d micro-ct images via uncertainty-guided self-training with very sparse annotation. In: *International Conference on Medical Image Computing and Computer-Assisted Intervention*. Springer, Cham, 2020. p. 802-812.





## Chapter 5 – Plasticity in postnatal development



In mammals, weaning is a key moment, characterized by transitions in feeding behaviors and loading in the feeding apparatus. As shown in the previous chapter, the skull and the mandible do not exhibit the same response to these changes. During this period, the tissues will have to accommodate to the various mechanical changes related to the modification of diet and behavior. The chewing muscles respond to the chewing forces and movements and develop to meet this need, as well as the need to gnaw or other adult behaviors. Thus, if the tissues must adapt to various stresses, one may wonder if this response varies according to changes in the stresses applied to the whole craniofacial complex during weaning.

In natural setting, this variation in strain may occur depending on availability of different food types in relation to seasons, dispersion in new environments, or at larger scale related to climate changes. The expression of the adult shape would thus be sensible to over-strain or under-strain, and the shape variation between spatial and/or temporal populations would partly relate to this plastic response. These variations in constraints could therefore lead to responses at different scales. At the individual scale, the organism may show developmental plasticity in relation to availability of resources (food type at weaning); when at the population scale, an evolution of the shape in response to environmental forcing through plasticity may occur by phenotypic accommodation (West-Eberhard 2005, Nijhout *et al.* 2021).

To assess the importance of strain variation on the adult shape, and thus of the plastic potentiality of the CF complex, the effect of diet could easily be controlled in animal experiments. The animals used in this study were therefore divided into two groups, one fed with conventional pellets (Hard diet) and the other with pellets boiled by hydration (Soft food). This type of experimentation is classically used to inform the plasticity of the cranium and the mandible. However, these studies have concerned pathological cases such as dystrophy (Renaud *et al.* 2010; Spassov *et al.* 2017), focused on the adult shape (Menegaz & Ravosa 2017), informed the reaction of the tissues by changing the diet during the study (Mitchell *et al.* 2021) or sought to apply over-stressing (Mavropoulos *et al.* 2005; Odman & Kiliaridis 2010), and in my knowledge none has been realized explicitly in a comparative setting.

Previous studies have shown that soft diet results in structural and morphological changes in the craniofacial complex due to functional load differences (Mavropoulos *et al.* 2010, 2014; Chen *et al.* 2011; Dias *et al.* 2011; Utreja *et al.* 2016; Ödman *et al.* 2019). At structural level, this type of diet leads to a decrease in bone volume, to bone thickness alveolar, bone trabecular volume and subchondral condylar bone volume (Odman *et al.*, 2008; Mavropoulos *et al.*, 2010; Anderson *et al.*, 2014), when at anatomical level, mandibles develop shorter processes (Mavropoulos *et al.* 2004; Anderson *et al.* 2014).

In the present study, the goal is to (1) document the effect of diet during postnatal development and thus assess the role of plasticity in the establishment of the craniofacial shape along ontogenetic trajectories, (2) to compare if this plasticity effect varies among species. Here I am

looking at whether there are inter-specific differences, as the anatomies of the three species are different. Indeed, the plastic response could depend on the specific anatomical setting and therefore be dependent of the systematics. Several scenarios are possible. Either the same timing of growth between the skull and the mandible is found in order to keep a complete cohesion between these two units; it has been shown previously in this manuscript that it was not the case in hard food diet. However, a less important constraint could slow down the forcing on the two structures and thus allow a better synchronized developmental timing, as it was shown in the previous chapter, the skull and the mandible can have different growth timings, while keeping a functional cohesion. It would thus be expected that, although most of the postnatal growth has already passed by the time of weaning, there would be a modification of the ontogenetic trajectory, notably that the vector lengths in soft diet group are potentially shorter than in hard food group. On the other hand, it would also be expected that inter-specific divergence would be less in soft food specimens, as the adult shape may be less expressed due to the lack of mechanical forcing applied by the muscles on the bone reducing the influences of differentiated adult behaviors. Anatomically speaking, the structures associated with the establishment of the masticatory muscles (ascending ramus processes) could be less developed in soft food specimens. Thus, the plasticity of the craniofacial complex could provide a rapid response to environmental factors, in modulating the mechanical performance and thus reducing the potential of maladaptation, the bone physiology allowing an almost instantaneous response to the availability of food resources.

### 5.1 Material and Methods

The specimens used in this study were bred in the central animal facility of the University of Burgundy (Project APAFIS#18405-2019011014262528). From weaning onwards, some individuals were fed with hard food pellets, others with pellets mixed with water. The specimens used were those corresponding to the post-weaning stages (35 and 63 days old). No dental problems, weight loss or different weight gain between diets were observed in either group during the experiment (Fig 5.1), meaning that the constraint applied by diet is weak.

The landmarks used on the mandible and the skull are the same as those used in the previous chapter as well as the statistical shape analysis. The ontogenetic trajectories were parallel transported prior to analysis; this time the 35-day-old expected marginal means of each species were superimposed.

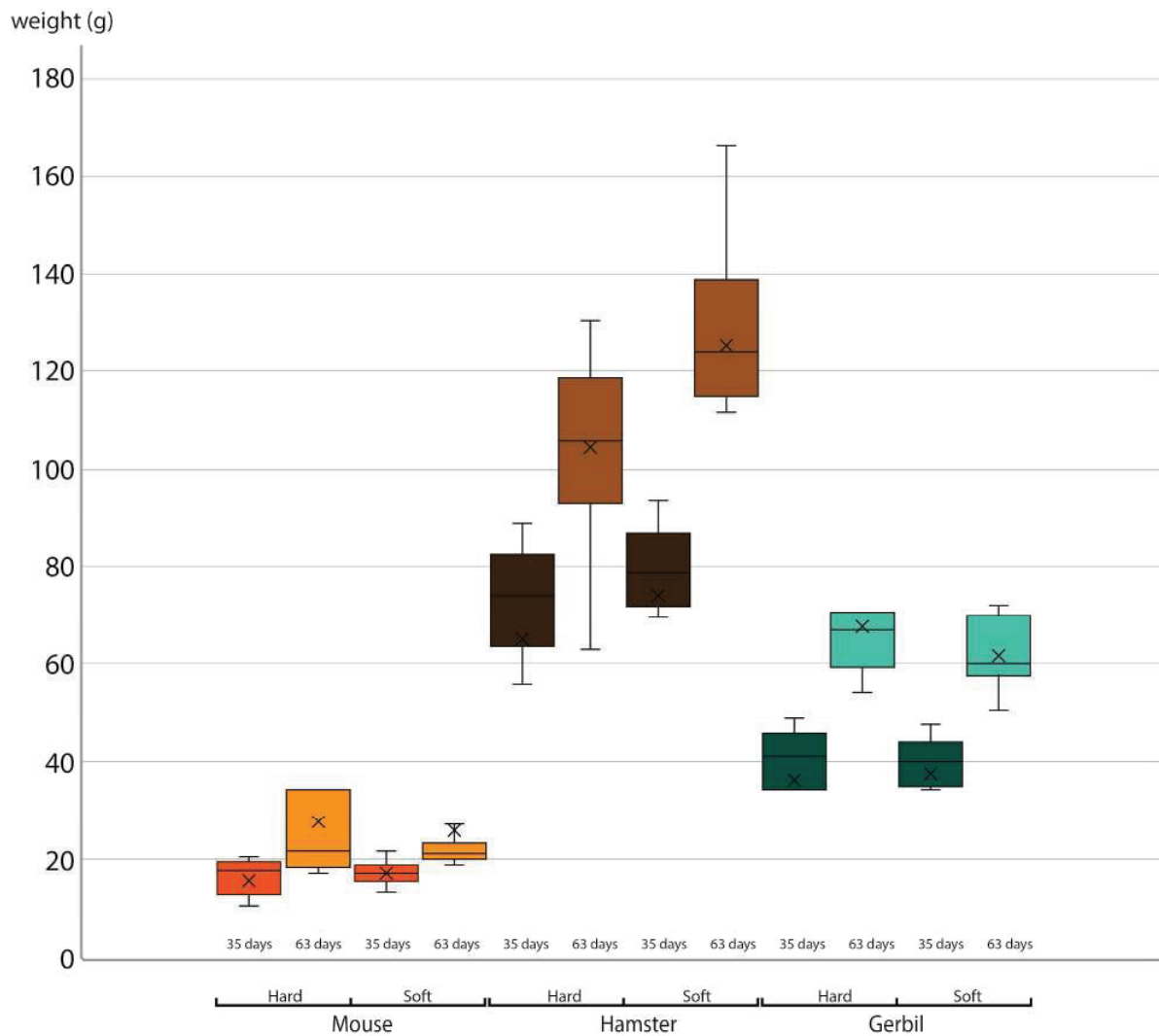


**Figure 5.1.** Weights measured during rearing of mice, hamsters and gerbils; at 35 and 63 days of age according to diet.

## 5.2 Results

For the mandible, the first two components of the PCA cumulate 72,53% of the total shape variation (Fig 5.2A). The 35-day-old are grouped together. Two major directions of development are represented. In one hand the trajectory of hamster projects well along PC1; in the other hand, the trajectory followed by mice and gerbils projects mostly along PC2. However, the directionality of the trajectories does not vary between soft and hard within each species. Moreover the soft and hard growth vectors within each species are of similar norms, indicating the same amount of change regardless of the associated diet. The ANOVA analysis reveals a diet effect on shape changes as well as a small age  $\times$  diet effect which reflects the duration of the treatment (Table 5.1). During the postweaning development, specimens fed with hard diet develop longer and more robust condylar and angular processes (Fig 5.2 C-D). The coronoid process is slightly longer also in hard diet fed specimens. In general, the entire posterior part of the mandible is less extended in soft diet fed specimens. The diastema is thicker in hard diet fed shape.

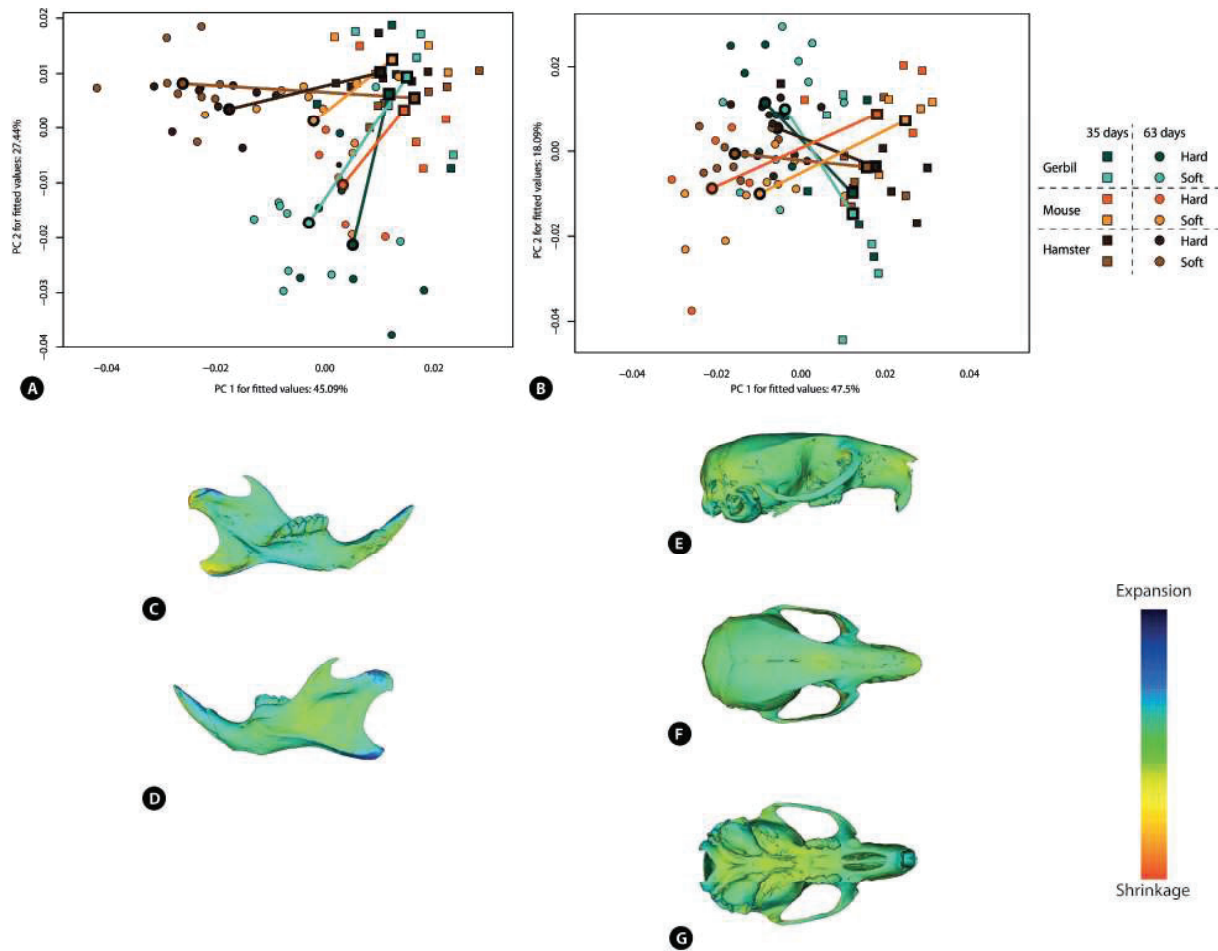


**Figure 5.2.** Analyses of post-weaning trajectories after parallel transport on the common reference (average of the expected marginal means at 35 days). A) First two parallel transported principal components (PC) on mandibles. B) First two parallel transported PCs on skulls. C-D) Shape changes between 35 and 63 day-old of the mandible with hard diet effect mapped on soft diet mean shape. C) Mandible in lateral internal view. D) Mandible in lateral external view. E-G) Shape changes between 35 and 63 day-old of the skull with hard diet effect mapped on soft diet mean shape. E) Skull in lateral view. F) Skull in upper view. G) Skull in lower view.

	Df	SS	MS	R <sup>2</sup>	F	Z	Pr(>F)	partial R <sup>2</sup>
<b>Species</b>	2	0.76528	0.38264	0.89447	430.1975	9.9471	0.001	0.926
<b>Age</b>	1	0.01227	0.01227	0.01434	13.7978	5.4491	0.001	0.169
<b>Diet</b>	1	0.00264	0.00264	0.00309	2.9717	3.3129	0.001	0.042
<b>Species × Age</b>	2	0.00554	0.00277	0.00648	3.1148	4.5000	0.001	0.084
<b>Species × Diet</b>	2	0.00182	0.00091	0.00213	1.0248	0.2019	0.405	0.029
<b>Age × Diet</b>	1	0.00138	0.00138	0.00161	1.5489	1.5348	0.068	0.022
<b>Species × Age × Diet</b>	2	0.00178	0.00089	0.00208	1.0016	0.1521	0.451	0.029

**Table 5.1.** ANOVA analysis on mandible.

	Df	SS	MS	R <sup>2</sup>	F	Z	Pr(>F)	partial R <sup>2</sup>
<b>Species</b>	2	0.43691	0.21845	0.69601	97.5999	7.0520	0.001	1.999
<b>Age</b>	1	0.01418	0.01417	0.02258	6.3335	4.7899	0.001	0.997
<b>Diet</b>	1	0.00154	0.001538	0.00245	0.6873	-0.8498	0.799	0.991
<b>Species × Age</b>	2	0.00752	0.00376	0.01198	1.6797	1.8767	0.034	1.966
<b>Species × Diet</b>	2	0.00389	0.00194	0.00620	0.8691	-0.3761	0.640	0.640
<b>Age × Diet</b>	1	0.00231	0.00231	0.00369	1.0338	0.3116	0.378	0.897
<b>Species × Age × Diet</b>	2	0.00256	0.00128	0.00408	0.5719	-2.1022	0.986	1.792

**Table 5.2.** ANOVA analysis on skull.

Concerning the skull, the first two components of the PCA cumulate 65,59% of the total shape variation (Fig 5.2B). The 35-day-old are opposed to the 63-day-old along PC1. As for the mandible, growth vectors are similar in direction and norm within each species. The ANOVA analysis reveals no effect of the diet on shape changes. There are few anatomical differences between the skull shapes associated with the two diets (Fig 5.2 E-G). Hard diet fed specimens show a very slightly more inflated cranial vault (parietal and interparietal).

### 5.3 Discussion

The results of this study show similar growth vectors between the different diets, both in the skull and the mandible. Although most of the postnatal growth had already occurred before weaning, it was expected that the vectors associated with the soft diet would be shorter than for the hard diet. Indeed, the masticatory muscles being less solicited in the soft diet, the constraints are lower, so the bone could have been less forced to adapt to the new chewing constraint induced by weaning (Renaud *et al.* 2010)

On the other hand, there is a notable difference in the shape of the mandible. The different processes of the ascending ramus are shorter than in the hard regime, thus reducing the whole posterior region of the mandible. However, a strong development of this part of the mandible is associated with the implementation of the major constraints applied by the masticatory muscles (Menegaz & Ravosa 2017). For the skull, the only difference observed is very small, the cranial vault is very slightly more inflated in the hard diet specimens. This observation was also made by Menegaz *et al.* in 2010 on rabbits.

Specimens were reared in the laboratory and kept as free as possible from easily gnawed objects in order to obtain results as characteristic as possible of the diet. For example, the incisor length of individuals reared on a soft diet could not have been maintained well after 63 days without intervention on the incisors. In contrast, in the wild, individuals have elements to gnaw on. Thus, in such an environment, the mandible would have the plastic capacity to respond to the resource constraints of the environment, while at the same time being able to gnaw without worrying

about maintaining incisors of a normal size, which would not present a health risk for the animal.

Here a net difference in plasticity between the skull and the mandible has been shown, and only the mandible exhibits a diet effect. Once again, it is important to note that the mandible is composed of fewer different tissues and could therefore more easily undergo a much greater bone remodeling in relation to bone loading than the skull. The mandible will then modify itself in accordance with the more or less strong need to create a lever capable of handling a more or less hard food and to support the tension applied by the muscles. At this stage, moreover, the skull has already seen the almost complete development of its internal structures (brain, olfactory and auditory organs), which are not compressible. There is therefore a desynchronization of the two units forming the craniofacial complex. Moreover, the areas impacted by food changes on the skull may be more localized at the muscle insertions which could not have been well captured with landmarks only.

The mandible allows for a slight adaptation to the diet and thus to the availability of resources. It is a possible rapid adaptation of the mandible to the environment and to the resources, as it allows to modify leverage in bite force without involving weight change of individuals. This plastic response could underline the adaptation of populations in aligning the mandible shape to the need in performance. This effect is observed regardless of the species in this study. It may possibly be extended to close species within Myomorpha and may highlight a possible mechanism of parallel evolution.

### 5.4 Conclusion

In this experiment, it was shown that the difference in diet after weaning had no effect on the timing of acquisition of adult shape, as the growth vectors were of similar length. However, anatomically speaking, the bony structures associated with muscle development are shorter on the mandibles associated with the soft diet. On the other hand, only slight differences are observed on the skull and no signal is found to associate them with the diet. Thus, the plasticity associated with the diet would only be carried by the mandible. However, this plasticity allows a rapid response to the availability of food resources and does not jeopardize the cohesion between the skull and mandible, allowing a functional craniofacial complex to be maintained and enabling the survival of individuals.

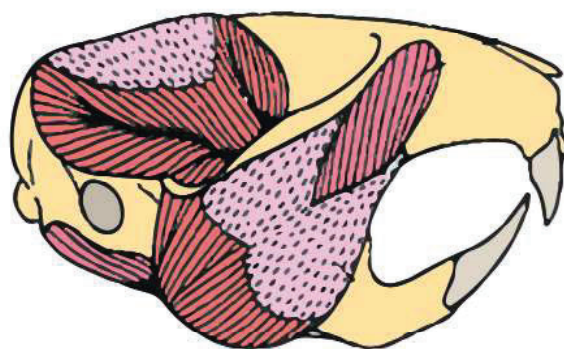
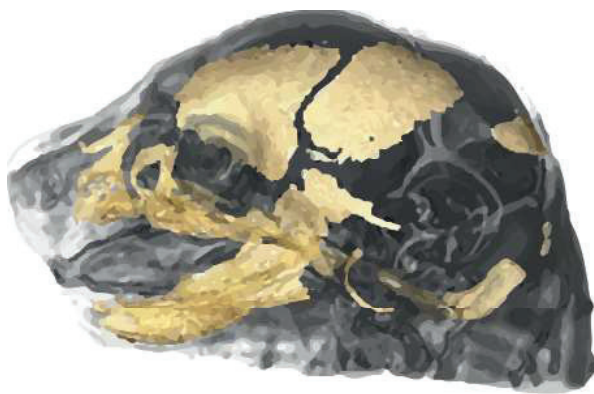
References

- ANDERSON, P. S., RENAUD, S., and RAYFIELD, E. J. Adaptive plasticity in the mouse mandible. *BMC Evolutionary Biology*, 2014, vol. 14, no 1, p. 1-9.
- CHEN, J., SOBUE, T., UTREJA, A., KALAJZIC, Z., XU, M., KILTS, T., YOUNG, M., and WADHWA, S. Sex differences in chondrocyte maturation in the mandibular condyle from a decreased occlusal loading model. *Calcified tissue international*, 2011, vol. 89, no 2, p. 123-129.
- DIAS, G. J., COOK, R. B., and MIRHOSSEINI, M. Influence of food consistency on growth and morphology of the mandibular condyle. *Clinical Anatomy*, 2011, vol. 24, no 5, p. 590-598.
- MAVROPOULOS, A., AMMANN, P., BRESIN, A., and KILIARIDIS, S. Masticatory demands induce region-specific changes in mandibular bone density in growing rats. *The Angle Orthodontist*, 2005, vol. 75, no 4, p. 625-630.
- MAVROPOULOS, A., KILIARIDIS, S., RIZZOLI, R., and AMMANN, P. Normal masticatory function partially protects the rat mandibular bone from estrogen-deficiency induced osteoporosis. *Journal of Biomechanics*, 2014, vol. 47, no 11, p. 2666-2671.
- MAVROPOULOS, A., KILIARIDIS, S., BRESIN, A., and AMMANN, P. Effect of different masticatory functional and mechanical demands on the structural adaptation of the mandibular alveolar bone in young growing rats. *Bone*, 2004, vol. 35, no 1, p. 191-197.
- MAVROPOULOS, A., ÖDMAN, A., AMMANN, P., and KILIARIDIS, S. Rehabilitation of masticatory function improves the alveolar bone architecture of the mandible in adult rats. *Bone*, 2010, vol. 47, no 3, p. 687-692.
- MENEGAZ, R. A., SUBLETT, S. V., FIGUEROA, S. D., HOFFMAN, T. J., RAVOSA, M. J., and ALDRIDGE, K. Evidence for the influence of diet on cranial form and robusticity. *The Anatomical Record: Advances in Integrative Anatomy and Evolutionary Biology*, 2010, vol. 293, no 4, p. 630-641.
- MENEGAZ, R. A. and RAVOSA, M. J. Ontogenetic and functional modularity in the rodent mandible. *Zoology*, 2017, vol. 124, p. 61-72.
- MITCHELL, D. R., WROE, S., RAVOSA, M. J., and MENEGAZ, R. A. More challenging diets sustain feeding performance: Applications toward the captive rearing of wildlife. *Integrative Organismal Biology*, 2021, vol. 3, no 1, p. obab030.
- NIJHOUT, H. F., KUDLA, A. M., and HAZELWOOD, C. C. Genetic assimilation and accommodation: Models and mechanisms. *Current Topics in Developmental Biology*, 2021, vol. 141, p. 337-369.
- ÖDMAN, A., BRESIN, A., and KILIARIDIS, S. The effect of retraining hypofunctional jaw muscles on the transverse skull dimensions of adult rats. *Acta Odontologica Scandinavica*, 2019, vol. 77, no 3, p. 184-188.
- ÖDMAN, A., and KILIARIDIS, S. Rat as a model for studying the effect of masticatory muscle function on craniofacial growth. In: *Seminars in Orthodontics*. WB Saunders, 2010. p. 92-98.
- ÖDMAN, A., MAVROPOULOS, A., and KILIARIDIS, S. Do masticatory functional changes influence the mandibular morphology in adult rats. *archives of oral biology*, 2008, vol. 53, no 12, p. 1149-1154.

- RENAUD, S., AUFRAY, J.-C., and DE LA PORTE, S. Epigenetic effects on the mouse mandible: common features and discrepancies in remodeling due to muscular dystrophy and response to food consistency. *BMC evolutionary biology*, 2010, vol. 10, no 1, p. 1-13.
- SPASSOV, A., TORO-IBACACHE, V., KRAUTWALD, M., BRINKMEIER, H., and KUPCZIK, K. Congenital muscle dystrophy and diet consistency affect mouse skull shape differently. *Journal of Anatomy*, 2017, vol. 231, no 5, p. 736-748.
- UTREJA, A., DYMENT, N. A., YADAV, S., VILLA, M. M., LI, Y., JIANG, X., NANDA, R., and ROWE, D. W. Cell and matrix response of temporomandibular cartilage to mechanical loading. *Osteoarthritis and cartilage*, 2016, vol. 24, no 2, p. 335-344.
- WEST-EBERHARD, Mary Jane. Phenotypic accommodation: adaptive innovation due to developmental plasticity. *Journal of Experimental Zoology Part B: Molecular and Developmental Evolution*, 2005, vol. 304, no 6, p. 610-618.



## Conclusions & Perspectives



### Conclusions

During this thesis, I first took a broad view through the macroevolutionary scale, in order to map general growth patterns of postnatal mandibular development in rodents, between and within clades. In order to provide precise information on the different processes undergone by the craniofacial complex during postnatal development, the other part of this work focused on a finer taxonomic and temporal scale. For this purpose, three model rodent species belonging to the same suborder (Myomorpha) were sampled at five different growth stages. Finally, in these three species, the role of mechanical constraints during growth was questioned using variations in diet

General postnatal growth patterns of the mandible were first mapped between and within the main clades of rodents to provide a macroevolutionary picture of the postnatal mandibular development. Rodentia is a very diverse and disparate mammal order, in which postnatal changes can be observed on a large scale. This study was focused on Hystricomorpha and Myomorpha which exhibit diverse life-history traits among species. Gestation and weaning are shorter in Myomorpha, which generally give birth to large litters several times a year, involving a short prenatal development and a rapid and therefore mechanically brutal weaning. Hystricomorpha give birth to small litters a few times a year. Parental care is therefore different, with longer behavioral weaning and less brutal dietary weaning, over a much longer period. The potential for postnatal plasticity could likely be different between the two suborders. A wide variety of diets is also found within these two groups. Changes in diet might correlate with evolutionary changes in muscle attachment, direction of mastication and mandible shape (Álvarez & Pérez, 2019). They also show diverse infraorbital morphologies, muscles attachment and types of molar growth. We observed trajectories between juvenile (before weaning) and adult stages. The results highlighted that the main evolutionary and developmental patterns appear to be along orthogonal directions of the shape space. Also, most of the shape divergences arise along postnatal directions of growth. Nevertheless, differences between suborders are raised. In Hystricomorpha, most of the development is apparently taking place during the gestational period as it presents short magnitude of changes in long postnatal periods and most trajectories are genus-specific. For Myomorpha, most of the development occur postnatally as it presents a much stronger magnitude of changes over a shorter growth period, also postnatal trajectories of Myomorpha subfamilies are closer to one another. Juvenile mandibles present similarities among suborders within rodents, with a flattened shape. Mandible shape then diversifies during growth in relation to muscle and tooth development, with epigenetic interactions coordinating the changes in the alveolar and muscle-bearing regions. During this study, only the mandible was considered but if we compare to the different studies conducted on the skull, we can highlight some differences between the two units constituted by the craniofacial complex. The skull is a composite unit constituted by multiple bones, and this assemblage is constrained by the development of teeth, facial muscles and internal organs. This complex entanglement of many tissues may explain the low skull disparity in relation to lineage diversification described in Rodentia (Alhajeri & Stepan 2018), or in the adaptive radiation of some families (Maestri *et al.* 2017), or the

relatively overlapping growth pattern of the skull observed among rodent clades (Wilson 2013). The higher complexity of skull development is likely to reduce its dependence on muscle and tooth development and this difference in complexity probably explains the contrast observed between these two skeleton elements of the head.

In the first study, the mandible shape change was analyzed at a large taxonomic scale but considering only two stages of the postnatal growth: an early phase after birth and the adult stage. Ontogenetic trajectories are well-known to be non-linear (Green *et al.* 2017, Mitteroecker & Gunz 2009). It was therefore essential to provide information on the change in morphology during growth at a finer scale using several subadult stages. Moreover, as the mandible is tightly link with the skull, it is essential to look at these changes on the entire craniofacial complex. The two units are closely related because anatomically linked. One would expect the skull and the mandible to follow similar timing and rate of development. However, these two elements are not totally constrained by the same tissue interactions as said before and therefore should not present the same developmental constraints. It is conceivable that these two structures could show different timing in ontogeny on the condition that they remain sufficiently integrated to maintain some efficiency in their common functions. So, I followed these trajectories on three model organisms, all three belonging to Myomorpha. After birth, a differential timing of shape changes is observed between mandible and skull. The mandible seems more sensible to different factors as gestational time, weaning and appears phylogeny-dependent. This bone undergoes an early shape divergence between families. After, changes seem to be driven by muscular loading and other mechanical stresses arising around weaning. The skull shows also an early shape divergence between subfamilies but does not undergo major changes during weaning. Despite this difference in developmental timing, the skull and the mandible covary slightly throughout development and maintain a functional head.

The changes in the mechanical constraint during the activation of the masticatory apparatus does not seem to influence the mandible and the skull in the same way. The idea was to document the effect of diet during postnatal development, thereby assessing the role of plasticity in the establishment of the craniofacial shape and comparing whether this plasticity effect varies among species. Thus, an experiment was designed to contrast two levels of this constraint by applying a classic diet (hard food) to the control group from weaning onwards and a sub-contractive diet (soft food) to another group. Several hypotheses were exposed. The timing of growth could be synchronized between the two structures in soft diet, an under-strain being less forcing on the mandible, despite a desynchronization already observed in hard diet. It was also expected that although most of the postnatal growth has already passed by the time of weaning, there would be a modification of the ontogenetic trajectory, notably that the vector lengths in soft diet group could be potentially shorter than in hard diet group. Another hypothesis was that inter-specific divergence would be less in soft diet group, as the adult shape may be less expressed due to the lack of mechanical forcing. Anatomically speaking, the structures associated with the establishment of the masticatory muscles (ascending ramus processes) were expected to be less developed in soft food specimens. The dif-

## Conclusions & Perspectives

ference in diet after weaning appears to have no effect on the timing of acquisition of adult shape. As expected, the bony structures associated with muscle development are shorter on the mandibles associated with the soft diet. Only slight differences were observed on the skull and no interaction with diet was found. Thus, the plasticity associated with the diet seems to only be carried by the mandible. This plasticity allows a rapid response to the availability of food resources as long as a cohesion between the skull and mandible is maintained, ensuring a functional craniofacial complex and survival of individuals.

Along this thesis manuscript, a difference in postnatal development between taxonomic groups and between the skull and the mandible was observed. The mandible seems to be more plastic than the skull, the latter is constrained by more tissues interactions than the mandible and must therefore follow a different development in terms of timing. But this obviously does not preclude the cohesion of these two units ensuring the viability of the individual. These elements allow a rapid plastic response of the organism to variations in the type of food available from weaning. Thus, postnatal trajectories of the mandible could be influenced throughout growth by the organismal environment (food, behaviors...) allowing mechanisms such as phenotypic accommodation to contribute to the evolutionary responses of populations.

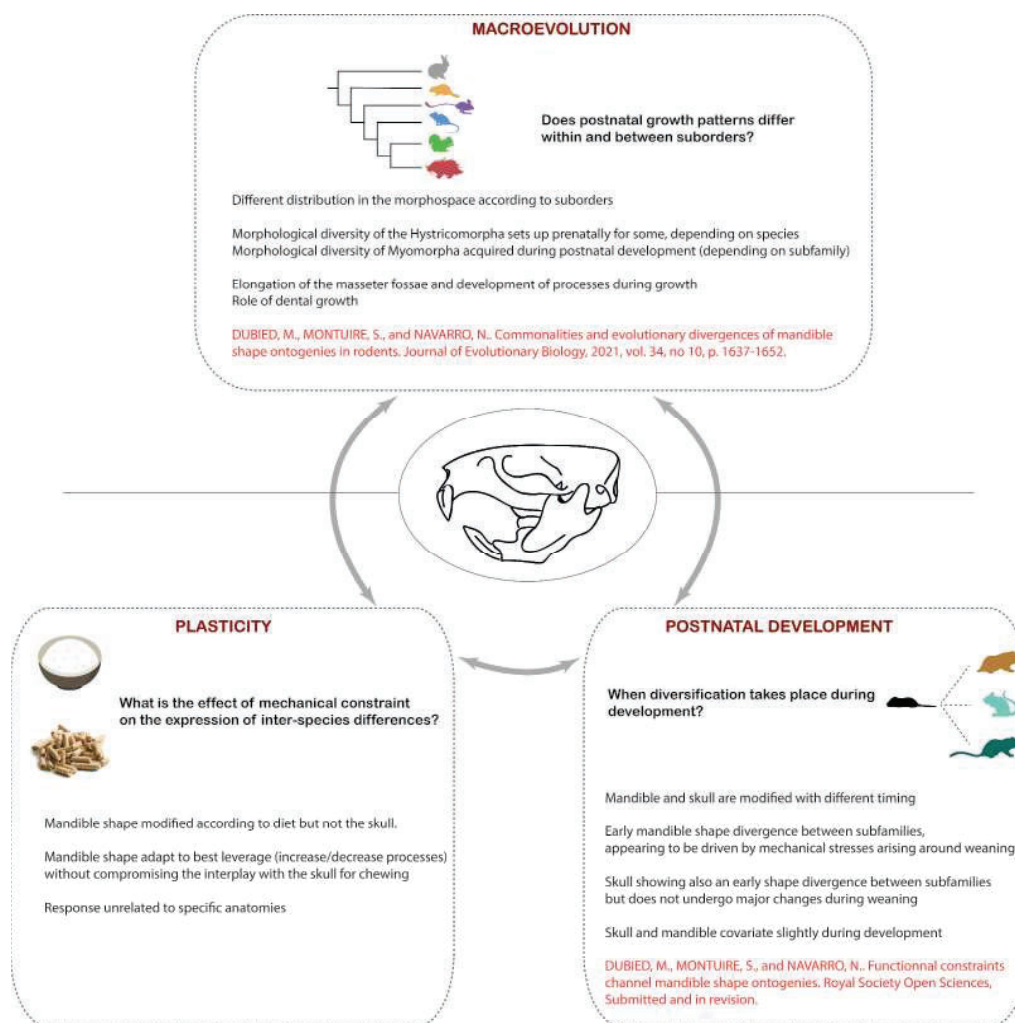


Figure 6.1. Diagram representing the conclusions.

## Perspectives

Throughout this thesis, scientific objectives to decipher the causal mechanisms of the craniofacial disparity onset and experimental setups were intertwined. Several experimental attempts were not successful, but could be improved without a doubt, allowing postnatal growth to be monitored by several proxies. Different perspectives on prenatal and soft tissue developments have also emerged to get an integrative view of the craniofacial development.

Regarding experimental improvement, the observation of growth by fluorochrome markings could be enhanced by having the injections checked by monitored ultrasound scan. As temperature and light do not seem to have a significant effect on the fluorescence capacity of the injected products, it does not seem relevant in the first instance to limit freezing and light exposure. Secondly, concerning the observation of microstructures of bone resorption and formation on the surface by SEM imaging, it would first be necessary to establish an atlas of these structures. This would require an important image compilation coupled with histological samples to decipher whether the structures are bone resorption or formation, and this should be done in a close model organism to the species under study to reduce anatomical differences of bones and soft tissues.

Unfortunately, the attempt to estimate myosin and actin expression was not successful due to contamination of the housekeeping gene to normalize the results. As the samples did not provide a sufficient amount of protein, this experiment could not be reproduced and will have required to replicate the animal breeding. In addition, only mouse samples were processed due to the availability of primers. This estimation of the expression of genes characteristic of muscle growth could be applied, with the design of new specific primers, to other laboratory species.

On a macroevolutionary scale, I was able to highlight that in the Hystricomorpha, the adult shape was already well established at birth in most of the species studied but it was not the case for Myomorpha. It would therefore be interesting to look at the development this time before birth. Studies on prenatal development are generally conducted on model organisms such as the mouse or the rat, based on 2D measurements (Sone *et al.* 2008, Wilson 2011) or histological observations (Frommer 1964, Struthers 1927). Moreover, these studies are conducted on pathological models (Barbeito-Andrès *et al.* 2016, Motch Perrine *et al.* 2014), or on the effect of intra-uterine stress, particularly in toxicology (Giglio *et al.* 1987, Ismail and Janjua 2001, Shen *et al.* 2013). There is therefore a lack of data, to my knowledge, on the prenatal monitoring of healthy organisms. It would therefore be possible to look at in-utero development in the various suborders, to characterize the ontogenetic timing and rates. As Hystricomorpha are born with a quasi-adult shape, their prenatal growth could present analogies with the postnatal growth of Myomorpha.

This thesis was mainly focused on bone development, it would also be possible to study the development of the muscles (masticatory and lingual), especially as different groups of rodents are defined by their infra-orbital and therefore musculofascial structure. In order to obtain an accurate picture of development, it is essential to take into account the different tissues

## Conclusions & Perspectives

that make up the craniofacial complex and thus to know the scenario of their setup. To do this, it is necessary to be able to characterize the muscular tissues very early in the growth process, which can be experimentally challenging. Indeed, masticatory muscles and their architecture are classically described via dissections or only on adult specimens for 3D reconstructions (Cox and Faulkes 2014, Cox and Jeffery 2011, Cox et al. 2012, Ginot et al. 2018a, b). This characterization of muscles could be considered first at the macroevolutionary scale, although it is conditioned by the availability of collections of the different stages of interest on potentially wild species. This study could also be conducted on a finer scale, on the three laboratory species already used in this manuscript. Attempts at iodine labelling of a 7-day-old juvenile mouse (DiceCT, Fig. 6.2) have already been made with results that assure me that this part may be feasible. High-resolution episcopic microscopy (Geyer *et al.* 2017) can also be added and confronted to the results obtained by iodine labelling to facilitate soft tissue recognition.



**Figure 6.2.** DiceCT tests on a 7-day-old mouse specimen (EasyTOM S 150, RX solutions, 5.8  $\mu\text{m}$ , 80kV, 50  $\mu\text{A}$ ). A-B) Different slides. C) positions of the slides.

Throughout the different aspects of this manuscript, I realized that there was a great lack of data on chewing movement. Only few data are available and emanate from direct visual observations (Gorniak 1977) or extrapolation from the wear of the dental occlusal surface (Charles *et al.* 2007, Coillot *et al.* 2013). This aspect was especially interesting when studying variable diets. It has already been shown that some rodents like the hamster could adapt this movement depending on whether they were feeding on pellets or seeds (Gorniak 1977). Indeed, this chewing movement could intuitively influence the way the masticatory muscles function and then their development. During this type of study, it might therefore be appropriate to equip the cages with a camera, or, to a different extent, to film the chewing of the individuals in a given time. These images could be processed with deep learning approach like DeepLabCut (Mathis *et al.* 2018, Nath *et al.* 2019) and compared to obtain an overview of chewing and mastication behavior.

### References

- ALHAJERI, B. H., and STEPPAN, S. J. A phylogenetic test of adaptation to deserts and aridity in skull and dental morphology across rodents. *Journal of Mammalogy*, 2018, vol. 99, no 5, p. 1197-1216.
- ÁLVAREZ, A., and PÉREZ, M. E. Deep changes in masticatory patterns and masseteric musculature configurations accompanied the eco-morphological evolution of cavioid rodents (Hystricognathi, Caviomorpha). *Mammalian Biology*, 2019, vol. 96, no 1, p. 53-60.
- BARBEITO-ANDRÉS, J., GONZALEZ, P. N., and HALLGRÍMSSON, B. Prenatal development of skull and brain in a mouse model of growth restriction. *Revista argentina de antropología biológica*, 2016, vol. 18, no 1, p. 0-0.
- CHARLES, C., JAEGER, J.-J., MICHAUX, J., VIRIOT, L. Dental microwear in relation to changes in the direction of mastication during the evolution of Myodonta (Rodentia, Mammalia). *Naturwissenschaften*, 2007, vol. 94, no 1, p. 71-75.
- COILLOT T., CHAIMANEE, Y., CHARLES, C., GOMES-RODRIGUES, H., MICHAUX J., TAFFOREAU, P., VIANEY-LIAUD, M., VIRIOT, L., and LAZZARI, V. Correlated changes in occlusal pattern and diet in stem Murinae during the onset of the radiation of Old World rats and mice. *Evolution*, 2013, vol. 67, no 11, p. 3323-3338.
- COX, P. G. and FAULKES, C. G. Digital dissection of the masticatory muscles of the naked mole-rat, *Heterocephalus glaber* (Mammalia, Rodentia). *PeerJ*, 2014, vol. 2, p. e448.
- COX, P. G. and JEFFERY, N. Reviewing the morphology of the jaw-closing musculature in squirrels, rats, and guinea pigs with contrast-enhanced microCT. *The Anatomical Record: Advances in Integrative Anatomy and Evolutionary Biology*, 2011, vol. 294, no 6, p. 915-928.
- COX, P. G., RAYFIELD, E. J., FAGAN, M. J., HERREL, A., PATAKY, T. C., and JEFFERY, N. Functional evolution of the feeding system in rodents. *PLoS One*, 2012, vol. 7, no 4, p. e36299.
- FROMMER, J. Prenatal development of the mandibular joint in mice. *The Anatomical Record*, 1964, vol. 150, no 4, p. 449-461.
- GEYER, S. H., MAURER-GESEK, B., REISSIG, L. F., and WENINGER, W. J. High-resolution episcopic microscopy (HREM)-simple and robust protocols for processing and visualizing organic materials. *Journal of Visualized Experiments*, 2017, no 125, p. e56071.
- GIGLIO, M. J., VIEIRO, M., FRIEDMAN, S., and BOZZINI, C. E. Effect of prenatal ethanol exposure on the growth of rat mandible skeletal units. *Journal de biologie buccale*, 1987, vol. 15, no 4, p. 211-216.
- GINOT, S., CLAUDE, J., and HAUTIER, L. One skull to rule them all? Descriptive and comparative anatomy of the masticatory apparatus in five mouse species. *Journal of Morphology*, 2018a, vol. 279, no 9, p. 1234-1255.
- GINOT, S., HERREL, A., CLAUDE, J., and HAUTIER, L. Skull size and biomechanics are good estimators of in vivo bite force in murid rodents. *The Anatomical Record*, 2018b, vol. 301, no 2, p. 256-266.
- GORNIK, G. C. Feeding in golden hamsters, *Mesocricetus auratus*. *Journal of Morphology*, 1977, vol. 154, no 3, p. 427-458.

- GREEN, R. M., FISH, J. L., YOUNG, N. M., SMITH, F. J., ROBERTS, B., DOLAN, K., CHOI, I., LEACH, C. L., GORDON, P., CHEVERUD, J. M., ROSEMAN, C. C., WILLIAMS, T. T., MARCUCIO, R. S., and HALLGRIMSSON, B. Developmental nonlinearity drives phenotypic robustness. *Nature communications*, 2017, vol. 8, no 1, p. 1-12.
- HAUTIER, L., CLAVEL, J., LAZZARI, V., GOMES-RODRIGUES, H., and VIANNEY-LIAUD, M. Biomechanical changes and remodeling of the masticatory apparatus during mammalian evolution: the case of the Issiodoromyinae (Rodentia). *Palaeos*, 2010, vol. 25, no 1, p. 6-13.
- MAESTRI, R., MONTEIRO, L., R., FORNEL, R., UPHAM, N. S., PATTERSON, B. D., and OCHOTORENA DE FREITAS, T. R. The ecology of a continental evolutionary radiation: Is the radiation of sigmodontine rodents adaptive?. *Evolution*, 2017, vol. 71, no 3, p. 610-632.
- MATHIS, A., MAMIDANNA, P., CURY, K. M., ABE, T., MURTHY, V. N., MATHIS, M. W. and BETHGE, M. DeepLabCut: markerless pose estimation of user-defined body parts with deep learning. *Nature neuroscience*, 2018, vol. 21, no 9, p. 1281-1289.
- MITTEROECKER, P., and GUNZ, P. Advances in geometric morphometrics. *Evolutionary Biology*, 2009, vol. 36, no 2, p. 235-247.
- MOTCH PERRINE, S. M., COLE, T. M., MARTÍNEZ-ABADÍAS, N., ALDRIDGE, K., JABS, E. W., and RICHTSMEIER, J. T. Craniofacial divergence by distinct prenatal growth patterns in Fgfr2 mutant mice. *BMC developmental biology*, 2014, vol. 14, no 1, p. 1-17.
- MOTCH PERRINE, S. M., STECKO, T., NEUBERGER, T., JABS, E. W., RYAN, T. M., and RICHTSMEIER, J. T. Integration of brain and skull in prenatal mouse models of Apert and Crouzon syndromes. *Frontiers in human neuroscience*, 2017, vol. 11, p. 369.
- MUHAMMAD, I., and MUHAMMAD ZAHOOR, J. Craniofacial alterations in adult rats after acute prenatal alcohol exposure. *Journal of Ayub Medical College Abbottabad*, 2001, vol. 13, no 3, p. 7-10.
- NATH, T., MATHIS, A., CHEN, A. C., PATEL, A., and MATHIS, M. W. Using DeepLabCut for 3D markerless pose estimation across species and behaviors. *Nature protocols*, 2019, vol. 14, no 7, p. 2152-2176.
- SHEN, L., AI, H., LIANG, Y., REN, X., ANTHONY, C. B., GOODLETT, C. R., WARD, R., and ZHOU, F. C. Effect of prenatal alcohol exposure on bony craniofacial development: a mouse MicroCT study. *Alcohol*, 2013, vol. 47, no 5, p. 405-415.
- SONE, K., KOYASU, K., KOBAYASHI, S., and ODA, S.-I. Fetal growth and development of the coypu (*Myocastor coypus*): Prenatal growth, tooth eruption, and cranial ossification. *Mammalian Biology*, 2008, vol. 73, no 5, p. 350-357.
- STRUTHERS, P. H. The prenatal skull of the Canadian porcupine (*Erethizon dorsatus*). *Journal of Morphology*, 1927, vol. 44, no 2, p. 127-216
- WILSON, L. A. B. Comparison of prenatal and postnatal ontogeny: cranial allometry in the African striped mouse (*Rhabdomys pumilio*). *Journal of Mammalogy*, 2011, vol. 92, no 2, p. 407-420.
- WILSON, L. A. B. Allometric disparity in rodent evolution. *Ecology and Evolution*, 2013, vol. 3, no 4, p. 971-984.



## **Annexes**

Annexe 1 - Supplementary materials: DUBIED, M., MONTUIRE, S., and NAVARRO, N.. Commonalities and evolutionary divergences of mandible shape ontogenies in rodents. *Journal of Evolutionary Biology*, 2021, vol. 34, no 10, p. 1637-1652.

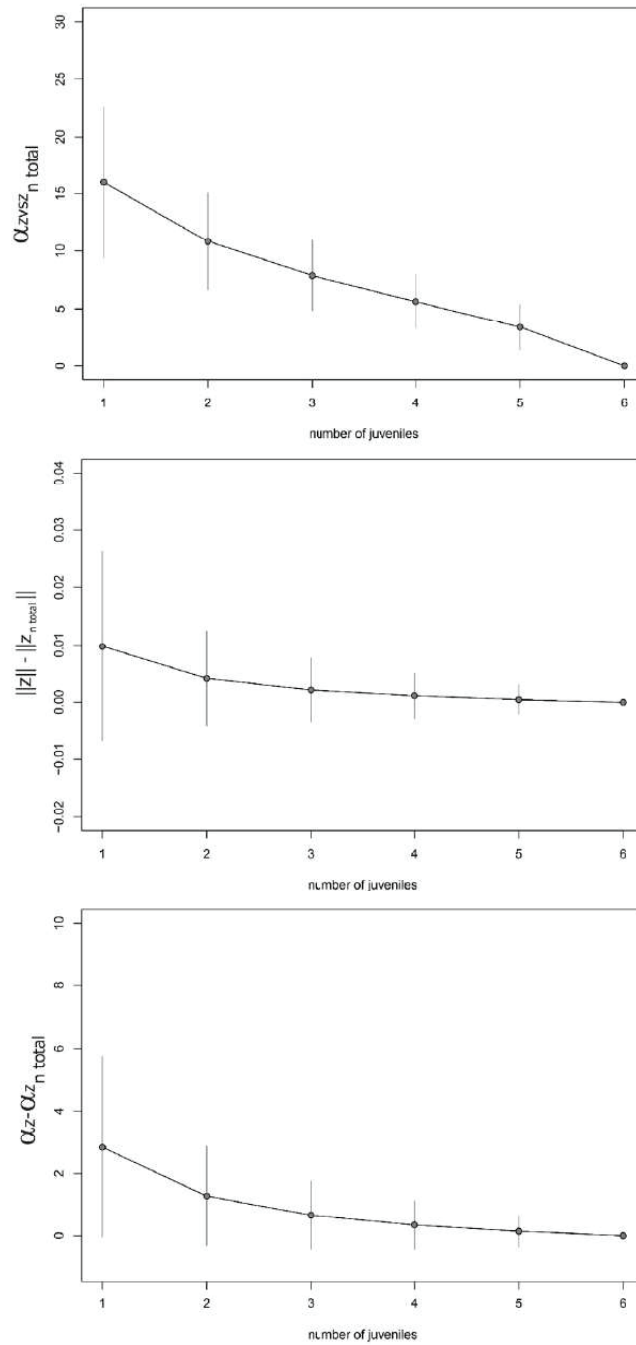
**Table S1.** List of specimens. IRSNB: Institut Royal des Sciences Naturelles de Belgique, Bruxelles. MHNG: Museum d'Histoire Naturelle de Genève. MNHN : Museum National d'Histoire Naturelle, Paris. NMB: Naturhistorisches Museum Basel. uB\_BGS: Université de Bourgogne, Biogéosciences, Dijon.

Species	Specimen	Age	Supp. Data
<i>Meriones unguiculatus</i>	uB_BGS-G-K-7J	Juvenile	
<i>Meriones unguiculatus</i>	uB_BGS-G-L-7J	Juvenile	
<i>Meriones unguiculatus</i>	uB_BGS-G-M-7J	Juvenile	
<i>Meriones unguiculatus</i>	uB_BGS-G-N-7J	Juvenile	
<i>Meriones unguiculatus</i>	uB_BGS-G-O-7J	Juvenile	
<i>Meriones unguiculatus</i>	uB_BGS-G-K-14J	Subadult	x
<i>Meriones unguiculatus</i>	uB_BGS-G-L-14J	Subadult	x
<i>Meriones unguiculatus</i>	uB_BGS-G-M-14J	Subadult	x
<i>Meriones unguiculatus</i>	uB_BGS-G-N-14J	Subadult	x
<i>Meriones unguiculatus</i>	uB_BGS-G-O-14J	Subadult	x
<i>Meriones unguiculatus</i>	uB_BGS-G-Dad-1	Adult	
<i>Meriones unguiculatus</i>	uB_BGS-G-Dad-2	Adult	
<i>Meriones unguiculatus</i>	uB_BGS-G-Mom-K	Adult	
<i>Meriones unguiculatus</i>	uB_BGS-G-Mom-L	Adult	
<i>Meriones unguiculatus</i>	uB_BGS-G-Mom-M	Adult	
<i>Meriones unguiculatus</i>	uB_BGS-G-Mom-N	Adult	
<i>Meriones unguiculatus</i>	uB_BGS-G-Mom-O	Adult	
<i>Mesocricetus auratus</i>	uB_BGS-H-C1-7J	Juvenile	
<i>Mesocricetus auratus</i>	uB_BGS-H-C4-7J	Juvenile	
<i>Mesocricetus auratus</i>	uB_BGS H C5-7J	Juvenile	
<i>Mesocricetus auratus</i>	uB_BGS-H-C6-7J-1	Juvenile	
<i>Mesocricetus auratus</i>	uB_BGS-H-C6-7J-2	Juvenile	
<i>Mesocricetus auratus</i>	uB_BGS-H-C7-7J	Juvenile	
<i>Mesocricetus auratus</i>	uB_BGS-H-C1-14J	Subadult	x
<i>Mesocricetus auratus</i>	uB_BGS-H-C3-14J	Subadult	x
<i>Mesocricetus auratus</i>	uB_BGS-H-C4-14J	Subadult	x
<i>Mesocricetus auratus</i>	uB_BGS-H-C5-14J	Subadult	x
<i>Mesocricetus auratus</i>	uB_BGS-H-C6-14J-1	Subadult	x
<i>Mesocricetus auratus</i>	uB_BGS-H-C6-14J-2	Subadult	x
<i>Mesocricetus auratus</i>	uB_BGS-H-C7-14J	Subadult	x
<i>Mesocricetus auratus</i>	uB_BGS-H-C1MH-1	Adult	
<i>Mesocricetus auratus</i>	uB_BGS-H-C3MH-1	Adult	
<i>Mesocricetus auratus</i>	uB_BGS-H-C4FH-1	Adult	
<i>Mesocricetus auratus</i>	uB_BGS-H-C6FH-1	Adult	

Species	Specimen	Age	Supp. Data
<i>Microtus arvalis</i>	MHNG-arv_4	Juvenile	
<i>Microtus arvalis</i>	MHNG-arv_5	Juvenile	
<i>Microtus arvalis</i>	MHNG_1477.019	Subadult	x
<i>Microtus arvalis</i>	MHNG_1477.020	Subadult	x
<i>Microtus arvalis</i>	MHNG_1477.021	Subadult	x
<i>Microtus arvalis</i>	MHNG_1477.023	Subadult	x
<i>Microtus arvalis</i>	MHNG_1477.024	Subadult	x
<i>Microtus arvalis</i>	MHNG_1477.025	Subadult	x
<i>Microtus arvalis</i>	MHNG_1477.026	Subadult	x
<i>Microtus arvalis</i>	uB_BGS-M.Arv-Lodesma-1	Adult	
<i>Microtus arvalis</i>	uB_BGS-M.Arv-Lodesma-2	Adult	
<i>Microtus arvalis</i>	uB_BGS-M.Arv-Mayorga-1	Adult	
<i>Microtus arvalis</i>	uB_BGS-M.Arv-Mayorga-2	Adult	
<i>Mus musculus</i>	uB_BGS-M-A-7J	Juvenile	
<i>Mus musculus</i>	uB_BGS-M-B-7J	Juvenile	
<i>Mus musculus</i>	uB_BGS-M-D-7J	Juvenile	
<i>Mus musculus</i>	uB_BGS-M-E-7J	Juvenile	
<i>Mus musculus</i>	uB_BGS-M-G1-7J	Juvenile	
<i>Mus musculus</i>	uB_BGS-M-A-15J	Subadult	x
<i>Mus musculus</i>	uB_BGS M B 15J	Subadult	x
<i>Mus musculus</i>	uB_BGS-M-D-15J	Subadult	x
<i>Mus musculus</i>	uB_BGS-M-E-15J	Subadult	x
<i>Mus musculus</i>	uB_BGS-M-G1-15J	Subadult	x
<i>Mus musculus</i>	uB_BGS-M-AMH-1	Adult	
<i>Mus musculus</i>	uB_BGS-M-BMH-1	Adult	
<i>Mus musculus</i>	uB_BGS-M-EMH-1	Adult	
<i>Mus musculus</i>	uB_BGS-M-EMH-2	Adult	
<i>Mus musculus</i>	uB_BGS-M-Mom-A	Adult	
<i>Mus musculus</i>	uB_BGS-M-Mom-B	Adult	
<i>Mus musculus</i>	uB_BGS-M-Mom-G	Adult	
<i>Mus musculus</i>	uB_BGS-M-Mom-E	Adult	
<i>Rattus rattus</i>	MHNG_766.94-1	Juvenile	
<i>Rattus rattus</i>	MHNG_766.94-3	Juvenile	
<i>Rattus rattus</i>	MI ING_766.94-4	Juvenile	
<i>Rattus rattus</i>	MHNG_1613-57	Adult	
<i>Rattus rattus</i>	MHNG_1613-59	Adult	
<i>Rattus rattus</i>	MHNG_1649-94	Adult	
<i>Rattus rattus</i>	MHNG_1649-95	Adult	

Species	Specimen	Age
<i>Oryctolagus cuniculus</i>	IRSNB_1591	Juvenile
<i>Oryctolagus cuniculus</i>	IRSNB_3261	Juvenile
<i>Oryctolagus cuniculus</i>	IRSNB_6255	Juvenile
<i>Oryctolagus cuniculus</i>	IRSNB_6754	Juvenile
<i>Oryctolagus cuniculus</i>	IRNSB_10552	Adult
<i>Oryctolagus cuniculus</i>	IRSNB_13161	Adult
<i>Oryctolagus cuniculus</i>	IRSNB_1590d	Adult
<i>Oryctolagus cuniculus</i>	IRSNB_6575	Adult
<i>Oryctolagus cuniculus</i>	IRSNB_9827	Adult
<i>Funisciurus lemniscatus</i>	MNHN_1960_3884	Juvenile
<i>Funisciurus lemniscatus</i>	MNHN_1961_308	Adult
<i>Funisciurus lemniscatus</i>	MNHN_1981_580	Adult
<i>Funisciurus lemniscatus</i>	MNHN_1981_583	Adult
<i>Funisciurus lemniscatus</i>	MNHN_1990_663	Adult
<i>Muscardinus avellanarius</i>	MNHN_1981-1015	Juvenile
<i>Muscardinus avellanarius</i>	MNHN_1932-4413	Adult
<i>Muscardinus avellanarius</i>	MNHN_1942-390	Adult
<i>Muscardinus avellanarius</i>	MNHN_1966-1032	Adult
<i>Muscardinus avellanarius</i>	MNHN_1981-449	Adult
<i>Capromys pilorides</i>	IRSNB_3281	Juvenile
<i>Capromys pilorides</i>	IRSNB_3282	Adult
<i>Cavia porcellus</i>	IRSNB_7114	Juvenile
<i>Cavia porcellus</i>	IRSNB_39533	Adult
<i>Cavia porcellus</i>	IRSNB_5893	Adult
<i>Cavia porcellus</i>	IRSNB_5894	Adult
<i>Dolichotis patagonum</i>	NMB_8409	Juvenile
<i>Dolichotis patagonum</i>	NMB_13517	Adult
<i>Dolichotis patagonum</i>	NMB_7325	Adult
<i>Dolichotis patagonum</i>	NMB_7647	Adult
<i>Dolichotis patagonum</i>	NMB_7979	Adult

Species	Specimen	Age
<i>Erethizon dorsatum</i>	NMB_13508	Juvenile
<i>Erethizon dorsatum</i>	NMB_1451	Juvenile
<i>Erethizon dorsatum</i>	NMB_6999	Adult
<i>Erethizon dorsatum</i>	NMB_7268	Adult
<i>Erethizon dorsatum</i>	NMB_7729	Adult
<i>Erethizon dorsatum</i>	NMB_872	Adult
<i>Hystrix cristata</i>	NMB_6193	Juvenile
<i>Hystrix cristata</i>	NMB_13309	Adult
<i>Hystrix cristata</i>	NMB_13308	Adult
<i>Hystrix cristata</i>	NMB_13311	Adult
<i>Hystrix cristata</i>	NMB_13313	Adult
<i>Lagostomus maximus</i>	NMB_6560	Juvenile
<i>Lagostomus maximus</i>	NMB_9995	Juvenile
<i>Lagostomus maximus</i>	NMB_13514	Adult
<i>Lagostomus maximus</i>	NMB_13515	Adult
<i>Lagostomus maximus</i>	NMB_5435	Adult
<i>Lagostomus maximus</i>	NMB_7239	Adult
<i>Myocastor coypus</i>	IRSNB_627D	Juvenile
<i>Myocastor coypus</i>	IRSNB_9099	Adult
<i>Myocastor coypus</i>	IRSNB_1773	Adult
<i>Myocastor coypus</i>	IRSNB_627	Adult
<i>Thryonomys swinderianus</i>	NMB_13344	Juvenile
<i>Thryonomys swinderianus</i>	NMB_13327	Adult
<i>Thryonomys swinderianus</i>	NMB_13328	Adult
<i>Thryonomys swinderianus</i>	NMB_13332	Adult
<i>Thryonomys swinderianus</i>	NMB_13349	Adult



**Supplementary figure S1.** Effect of the number of sampled juveniles. A) Angle between the postnatal trajectories  $z$  estimated from the complete or the downsampled sets of juveniles. B) Differences in the amount of postnatal changes between the complete and the downsampled sets of juveniles. C) Differences in angles between the ancestral postnatal trajectory ( $\bar{z}_{pgls}$ ) and the species trajectories estimated either with the complete or the downsampled sets of juveniles.

**Supplementary Table S2.** Effect of the variation in age of juveniles.

Species	alpha*	theta**	prop.norm***
<i>Mus musculus</i>	48.98	13.44	0.39
<i>Mesocricetus auratus</i>	30.74	9.52	0.73
<i>Meriones unguiculatus</i>	29.19	4.91	0.85
<i>Microtus arvalis</i>	42.38	18.06	0.68

\*alpha: angle between Adult-Juvenile and Adult-subAdult

\*\*theta: diff. between angles with common trajectory  $\bar{z}_{pGLS}$

\*\*\*Proportion of the norm of the Adult-Juvenile vector

**Supplementary Table S3.** Disparity (Procrustes variances) of clade × age groups.

suborder	age	disparity
Hystricomorpha	all	0.0169 ± 0.0014
Myomorpha	all	0.0213 ± 0.0018
Hystricomorpha	juvenile	0.0163 ± 0.0020
Myomorpha	juvenile	0.0110 ± 0.0019
Hystricomorpha	adult	0.0149 ± 0.0019
Myomorpha	adult	0.0135 ± 0.0031

#### Error rate and power of the phylogenetic generalized least-squares using Procrustes sum of squares and residual permutations

Shapes were simulated in the tangent space following its linear approximation (Bookstein 2016; Klingenberg 2020) given the mean shape of our sample and an isotropic variation. This simulation scheme respects the constraints that the Procrustes superimposition imposes on the variation. This is the main difference to the simulations of Adams and Collyer (2018) where multiple traits were simulated with a similar effect on each dimension. Also, our focal tree is half smaller than the tree used in this previous study.

The norm of the simulated shape change was scaled to a certain proportion of the total Procrustes variance (at most 50%). 100 simulations of shape effect and residuals were done and for each of them 100 Brownian evolution of the covariate were simulated. Two kind of covariate were simulated: a continuous one and a three-state character. Analysis with a random binary classification was also realized. Probability of the effect was estimated with phylogenetic GLS within the package geomorph 3.2.1 (Adams et al. 2020) and evaluated using 1000 residual permutations with the package RRPP 0.5.2 (Collyer and Adams 2018). The family-wise error rate was computed on as the proportion of significant pGLS when no covariate effect was simulated and again this error rate was averaged across the 100 shape configurations (Table S4). For each of the three models, the expected FWER is lower than 5%.

**Supplementary Table S4.** Error rate for the pGLS given the 16 species tree

Effect	fwcr	2.5 <sup>th</sup> quantile	97.5 <sup>th</sup> quantile
Quantitative covariate	0.042	0.005	0.08
3-state covariate	0.049	0.01	0.11
Binary class	0.039	0.01	0.08

Power was computed as the proportion of the simulations where the probability was lower than 0.05 and the average across the 100 shape configurations was reported (Figure S2).

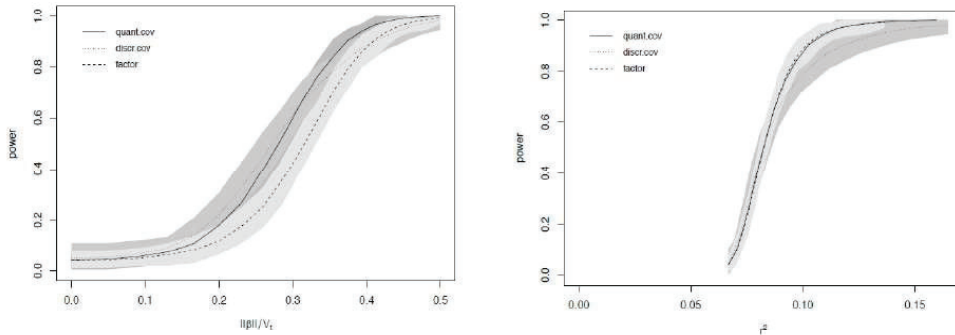


**Figure S2.** Power of pGLS given the 16 species tree and the three kind of covariate or grouping. X-axis on the left panel reported the ratio of the norm of the effect  $\beta$  (effect to be simulated) to the total variance (the sum of eigenvalues), and the observed  $r^2$  on the right. Shade area represent 95<sup>th</sup> interval of the 100 shape simulations and lines their averages. Power reaches 80% for an effect size equal to 0.35 (quantitative covariate), 0.37 (3-state covariate), and 0.39 (binary classification).

**Movies S1.** Shape changes according to the ancestral estimate of postnatal growth trajectory apply to the estimate of the juvenile mean shape of either the Myomorpha or the Hystricomorpha.

**Movies S2.** Shape changes according to the effect of the hypselodonty estimated from the pGLS and applied to the Myomorpha mean shape (based on a brachyodont shape).

## Annexe 2 - Specimens used during experiments

Species	Litter	Name	Cage	Sexe	Diet	Age (Days)	Weight (g)
Hamster	C1	H-Mom-C1		F	Hard	100	127,5
Hamster	C1	H-C1-7J		N	N	7	8,2
Hamster	C1	H-C1-14J		N	N	14	14
Hamster	C1	H-C1-29J-1		N	N	29	59,2
Hamster	C1	H-C1-29J-2		N	N	29	57,8
Hamster	C1	H-C1MH-1	J2	M	Hard	35	84,6
Hamster	C1	H-C1FH-1	H2	F	Hard	63	93,2
Hamster	C1	H-C1FS-1	A2	F	Soft	35	84,9
Hamster	C1	H-C1FS-2	A2	F	Soft	63	127,7
Hamster	C1	H-C1FS-3	A2	F	Soft	63	138,6
Hamster	C3	H-Mom-C3		F	Hard	100	136
Hamster	C3	H-C3-14J		N	N	14	15,4
Hamster	C3	H-C3-29J-1		N	N	29	58,9
Hamster	C3	H-C3-29J-2		N	N	29	60,1
Hamster	C3	H-C3MH-1	J2	M	Hard	35	96,2
Hamster	C3	H-C3MH-2	J2	M	Hard	63	99,4
Hamster	C3	H-C3MS-1	D2	M	Soft	35	88,1
Hamster	C3	H-C3MS-2	D2	M	Soft	63	120
Hamster	C3	H-C3FS-1	B2	F	Soft	63	123,6
Hamster	C3	H-C3FH-1	G2	F	Hard	63	115,8
Hamster	C4	H-Mom-C4		F	Hard	100	132,8
Hamster	C4	H-C4-7J		N	N	7	9,5
Hamster	C4	H-C4-14J		N	N	14	18,9
Hamster	C4	H-C4-29J		N	N	29	61,3
Hamster	C4	H-C4FH-1	G2	F	Hard	35	85,9
Hamster	C4	H-C4FS-1	B2	F	Soft	35	105,8
Hamster	C4	H-C4MH-1	K2	M	Hard	63	105,9
Hamster	C4	H-C4MS-1	E2	M	Soft	63	166
Hamster	C5	H-Mom-C5		F	Hard	100	129
Hamster	C5	H-C5-7J		N	N	7	9
Hamster	C5	H-C5-14J		N	N	14	13,6
Hamster	C5	H-C5-29J		N	N	29	53,6
Hamster	C5	H-C5FH-1	I2	F	Hard	63	106
Hamster	C5	H-C5FH-2	I2	F	Hard	63	105,4
Hamster	C5	H-C5FS-1	C2	F	Soft	63	114,9
Hamster	C5	H-C5MH-1	L2	M	Hard	35	80,8
Hamster	C5	H-C5MH-2	L2	M	Hard	63	92,5
Hamster	C5	H-C5MS-1	F2	M	Soft	35	79,4
Hamster	C6	H-Mom-C6		F	Hard	100	154
Hamster	C6	H-C6-7J		N	N	7	7,9
Hamster	C6	H-C6-14J-1		N	N	14	15,1
Hamster	C6	H-C6-14J-2		N	N	14	14,9
Hamster	C6	H-C6-29J-1		N	N	29	60,7
Hamster	C6	H-C6-29J-2		N	N	29	62,5
Hamster	C6	H-C6FS-1	C2	F	Soft	35	98,8
Hamster	C6	H-C6FS-2	C2	F	Soft	63	119,6
Hamster	C6	H-C6FS-3	C2	F	Soft	63	111,8
Hamster	C6	H-C6FH-1	I2	F	Hard	35	93,4
Hamster	C6	H-C6FH-2	I2	F	Hard	63	122,4
Hamster	C6	H-C6MS-1	F2	M	Soft	63	127,8
Hamster	C6	H-C6MH-1	L2	M	Hard	63	118,6
Hamster	C7	H-Mom-C7		F	Hard	100	146
Hamster	C7	H-C7-7J		N	N	7	10,1
Hamster	C7	H-C7-14J		N	N	14	17,3
Hamster	C7	H-C7-29J		N	N	29	63,7
Hamster	C7	H-C7FH-1	G2	F	Hard	63	129,8
Hamster	C7	H-C7FS-1	B2	F	Soft	63	156
Hamster	C7	H-C7MH-1	K2	M	Hard	35	93,7
Hamster	C7	H-C7MS-1	E2	M	Soft	35	100,1

Species	Litter	Name	Cage	Sexe	Diet	Age (Days)	Weight (g)
Gerbil		G-Dad-1		M	Hard	100	90,1
Gerbil		G-Dad-2		M	Hard	100	89,4
Gerbil	K	G-Mom-K		F	Hard	100	82,4
Gerbil	K	G-K-7J		N	N	7	6,7
Gerbil	K	G-K-14J		N	N	14	11,3
Gerbil	K	G-KFS-1	A3	F	Soft	63	60,1
Gerbil	K	G-KFH-1	B3	F	Hard	63	54,3
Gerbil	K	G-KMS-1	C3	M	Soft	35	42,1
Gerbil	K	G-KMS-2	C3	M	Soft	63	59,3
Gerbil	K	G-KMS-3	C3	M	Soft	63	71,8
Gerbil	K	G-KMH-1	E3	M	Hard	35	55,1
Gerbil	K	G-KMH-2	E3	M	Hard	63	65,4
Gerbil	L	G-Mom-L		F	Hard	100	83
Gerbil	L	G-L-7J		N	N	7	6,8
Gerbil	L	G-L-14J		N	N	14	12,8
Gerbil	L	G-LFS-1	A3	F	Soft	63	50,8
Gerbil	L	G-LMS-1	D3	M	Soft	35	42,2
Gerbil	L	G-LMS-2	D3	M	Soft	63	71,2
Gerbil	L	G-LMH-1	F3	M	Hard	35	49,2
Gerbil	L	G-LMH-2	F3	M	Hard	63	69,2
Gerbil	M	G-Mom-M		F	Hard	100	80,7
Gerbil	M	G-M-7J		N	N	7	7,5
Gerbil	M	G-M-14J		N	N	14	12,7
Gerbil	M	G-MFS-1	A3	F	Soft	35	46,5
Gerbil	M	G-MFH-1	B3	F	Hard	35	48
Gerbil	M	G-MMS-1	D3	M	Soft	63	69,2
Gerbil	M	G-MMH-1	F3	M	Hard	63	70,4
Gerbil	N	G-Mom-N		F	Hard	100	85,1
Gerbil	N	G-N-7J		N	N	7	6,5
Gerbil	N	G-N-14J		N	N	14	11,9
Gerbil	N	G-NFS-1	G3	F	Soft	35	50
Gerbil	N	G-NFS-2	G3	F	Soft	63	54,2
Gerbil	N	G-NFH-1	H3	F	Hard	35	53,4
Gerbil	N	G-NFH-2	H3	F	Hard	63	58,4
Gerbil	N	G-NMS-1	I3	M	Soft	63	60,1
Gerbil	N	G-NMH-1	J3	M	Hard	63	70,4
Gerbil	O	G-Mom-O		F	Hard	100	79,3
Gerbil	O	G-O-7J		N	N	7	7,9
Gerbil	O	G-O-14J		N	N	14	13
Gerbil	O	G-OFS-1	G3	F	Soft	63	58,9
Gerbil	O	G-OMH-1	J3	M	Hard	63	88,8
Gerbil	O	G-OMS-1	I3	M	Soft	35	49,9

Species	Litter	Name	Cage	Sexe	Diet	Age (Days)	Weight (g)
Mouse	A	M-Mom-A		F	Hard	100	24,2
Mouse	A	M-A-7J		N	N	7	5,6
Mouse	A	M-A-15J		N	N	14	9,5
Mouse	A	M-AFH-1	A1	F	Hard	35	19,3
Mouse	A	M-AMH-1	B1	M	Hard	63	25
Mouse	B	M-Mom-B		F	Hard	100	21,1
Mouse	B	M-B-7J		N	N	7	5,4
Mouse	B	M-B-15J		N	N	14	9,7
Mouse	B	M-BMH-1	B1	M	Hard	35	20,9
Mouse	B	M-BFH-1	A1	F	Hard	63	19,9
Mouse	D	M-Mom-D		F	Hard	100	22,4
Mouse	D	M-D-7J		N	N	7	5,2
Mouse	D	M-D-15J		N	N	14	8,2
Mouse	D	M-DFH-1	A1	F	Hard	63	17,7
Mouse	D	M-DMH-1	B1	M	Hard	35	18,6
Mouse	E	M-Mom-E		F	Hard	100	23
Mouse	E	M-E-7J		N	N	7	6
Mouse	E	M-E-15J		N	N	14	10,5
Mouse	E	M-EMH-1	B1	M	Hard	35	19,9
Mouse	E	M-EMH-2	B1	M	Hard	63	24,1
Mouse	E	M-EFS-1	C1	F	Soft	35	13,9
Mouse	E	M-EFS-2	C1	F	Soft	63	22
Mouse	E	M-EFS-3	C1	F	Soft	63	19,5
Mouse	G	M-Mom-G		F	Hard	100	23,6
Mouse	G	M-G1-7J		N	N	7	5,5
Mouse	G	M-G1-15J		N	N	14	10,2
Mouse	G	M-G1FH-1	A1	F	Hard	35	14,9
Mouse	G	M-G2MS-1	E1	M	Soft	63	27,3
Mouse	G	M-G2FS-1	F1	F	Soft	35	15
Mouse	G	M-G2FS-2	F1	F	Soft	35	16,5
Mouse	G	M-G2FS-3	F1	F	Soft	35	15,7
Mouse	G	M-G2FS-4	F1	F	Soft	63	20,2
Mouse	G	M-G2FS-5	F1	F	Soft	63	22,1
Mouse	J	M-Mom-J		F	Hard	100	25,1
Mouse	J	M-JFH-1	G1	F	Hard	63	18,9
Mouse	J	M-JFS-1	H1	F	Soft	63	19,4
Mouse	J	M-JFS-2	H1	F	Soft	63	20,5
Mouse	J	M-JMS-1	I1	M	Soft	63	21,2
Mouse	J	M-JMS-2	I1	M	Soft	63	21,4
Mouse	J	M-JMS-3	I1	M	Soft	63	21,2

Annexe 3 - Supplementary materials: DUBIED, M., MONTUIRE, S., and NAVARRO, N.. Functional constraints channel mandible shape ontogenies. *Royal Society Open Science*, Accepted.

Supplementary Table 1. Analysis of Variance

	Df	SS	MS	Rsq	F_perm	Z_perm	Pr(>F)_perm	Pillai	Z	F approx	Df1	Df2	Pr(>F)	Pr(<Pillai)_perm
species	2	0.77349	0.38675	0.51376	324.397	8.2790	0.001	1.999928	1.602031	759.23	146	4	3.511e-06	0.001
age	4	0.52173	0.13043	0.34654	109.406	7.0232	0.001	3.985144	2.878793	14.70	292	16	1.387e-07	0.001
species:age	8	0.12263	0.01533	0.08145	12.858	16.3280	0.001	7.825837	5.435799	4.92	584	64	2.032e-12	0.001
Residuals	73	0.08703	0.01533	0.05781										

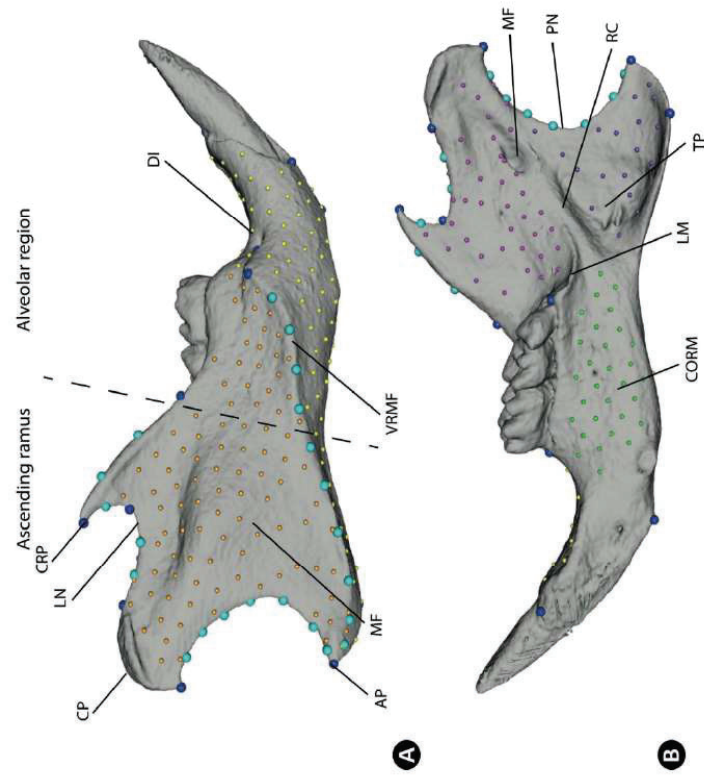
Supplementary Table 2. Path distances (SE)

Gerbil	Hamster	Mouse
0.2609273 (0.009902233)	0.2854395(0.009556840)	0.2632860 (0.010739087)

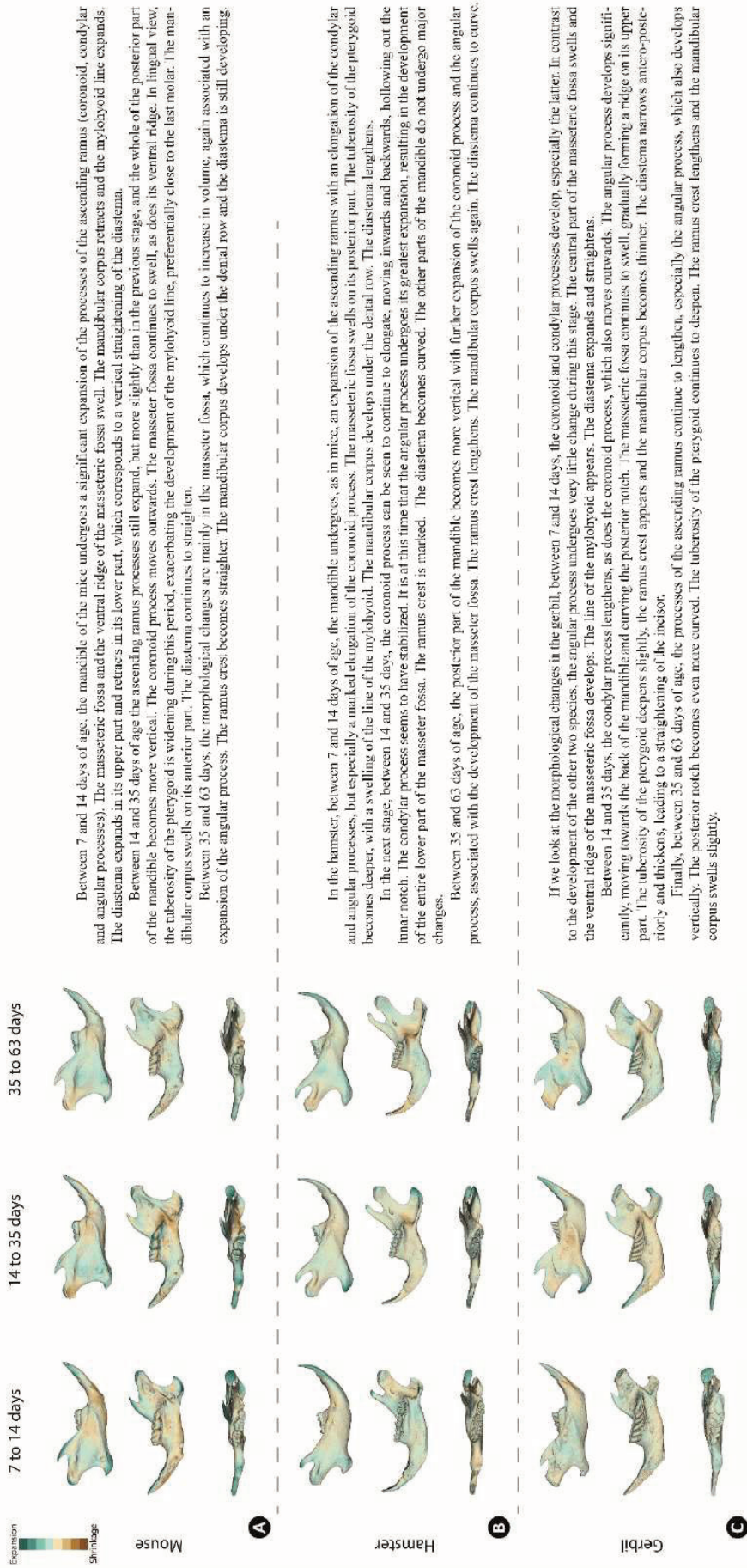
Supplementary Table 3. Trajectory analysis

	r_path_dist	d_path_dist	UCL (95%)	Z Pr > d	r_path_dist	r_angle	r_angle	angle	UCL (95%)	Z Pr > angle	r_shape	d_shape	UCL (95%)	Z Pr > d shape
Gerbil:Hamster	0.024512237	0.03725481	0.9538886	0.186	0.7877686	38.02253	38.02253	11.75462	0.001	0.08612659	0.1935579	-1.235703	0.886	
Gerbil:Mouse	0.002358729	0.03906131	-1.3787924	0.910	0.8325332	33.64015	33.64015	11.88610	0.001	0.41773173	0.1971286	6.104168	0.001	
Hamster:Mouse	0.022153508	0.03951145	0.6858120	0.267	0.7829233	38.47098	38.47098	12.01749	0.001	0.42963305	0.1917990	5.776478	0.001	

Supplementary Figure 1. Landmarks and semilandmarks on 3D mandibular surface. Blue dots are manual 3D landmarks, light blue dots represent semilandmark curves, other dots colored similarly belong to the same patch of surface semilandmarks. (AP: angular process, CORM: mandibular corpus, CRP: condylar process, CP: coronoid process, DI: diastema, LM: line of the mylohyoid, LN: lunar notch, MF: masseteric fossa, PN: posterior notch, RC: ramus crest, RF: ramus fossa, TP: tuberosity of the pterygoid, VRMF: ventral ridge of masseteric fossa). A: labial view; B: lingual view.



Supplementary Figure 2. Shape changes along postnatal development of each species. Reference shapes were initially parallel transported prior to be deformed according to growth vectors.



Between 7 and 14 days of age, the mandible of the mice undergoes a significant expansion of the processes of the ascending ramus (coronoid, condylar and angular processes). The masseteric fossa and the ventral ridge of the masseteric fossa swell. The mandibular corpus retracts and the mylohyoid line expands. The diastema expands in its upper part and retracts in its lower part, which corresponds to a vertical straightening of the diastema.

Between 14 and 35 days of age the ascending ramus processes still expand, but more slightly than in the previous stage, and the whole of the posterior part of the mandible becomes more vertical. The coronoid process moves outwards. The masseter fossa continues to swell, as does its ventral ridge. In lingual view, the tuberosity of the pterygoid is widening during this period, exacerbating the development of the mylohyoid line, preferentially close to the last molar. The mandibular corpus swells on its anterior part. The diastema continues to straighten.

Between 35 and 63 days, the morphological changes are mainly in the masseter fossa, which continues to increase in volume, again associated with an expansion of the angular process. The ramus crest becomes straighter. The mandibular corpus develops under the dental row and the diastema is still developing.

In the hamster, between 7 and 14 days of age, the mandible undergoes, as in mice, an expansion of the ascending ramus with an elongation of the condylar and angular processes, but especially a marked elongation of the coronoid process. The masseteric fossa swells on its posterior part. The tuberosity of the pterygoid becomes deeper, with a swelling of the line of the mylohyoid. The mandibular corpus develops under the dental row. The diastema lengthens.

In the next stage, between 14 and 35 days, the coronoid process can be seen to continue to elongate, moving inwards and backwards, following out the linear notch. The condylar process seems to have stabilized. It is at this time that the angular process undergoes its greatest expansion, resulting in the development of the entire lower part of the masseter fossa. The ramus crest is marked. The diastema becomes curved. The other parts of the mandible do not undergo major changes.

Between 35 and 63 days of age, the posterior part of the mandible becomes more vertical with further expansion of the coronoid process and the angular process, associated with the development of the masseter fossa. The ramus crest lengthens. The mandibular corpus swells again. The diastema continues to curve.

If we look at the morphological changes in the gerbil, between 7 and 14 days, the coronoid and condylar processes develop, especially the latter. In contrast to the development of the other two species, the angular process undergoes very little change during this stage. The central part of the masseteric fossa swells and the ventral ridge of the masseteric fossa develops. The line of the mylohyoid appears. The diastema expands and straightens.

Between 14 and 35 days, the condylar process lengthens, as does the coronoid process, which also moves outwards. The angular process develops significantly, moving towards the back of the mandible and curving the posterior notch. The masseteric fossa continues to swell, gradually forming a ridge on its upper part. The tuberosity of the pterygoid deepens slightly, the ramus crest appears and the mandibular corpus becomes thinner. The diastema narrows antero-posteriorly and thickens, leading to a straightening of the incisor.

Finally, between 35 and 63 days of age, the processes of the ascending ramus continue to lengthen, especially the angular process, which also develops vertically. The posterior notch becomes even more curved. The tuberosity of the pterygoid continues to deepen. The ramus crest lengthens and the mandibular corpus swells slightly.

In all three species, the growth of the ascending ramus processes (coronoid, condylar and angular processes) is a key point in the development of the mandible, but the timing of this growth varies between taxa. In mice, these processes undergo increased growth from the first stage studied (7 to 14 days) and slow down progressively in the following stages. On the other hand, in hamsters and gerbils, the development of the angular process only starts at a second stage (between 14 and 35 days) and continues for the rest of the time studied. The coronoid process being longer in the adult hamster, its growth is over the whole period studied. The masseteric fossa develops significantly throughout the stages in the mouse. In the hamster, it develops first on its posterior part, and undergoes major changes between 35 and 63 days. The gerbil's one shows a major remodelling in the third stage. The ramus crest develops in the same way in both murids, becoming more massive and straight in the second stage. It is already well formed in the first stage when looking at the hamster. The mandibular corpus does not develop immediately in the mouse, its remodelling only starts at the second stage and especially on its anterior part. In the hamster, it starts to develop between 7 and 14 days, slows down in the second stage, and starts again in the third. This part in the gerbil is generally little modified and its development is especially notable between 35 and 63 days. Finally, in all three species the diastema is long and flat at the beginning of growth and deepens, with the incisor outlet becoming more vertical later on.







**Titre :** Développement postnatal et évolution du complexe craniofacial chez les rongeurs

**Mots clés :** Développement, Morphométrie géométrique, Epigénétique, Craniofacial, Rongeurs, Croissance

**Résumé :** Le crâne est une structure fortement intégrée, complexe architecturalement et fonctionnellement. En même temps et paradoxalement, cette unité est très évolvable et présente une très grande diversité de formes. Les interactions épigénétiques lors de la croissance vont permettre de répondre aux stimulations mécaniques, de compenser et coordonner la croissance des différents organes composant la tête afin d'acquérir et/ou de maintenir certaines fonctions. Elles vont permettre un développement normal en contrôlant la remodelisation osseuse. Malgré ce rôle central, l'importance de ces interactions dans l'expression des différences entre espèces et à plus long terme dans la dynamique des clades reste peu comprise.

Le projet de thèse vise à étudier I) la mise en place de la disparité craniofaciale chez les rongeurs au cours du développement et II) d'évaluer l'importance des processus épigénétiques lors de cette croissance postnatale.

**Title :** Postnatal development and evolution of the rodents' craniofacial complex

**Keywords :** Development, Epigenetic, Geometric morphometrics, Craniofacial, Rodents, Growth

**Abstract:** The skull is, architecturally and functionally, a strongly integrated and complex structure. At the same time and somehow paradoxically, this unit is highly evolvable and presents a high diversity of shapes. Epigenetic interactions in response to mechanical stimulations will compensate and coordinate the growth of the different organs constituting the head, in order to acquire and/or to maintain certain functions. These interactions will allow the normal development by controlling the bone remodeling. In spite of its central role, the importance of these interactions in the expression of differences between species and at a large time-scale in the dynamics of clades remains poorly understood.

The project of the PhD thesis aims I) at studying the onset of the craniofacial disparity in rodents during development, and II) at estimating the importance of the epigenetic processes during this postnatal growth.